



**FACULDADE DE CIÊNCIAS E TECNOLOGIA**

**UNIVERSIDADE NOVA DE LISBOA**

**STOCHASTIC MODELLING OF THE RESERVOIR LITHOLOGICAL  
AND PETROPHYSICAL ATTRIBUTES. A CASE STUDY OF THE  
MIDDLE EAST CARBONATE RESERVOIR**

**Svetlana Kravets**

(Licenciada)

Dissertação para obtenção do Grau de Mestre em Engenharia Geológica (Georrecursos)

**Orientador:** Doutor José António de Almeida, Prof. Auxiliar – FCT/UNL

**Co-orientador:** Doutor José Carlos Ribeiro Kullberg, Prof. Auxiliar – FCT/UNL

**Júri:**

Presidente: Doutor Paulo Alexandre Rodrigues Roque Legoinha, Prof. Auxiliar – FCT/UNL

Vogais: Doutor Herlander Mata Lima, Investigador. Auxiliar – Cerena/IST – UTL

Doutor Martim Afonso Ferreira de Sousa Chichorro, Investigador. Auxiliar – FCT/UNL

Doutor José António de Almeida, Prof. Auxiliar – FCT/UNL

Doutor José Carlos Ribeiro Kullberg, Prof. Auxiliar – FCT/UNL

July 2012



**FACULDADE DE  
CIÊNCIAS E TECNOLOGIA  
UNIVERSIDADE NOVA DE LISBOA**

**STOCHASTIC MODELLING OF THE RESERVOIR LITHOLOGICAL AND PETROPHYSICAL ATTRIBUTES. A CASE STUDY OF THE MIDDLE EAST CARBONATE RESERVOIR**

Copyright em nome de Svetlana Kravets, da FCT/UNL e da UNL

A Faculdade de Ciências e Tecnologia e a Universidade Nova de Lisboa tem o direito, perpétuo e sem limites geográficos, de arquivar e publicar esta dissertação através de exemplars impressos reproduzidos em papel ou de forma digital, ou por qualquer outro meio conhecido ou que venha a ser inventado, e de a divulgar através de repositórios científicos e de admitir a sua cópia e distribuição com objectivos educacionais ou de investigação, não comerciais, desde que seja dado crédito ao autor e editor.

## **ACKNOWLEDGEMENTS**

I would like to express my greatest gratitude to the professors of FCT UNL Doctor José António de Almeida and Doctor José Carlos Kullberg for the support and guidance throughout my thesis; from initial idea and conceptual advices to supervising and inspiration during the work and great instrumental and technical assistance. It is a great pleasure to work with them and constantly learn something new.

This work was performed under the support of Erasmus Mundus Action II Multic Programme.

## ABSTRACT

Carbonate reservoirs represent the significant part of oil and gas production. They produce about 50% of hydrocarbons globally. In order to provide the rational exploitation of deposits in carbonate reservoirs it is necessary to ensure accurate prediction and effectively overcome the technical barriers that occur in a complex carbonate formations. The main rules for successful project are to develop and apply reservoir characteristics, to predict performance and productivity, effectively manage diagenesis to optimize production and maximize recovery through reservoir simulation technology. The great development of digital modelling technologies gives the opportunities to solve these problems.

Generation of models of carbonate reservoir rocks by simulating the results of the geological processes involved is very complicated. Mainly because the rock may have undergone several phases of diagenetic processes that might have modified or even completely overprinted texture and fabrics of the original carbonate rock. In spite of this problem, a modelling technique, originally developed for sandstones, has successfully been extended for the 3D modeling of carbonate reservoir rocks. The input data to the modelling is obtained from the geophysical data and logging. In the present work, the virtual pore scale models of carbonates were produced by simulating the results of the geological processes.

The implemented methodology was divided into two main steps. The first stage was a Lithoclasses Modelling. The 3D stochastic geological model of the lithology was produced by the Sequential Indicator Simulation (SIS) algorithm. The second stage was an attribute modelling. The main properties such as porosity and permeability were computed according to the lithoclasses via Direct Sequential Simulation (DSS) algorithm with local histograms. The comparison of the two data sets showed high convergence for the main calculated properties. In the final stage of the work the geobody analysis was conducted. This type of the connectivity analysis performed the geometry of geological facies, trends for property distribution and permeability barriers.

**Key-words:** carbonate reservoir, stochastic modelling, sequential simulation, geobody analysis.

## RESUMO

Rochas reservatório carbonáticos representam parte significativa da produção de petróleo e gás. Eles produzem cerca de 50% de hidrocarbonetos em todo o mundo. A fim de fornecer a exploração racional dos depósitos em reservatórios de carbonato, que é necessário para assegurar a previsão precisa e eficaz superar as barreiras técnicas que podem ocorrer numa formações de carbonato de complexos. As principais regras para projeto de sucesso são desenvolver e aplicar características do reservatório, para prever o desempenho e produtividade, gerir eficazmente diagênese para otimizar a produção e maximizar a recuperação através da tecnologia de simulação de reservatórios. O grande desenvolvimento das tecnologias de modelagem digital dá as oportunidades para resolver estes problemas.

Geração de modelos de rochas reservatório de carbonato através da simulação dos resultados dos processos geológicos envolvidos é muito complicado. Principalmente porque a rocha pode ter sofrido várias fases de processos diagenéticos que poderiam ter modificados ou até mesmo completamente sobreposta textura e tecidos da rocha carbonática original. Apesar deste problema, uma técnica de modelagem, originalmente desenvolvido para arenitos, com sucesso, foi estendido para a modelagem 3D de rochas reservatórios de carbonato. Os dados de entrada para a modelagem é obtida a partir dos dados geofísicos e madeireiras. No presente trabalho, os modelos de poros virtuais escala de carbonatos foram produzidos através da simulação dos resultados dos processos geológicos.

A metodologia implementada foi dividida em duas etapas principais. A primeira etapa foi uma Modelagem Lithoclasses. O modelo estocástico 3D geológica da litologia foi produzido pelo Indicador de Simulação Seqüencial (SIS) algoritmo. A segunda etapa foi uma modelagem atributo. As principais propriedades como porosidade e permeabilidade foram calculados de acordo com as lithoclasses via Directa Seqüencial Simulação algoritmo (DSS), com histogramas locais. A comparação dos dois conjuntos de dados mostrou convergência elevada para as principais propriedades calculados. Na fase final do trabalho a análise geobody foi conduzido. Este tipo de análise realizada conectividade a geometria de fácies geológicas, as tendências de distribuição de propriedade e as barreiras de permeabilidade.

**Palavras-chave:** reservatórios de carbonato, modelagem estocástica, simulação seqüencial, análise geobody.

# CONTENT

1	INTRODUCTION	13
1.1	Carbonate reservoir distribution	14
1.2	Current economic situation	15
1.3	Organization of the work	18
2	GEOLOGICAL ENVIRONMENTS	19
2.1	Carbonate rocks: main characteristics	19
2.2	Classification of the carbonate rocks	20
2.3	Depositional environments	26
2.4	Properties	32
	2.4.1 Porosity	32
	2.4.2 Molds and vugs in carbonate reservoirs	35
	2.4.3 Fractured porosity	36
	2.4.4 Permeability	38
	2.4.5 Pore Size and fluid saturation	39
2.5	Diagenetic process	41
2.6	Reservoir potential. Seals and traps	42
3	PROSPECTING METHODS AND INTEREST VARIABLES	47
3.1	Core description	48
3.2	Seismic surveys	50
3.3	Geophysical well logging	53
4	MODELLING METHODOLOGY	58
4.1	Workflow description	58
4.2	Background of geostatistics	61
4.3	Variograms and spatial continuity	63
4.4	Estimation	67
4.5	Indicator background	68
4.6	Simulation	71
	4.6.1 Sequential Indicator Simulation	72
	4.6.2 Direct Sequential Simulation	73
4.7	Geobody analysis	75
5	CASE STUDY	77
5.1	Data presentation and basic statistics	77
5.2	Layer top and bottom morphology	79

5.3	Transformation into stratigraphic units	81
5.4	3D geological model of lithoclasses	83
5.5	3D Model of porosity	87
5.6	3D model of permeability	95
5.7	Analysis of geobodies	100
6	FINAL REMARKS	102
	References	104

## List of figures

Figure 1.1.1 – Worldwide distribution of carbonate reservoirs (BP Statistical Review, 2007; Schlumberger Market Analysis, 2007)	15
Figure 1.2.1 – The main oil producers and consumers (BP statistical Review of World Energy, 2005)	17
Figure 1.2.2 – Proven oil and gas reserves by region (OPEC Annual Statistic Bulletin, 2007)	18
Figure 2.2.1 Textural maturity classification of limestone proposed by Folk (Ham, 1962)	22
Figure 2.2.2 – Folk System classification (Archie, 1952)	23
Figure 2.2.3 – Classification of limestone proposed by Dunham (1962), (Schlumberger, 2010)	24
Figure 2.2.4 – Carbonate rock examples (Ham, 1962)	25
Figure 2.3.1 – Some typical environments that carbonates can form (Tucker and Wright, 1990).	26
Figure 2.3.2 – Carbonates depositional environments (reefs and ramps) (Schlumberger, 2010)	29
Figure 2.3.3 – Idealized shelf cross-section (Schlumberger, 2010)	30
Figure 2.3.4 – Idealized ramp cross-section (Schlumberger, 2010)	30
Figure 2.3.5 – Classification of reefs: fringing reefs (top), barrier reefs (middle), atolls (bottom) (Schlumberger, 2010)	31
Figure 2.4.1.1 – Changings of the porosity of carbonate sediments from deposition (Schlumberger, 2010)	33
Figure 2.4.1.2 – Comparison of the primary porosity of carbonate sediments (Schlumberger, 2010)	34
Figure 2.4.1.3 – Types of microporosity in carbonate rock (Schlumberger, 2010)	34
Figure 2.4.2.1 – Stages in the development of molds and vugs (Schlumberger, 2010)	36
Figure 2.4.3.1 – Examples of fracture porosity in carbonate reservoirs (adopted from Lucia, 1999)	37
Figure 2.4.3.2 – Diagram illustrating the relationship between fracture porosity, fracture volume, and reservoir drainage area. Intuitively, smaller drainage areas have smaller fracture volume. (Ahr, 2008)	38



Figure 2.4.5.1 – Plot of porosity and permeability for carbonate rocks, illustrating that there is no relationship between porosity and permeability in carbonate rocks without including pore-size distribution (Lucia, 1999)	40
Figure 2.4.5.2 – Diagram showing smaller pores being filled with a non-wetting fluid (oil) displacing a wetting fluid (water) as capillary pressure increases linearly with reservoir height (Lucia, 1999)	40
Figure 2.6.1 – Structural traps (Discovery Drilling Funds, 2005)	43
Figure 2.6.2 – Stratigraphic Pinch-Out trap: limestone reservoir loses its porosity and becomes impermeable limestone (Discovery Drilling Funds, 2005)	43
Figure 2.6.3 – Secondary diagenetic stratigraphic traps. A – Traps were created by post-depositional updip porosity occlusion. B – Traps were created by post-depositional porosity and permeability enhancement (Archie, 1952).	44
Figure 2.6.4 – Stratigraphic sedimentological trap – reef (Discovery Drilling Funds, 2005)	45
Figure 3.1.1 – The examples of core sampling of carbonates (Western Siberia) (TNK, 2005)	49
Figure 3.2.1 – The example of seismic facies analysis of the form seismic traces (Levyant, 2010)	52
Figure 3.2.2 – Example of FMI images (Schlumberger, 2009)	53
Figure 3.3.1 – EcoScope LWD tool. The EcoScope tool incorporates resistivity, neutron porosity, sigma and neutron capture spectroscopy sensors into a single compact device. Wireline and LWD tools generally use chemical sources for neutron porosity and neutron capture spectroscopy measurements. The EcoScope tool generates neutrons with a pulsed-neutron generator that operates only when mud is being pumped through the tool (Schlumberger, 2010)	56
Figure 3.3.2 – Pore size and geometry. Measurements from NMR logging tools are more sensitive to pore size and geometry than are resistivity and other porosity measurements. The gamma ray log (Track 1), resistivity logs (Track 2) and porosity measurements (Track 3) are consistent throughout the interval shown. The NMR data (Track 4) indicate a large increase in pore size above X,040 ft that is not seen in the other measurements (adapted from Ramamoorthy, 2010)	57

Figure 4.1.1 – Basic scheme of modelling process presented in this work: SIS – Sequential Indicator Simulation; DSS – Direct Sequential Simulation; POIP – Potential Oil in place	59
Figure 4.1.2 – Example of transformation into a stratigraphical referential	60
Figure 4.3.1 – Representation of the main variogram parameters	65
Figure 4.3.2 – Representation of theoretical models with the same range (adapted from Matheron, 1989)	66
Figure 4.5.1 – Representation of a binary map and a binary variable	69
Figure 5.1.1 – Aerial view of the entire field with superposition of the stochastic simulation grid and well locations.	77
Figure 5.1.2 – Cumulative curves of PHIE for each lithoclass	78
Figure 5.1.3 – Cumulative curves of permeability	78
Figure 5.1.4 – Proportion of each lithoclasses	79
Figure 5.2.1 – Omnidirectional variograms for every surface	80
Figure 5.2.2 – Map of the top of the first layer	81
Figure 5.2.3 – Obtained morphology of the studied layer and location of wells	81
Figure 5.3.1 – The example of coordinate geometric transformation for PHIE parameter	82
Figure 5.3.2 – Cumulative curves of PHIE parameter for each lithoclass	82
Figure 5.3.3 – Cumulative curves of LDperm parameter for each lithoclass	83
Figure 5.4.1 – Variograms for lithoclasses 2 and 5 for both directions (horizontal and vertical)	84
Figure 5.4.2 – Multi-phase variograms for lithoclasses with fitted theoretical model	84
Figure 5.4.3 – Two realization of simulation of the lithoclasses: left – horizontal; right – cross-section, where colors represent each lithoclass	85
Figure 5.4.4 – Comparison of the well and simulated data	86
Figure 5.4.5 – Multi-phase variogram of one simulated image (horizontal and vertical) and the theoretical model fitted to the well data	87

Figure 5.5.1 – Variograms of PHIE for each lithoclass and fitted theoretical models	88-89
Figure 5.5.2 – The obtained maps of PHIE for first and second images of lithoclasses (horizontal and cross-section) and an average map of phie (30)	91-92
Figure 5.5.3 – Simulated map of Phie with overlaid well data	93
Figure 5.5.4 – Univariate statistics of grid	93
Figure 5.5.5 – Univariate statistics of well data	94
Figure 5.5.6 – Variograms for one simulated images of PHIE conditioning to the lithoclasses	94
Figure 5.6.1 – Variograms of LDperm for all lithoclasses with fitted theoretical model	95
Figure 5.6.2 – Two realizations of LDperm for the first and second images of lithoclasses (horizontal and cross-section) and the average map of LDperm (logarithmic scale)	96-97
Figure 5.6.3 – Simulated map of LDperm with overlaying well data	97
Figure 5.6.4 – Univariate statistic for one simulated image of LDperm	98
Figure 5.6.5 – Univariate statistic for well data	99
Figure 5.6.6 – Variograms for simulated maps of LDperm	99
Figures 5.7.1 – Potential oil in place curves for case a)	101
Figures 5.7.2 – Potential oil in place curves for case b)	101

## **List of tables**

Table 5.1.1 – Lithoclasses identified in the present oil field: typical rock types and porosity and permeability mean and variance	79
Table 5.2.1 – Parameters of grid used for computing variograms and kriging process	80
Table 5.4.1 – Theoretical model parameters for the multi-phase variograms of lithoclasses	83
Table 5.4.2 – Main univariate statistic parameters for well and simulated data	86
Table 5.5.1 – Parameters of the theoretical models of variograms for PHIE	90
Table 5.6.1 – Parameters of the theoretical model fitted for Ldperm for all lithoclasses	95

## **1 INTRODUCTION**

Hydrocarbon energy sources – oil, gas and coal are the foundation of modern society. There are a lot of hydrocarbon deposits all over the world which are in different geological and tectonic environment.

It is estimated that more than 60% of the world's oil and 40% of the world's gas reserves are held in carbonate reservoirs. The Middle East, for example, is dominated by carbonate fields, with around 70% of oil and 90% of gas reserves held within these reservoirs (BP Statistical Review of World Energy, 2011). Carbonates can exhibit highly varying properties (e.g., porosity, permeability, flow mechanisms) within small sections of the reservoir, making them difficult to characterize. A focused approach is needed to better understand the heterogeneous nature of the rock containing the fluids and the flow properties within the porous and often fractured formations. This involves detailed understanding of the fluids saturation, pore-size distribution, permeability, rock texture, reservoir rock type, and natural fracture systems at different scales.

The key point in a rational development of hydrocarbon deposits in carbonate reservoirs is an accurate forecasting of a structure, lithology and main properties of reservoir. In turn it provides effective and successful production of deposit and maximizing the economic benefit. The most powerful technology to solve these issues is modelling.

Exploration, development and production of hydrocarbons are a very complex issues and many factors influence on them. Looking through historical development it can be noticed that all industry of oil and gas development depends on not only industry themselves but the great role have also politics, economics, prices and costs and even social stability in country where hydrocarbons are developed. For oil and gas industry is almost impossible to influence on social and political reasons. The other side is technology. In order to enhance current situation on oil and gas market in condition of occurrence more and more difficulties and problems connected with exploration and production of hydrocarbon deposits we can better develop technology (Montaron, et. al., 2009). Nowadays the situation is that opening the great deposits of hydrocarbon is very seldom case. All discovered ones are not so big and it occurs on great depth in the earth crust or under the sea. Also there are a lot of environmental restrictions in such regions as Alaska and other places of the world, global condition of existing number of pollution problems. All complex of issues creates a great number of limits of exploration, development and production of oil and gas. The main way to improve the situation is developing technology.

Modern technology improves our ability to virtually “see” and distinguish the oil and gas before we drill. The key technology for doing this is modeling of georesources. Modelling is the applied science of creating digital representations of rock features or properties based on geophysical and geological observations. A model is the numerical equivalent of a three-dimensional geological map complemented by a description of physical quantities in the domain of interest. Modeling is commonly used for managing natural resources and natural hazards and quantifying geological processes, in the oil and gas industry, realistic geologic models are designed to simulate reservoirs structure, predict the behavior of the rocks under various hydrocarbon recovery scenarios. An actual reservoir can only be developed and produced once, and mistakes can be wasteful. Using geological models and reservoir simulation allows reservoir engineers to identify based on the data obtained and predicted from model, which recovery options offer the safest and most economic, efficient, and effective development plan for a particular reservoir.

An important part of geologic modelling is related to geostatistics. In order to represent the observed data, often not on regular grids, we have to use certain interpolation techniques. The most widely used technique is kriging which uses the spatial correlation among data and intends to construct the interpolation via variograms. To reproduce more realistic spatial variability and help assessing spatial uncertainty between data, geostatistical simulation is often used, based on variograms, different simulation algorithms or parametric geological objects (Goovaerts 1997).

### **1.1 Carbonate reservoir distribution**

Carbonate rocks in many areas developed widely, making a whole, as in the stratigraphic section sedimentary strata, and in the vast space of complex deposits oil and gas prospects are evaluated on the merits due way recently. Carbonate rocks are characteristic of all geological scale, from the Precambrian to the Neogene system. According to various estimates, carbonate reservoirs are concentrated between 35 and 48% oil and about 23-28% of the gas in the world. In some countries, like Iran, Oman, Syria, Mexico, the share of oil reserves, confined to carbonate collectors, is almost 100% (BP, 2007). In the figure 1.1.1 the global distribution of carbonate reservoirs is presented.

From the statistics above it is clear that the relative importance of carbonate reservoirs compared with other types of reserves will increase dramatically during the first half of the 21st century. However, there are significant challenges in terms of recovery due to the highly complex internal

structure and specificity of carbonate reservoirs. In consequence with such wide spreading of carbonates and therefore its importance in hydrocarbons production and considering the fact that the leading production regions is also presented with carbonates rocks, currently, their careful investigation is becoming more and more important. It allows to point out the relevance of this work.

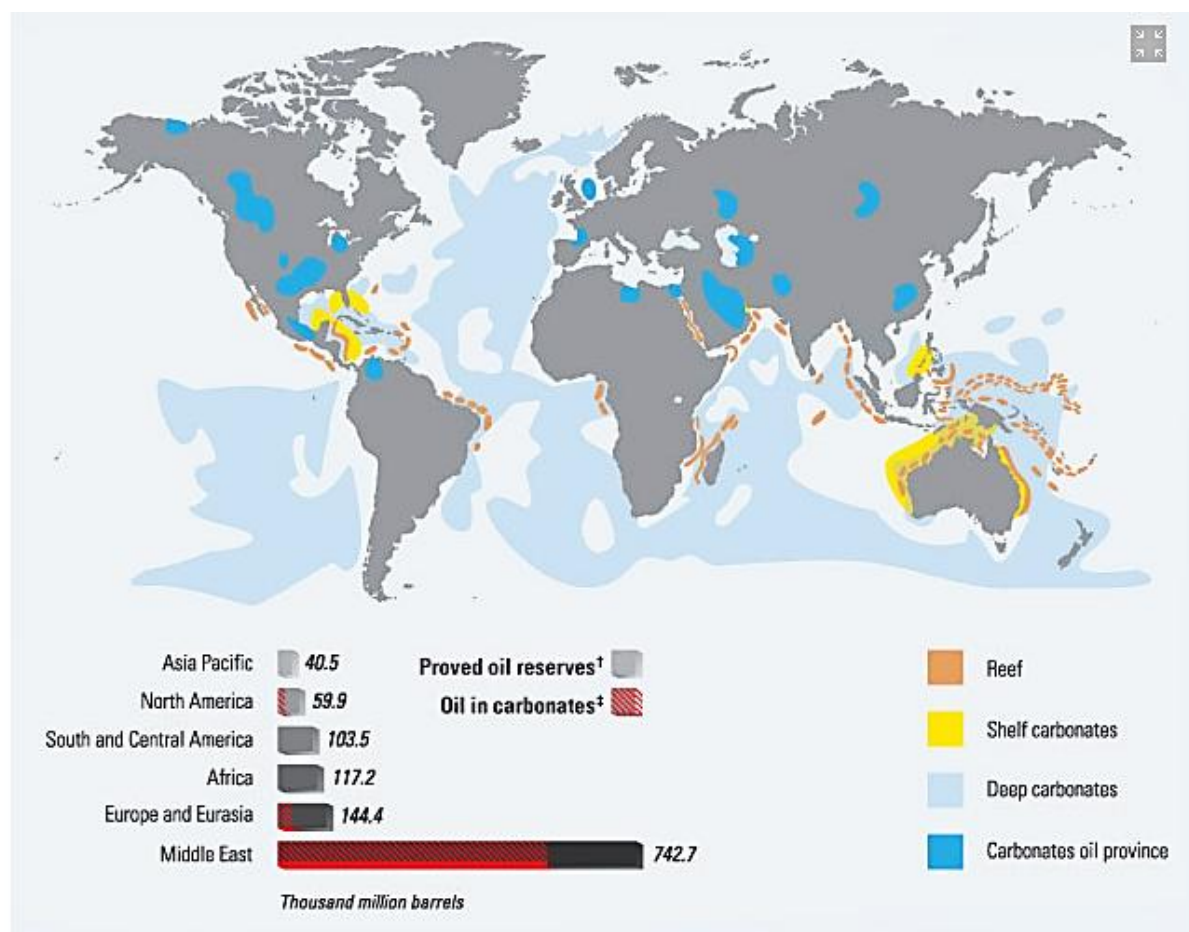


Figure 1.1.1 – Worldwide distribution of carbonate reservoirs (BP Statistical Review, 2007; Schlumberger Market Analysis, 2007)

## 1.2 Current economic situation

In the twentieth century the average annual of consumption of hydrocarbon energy resources have changed. It was dominated by the following trends: decreasing of the share of coal in the global fuel mix from 89% to 29%; increasing the share of oil and gas from 3.5% to 33% and from 1% to 24%, respectively. In the last decade, a trend increase in the share of alternative and renewable energy. This is partly due to the fear climate change and human impact on the search

for alternative sources with low emissions of carbon dioxide, on the other hand, is associated with rising prices for traditional energy resources. The growing of the price was caused by increasing of exploration and exploitation costs, which in turn, rising due to complicated condition of reservoirs involved in production and the depletion stage of the most part of hydrocarbon deposits (Sokolov, 2011).

The structure of energy consumption and production across regions of the world is inhomogeneous. There are the following features for the world oil market. The greater volume of oil produced is consumed in Asia Pacific and North America. At the same time, oil production in these regions is less than the consumption (figure 1.2.1). This difference in volume production and consumption is characteristic for all the world oil market. On 01.01.2011 the amount of recoverable oil reserves in the world amounted to 188 billion tons (in the figure 1.2.2 the proven reserves of oil and gas is shown) (BP., Schlumberger, 2011). At current levels of consumption security reserves is 46 years old. In this case, it is understood that the value of 46 years is largely arbitrary. In indeed, as the depletion of prey is a natural way decline and reduced production even at 30% would have a negative impact on the global economy (Burkhard, 2010). Thus, it is obvious that the world economy faces significant challenges long before they fully exhausted all oil reserves.

Sustaining global oil and gas demands requires advanced and appropriate oilfield technology in carbonate reservoirs. There is the up-to-date resource of improving the situation – advanced remote technologies of reservoir investigation – modelling methodologies. In this work the last reliable methodologies of reservoirs modelling is presented.



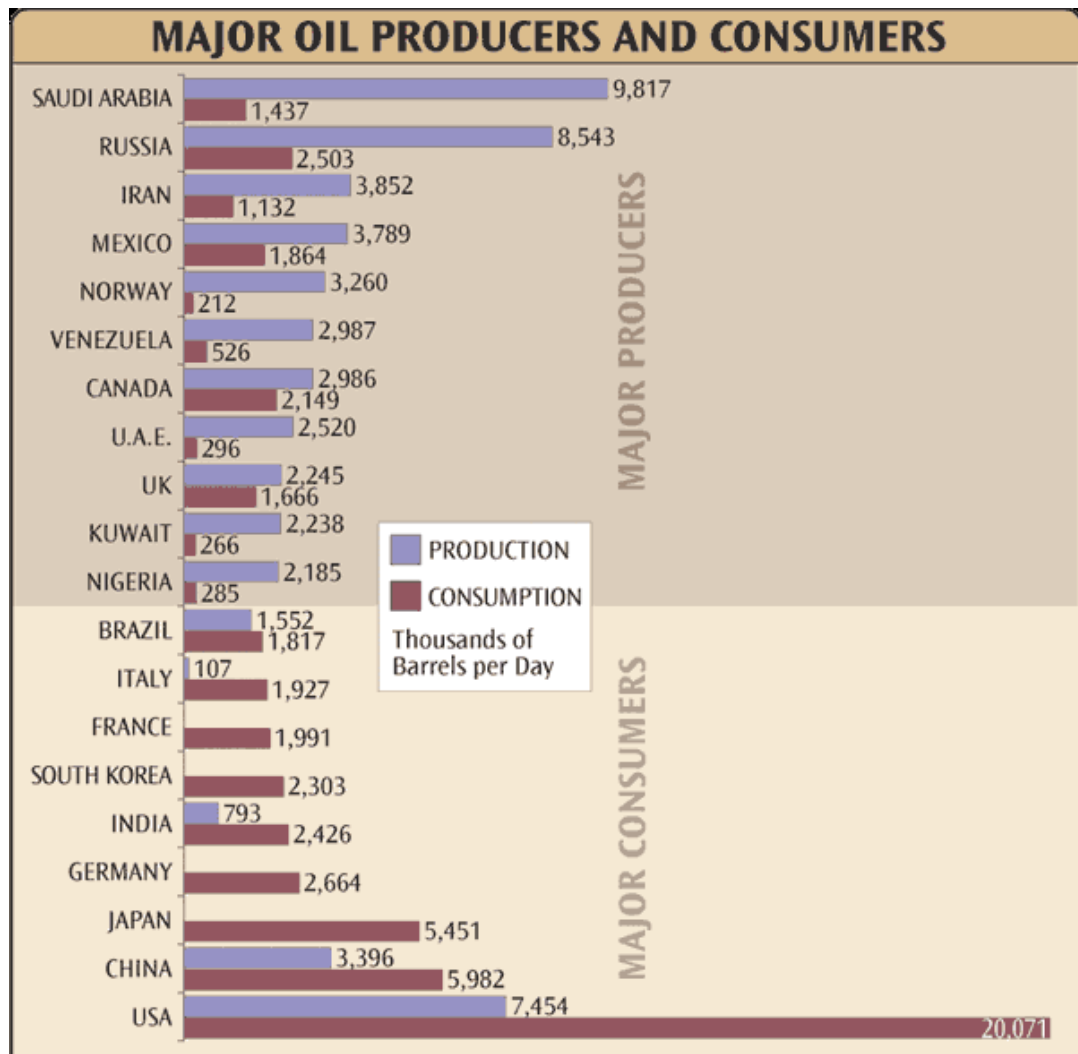


Figure 1.2.1 – The main oil producers and consumers (BP statistical Review of World Energy, 2005)

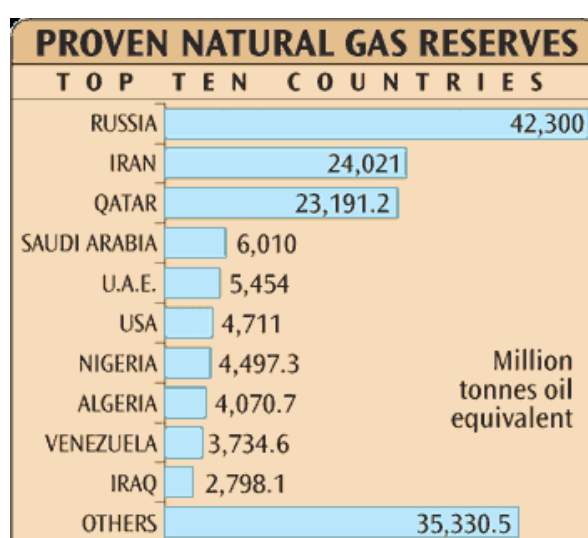
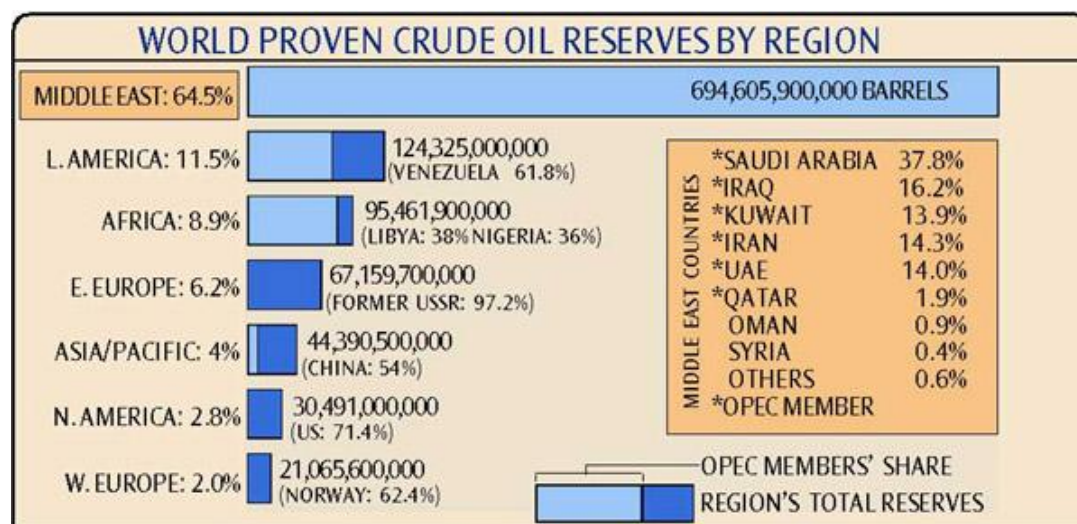


Figure 1.2.2 – Proven oil and gas reserves by region (OPEC Annual Statistic Bulletin, 2007)

### 1.3 Organization of the work

In compliance with the main subject of this work it has following organisation. On the second chapter the basic information about carbonate reservoir rocks and their composition, classification, morphology, properties and geological environments is presented as an introduction to the challenges in their characterization. In the third chapter the main ways of obtaining geological information for further modelling is described. Then the theoretical base of modelling methodologies is presented. In the case study the process of creation of the reservoir model by estimation and simulation morphology, lithology and attributes is described in accordance with the performed work. In conclusion there is a discussion of the obtained results.

## 2 GEOLOGICAL ENVIRONMENTS

### 2.1 Carbonate rocks: main characteristics

Carbonate rocks are sedimentary formations, composed of 50% and more carbonate minerals. The basic minerals are calcite (and aragonite) –  $\text{CaCO}_3$ , dolomite –  $\text{CaMg}(\text{CO}_3)_2$ , as well as some of the considerably more rarely occurred minerals – magnesium carbonate –  $\text{MgCO}_3$ , ankerite –  $\text{Fe,Ca}(\text{CO}_3)_2$ , siderite –  $\text{FeCO}_3$  and others. In nature only calcite and dolomite are widely distributed and the rest ones are found in the form of dispersed precipitates or individual lenses. Sometimes they formed more or less significant solid accumulations. Calcite and dolomite as a main rock forming carbonate minerals form limestone, dolomite and others different types of lime-dolomite composition rocks. These rocks are found in sediments of different tectonic structures (platform and geosynclinals) and the very different age from the Precambrian to Neogene (North, 1985; Ahr, 2008).

Limestones and dolomites form some of the largest petroleum reservoirs in the world. Many of the biggest occur in the Middle East (Harris, 1984). Other areas in which carbonate reservoirs deliver large quantities of oil and gas are western Canada, Mexico, Texas (USA), Norway (central North Sea), Poland, Kazakhstan, western and southeastern China, Iran, and Libya. The range of carbonate depositional environments likely to produce significant petroleum reservoirs is more restricted than that for clastics (Russell, et. al., 2009). Almost all of the major petroleum reservoirs in carbonates accumulated as shallow-marine sediment. Also some exceptions such as relatively deep-water pelagic chalks in the North Sea; or the similarly deep-water resedimented reservoir carbonates in Mexico exists.

Carbonate rocks have some unique attributes. One of the key differences between clastic and carbonate rocks is the distance between the site where the sediment was created and where it was deposited. While sand and silt may travel hundreds of miles down river systems before deposition and lithification, the grains that comprise carbonate sediments are usually deposited very close to the place where they were created. Transport related abrasion of carbonate grains is uncommon, and size sorting is generally very poor. Carbonate rock do not owe their mineralogical composition to weathered, parent rocks and their textures do not result from transport down streams and rivers (Lucia, 1999; Harris, et. al., 1984).

Carbonates are formed within the basin deposition by biological, chemical, and detrital processes. Organisms have an essential role in their formation. They extract dissolved components from sea-water to manufacture shells or skeletons that later are incorporated in the

sedimentary record. They can also modify the geochemical setting enough to cause mineral precipitation. So carbonates are largely made up of skeletal remains and other biological constituents that include fecal pellets, limemud (skeletal), and microbially mediated cements and lime muds (Ahr, 2008).

It is also should be mentioned that carbonates are susceptible to rapid and extensive diagenetic change. Carbonate minerals are susceptible to rapid dissolution, cementation, recrystallization, and replacement at ambient conditions in a variety of diagenetic environments. In short, porosity and permeability in carbonate reservoirs depend on a broad array of rock properties, on diagenetic episodes that may continue from just after deposition through deep burial, and on fracture patterns related more to the geometry of stress fields than to rock type (Lucia, 1999).

## **2.2 Classification of the carbonate rocks**

Numerous methods for carbonate rock classification have been proposed over the past 40 years. The most two widely accepted methods were devised by R.L. Folk (1959, 1962), for laboratory classification mostly, and R.J. Dunham (1962), for industry implement. The classification of carbonates is generally based on the textural and structural peculiarities instead of mineral composition.

The main principles of Folk classification that carbonate rock names consist of a conjunction of two names, one describing the allochems, the large pieces, the other describing the interstitial material. Allochems are equivalent to gravel, sand, lithics or feldspars in the siliciclastics. Interstitial material is equivalent to clay or cements in clastics. There are four kinds of allochems:

Fossils – may be whole fossils, or broken and abraded fossils; all are called "bio" fragments;

Oolites – small, pearl-like spheres;

Pellets – fecal pellets produced by invertebrate animals; look superficially like oolites but are dull and not pearl-like;

Intraclasts – chunks of eroded limestone deposited as a conglomerate;

Micrite is "lime mud", the dense, dull-looking sediment made of clay sized crystals of  $\text{CaCO}_3$ . Much micrite today forms from the breakdown of calcareous algae skeletons. It is not clear if all

ancient micrites formed in the same way. Many carbonates are composed of nearly 100% micrite. Such rocks are simply called micrites (Folk, 1962).

With carbonates containing allochems the question is whether micrite is present or absent as an interstitial material, and if present by how much. If micrite is present during deposition then it fills the spaces between the allochems and the rock will be given a name which describes the allochems in a micrite matrix. For example, a rock with fossil fragments embedded in micrite is called a "biomicrite". Biomicrite is analogous to a siliciclastic wacke, sand imbedded in a lot of matrix.

If, on the other hand, the depositional environment has strong currents, only allochems may be deposited. This is analogous to a 100% siliciclastic sand on a beach with no silt or clay. Micrite in these cases, being clay sized, has been washed away. The rock formed is then composed only of allochems, held together by clear to translucent calcite crystals with rhombohedral cleavage (called spar or sparite) acting as a cement. The spar is precipitated from fresh or marine water percolating through the sediment after deposition, but before final cementation. This oosparite shows well the spar cement (Folk, 1962).

Thus the classification of carbonates using the allochem/interstitial material system is very systematic and straight forward. The allochem name is combined with the interstitial name (micrite or spar). The figure 2.2.1 below shows the major categories of carbonate rocks based on their allochems and interstitial material.

This system goes through other levels of refinement, such as the table below where the abundance of allochems is dealt with. Other modifiers deal with different sizes of allochems. The scheme of classification is presented in the 2.2.2.

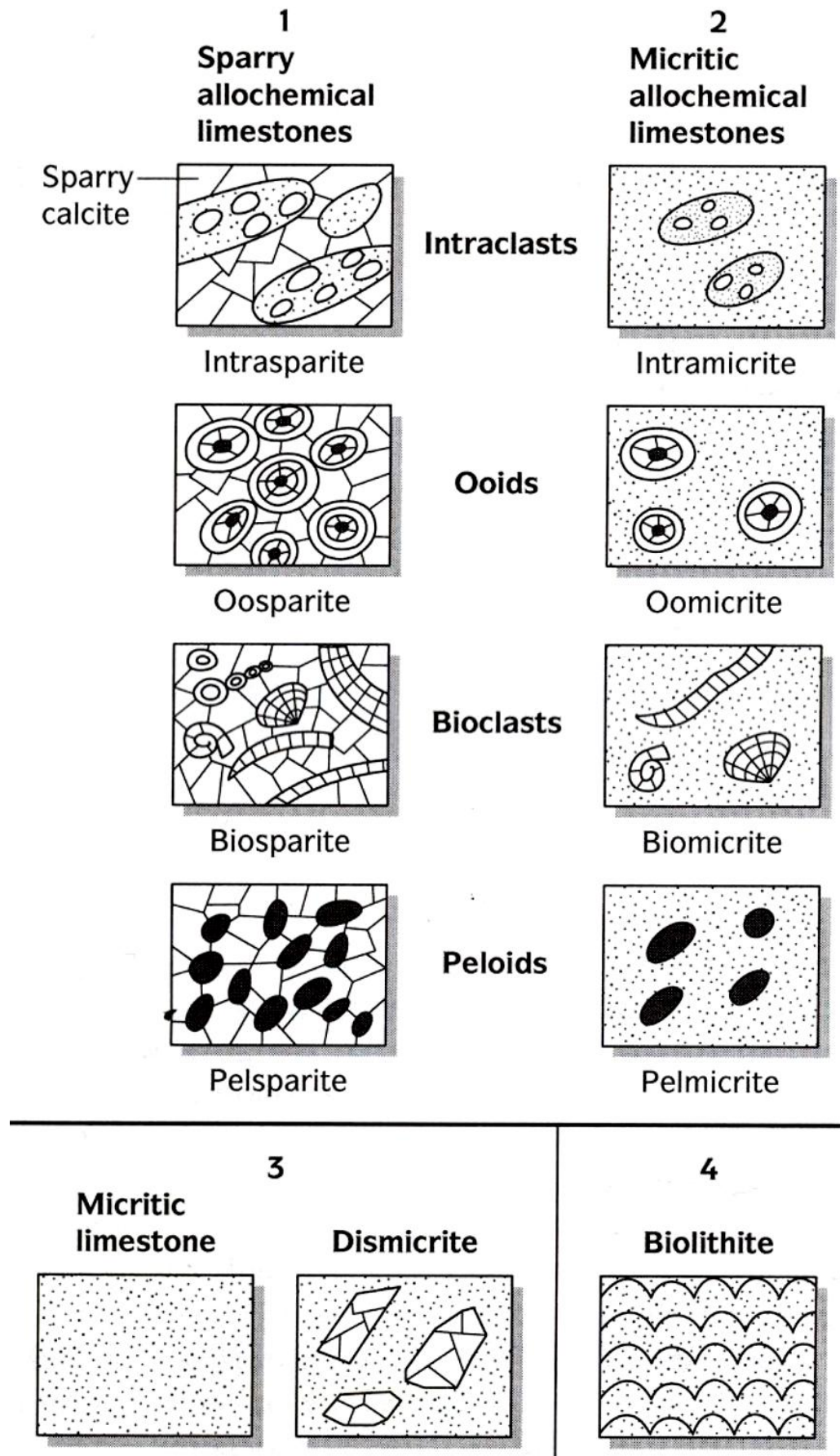


Figure 2.2.1 Textural maturity classification of limestone proposed by Folk (Ham, 1962)

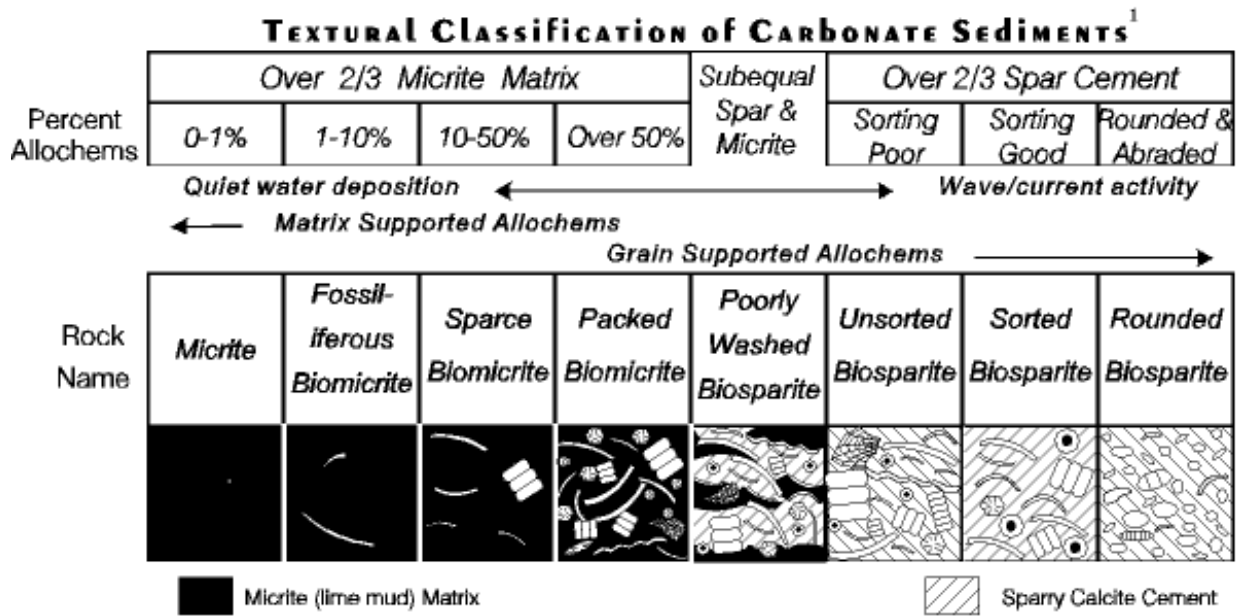


Figure 2.2.2 – Folk System classification (Archie, 1952)

The Dunham system is based on depositional texture that is, the amount of matrix surrounding the grains at the time of deposition. This scheme focuses on the depositional fabric of carbonate rocks. It divides the rocks into four main groups based on relative proportions of coarser clastic particles and deal with the question of whether or not the grains were originally in mutual contact; and therefore self-supporting, or whether the rock is characterized by the presence of frame builders and algal mats. Unlike the Folk classification scheme, Dunham one deals with the original porosity of the rock. The Dunham scheme is more useful industry because of basing on texture not the grains in the sample (Ham, 1962; Tucker, et. al., 1990). The classification is shown in the figure 2.2.3: the figure 2.2.4 represents the images of carbonates based on the Dunham scheme.

According to this classification, grainstones with very little mud blocking pore space, often exhibit high porosity and permeability at time of deposition and after diagenesis. They have the potential to become excellent reservoir rocks. Many of the Middle East's biggest and best known carbonate reservoirs are grainstones (Harris, 1985).



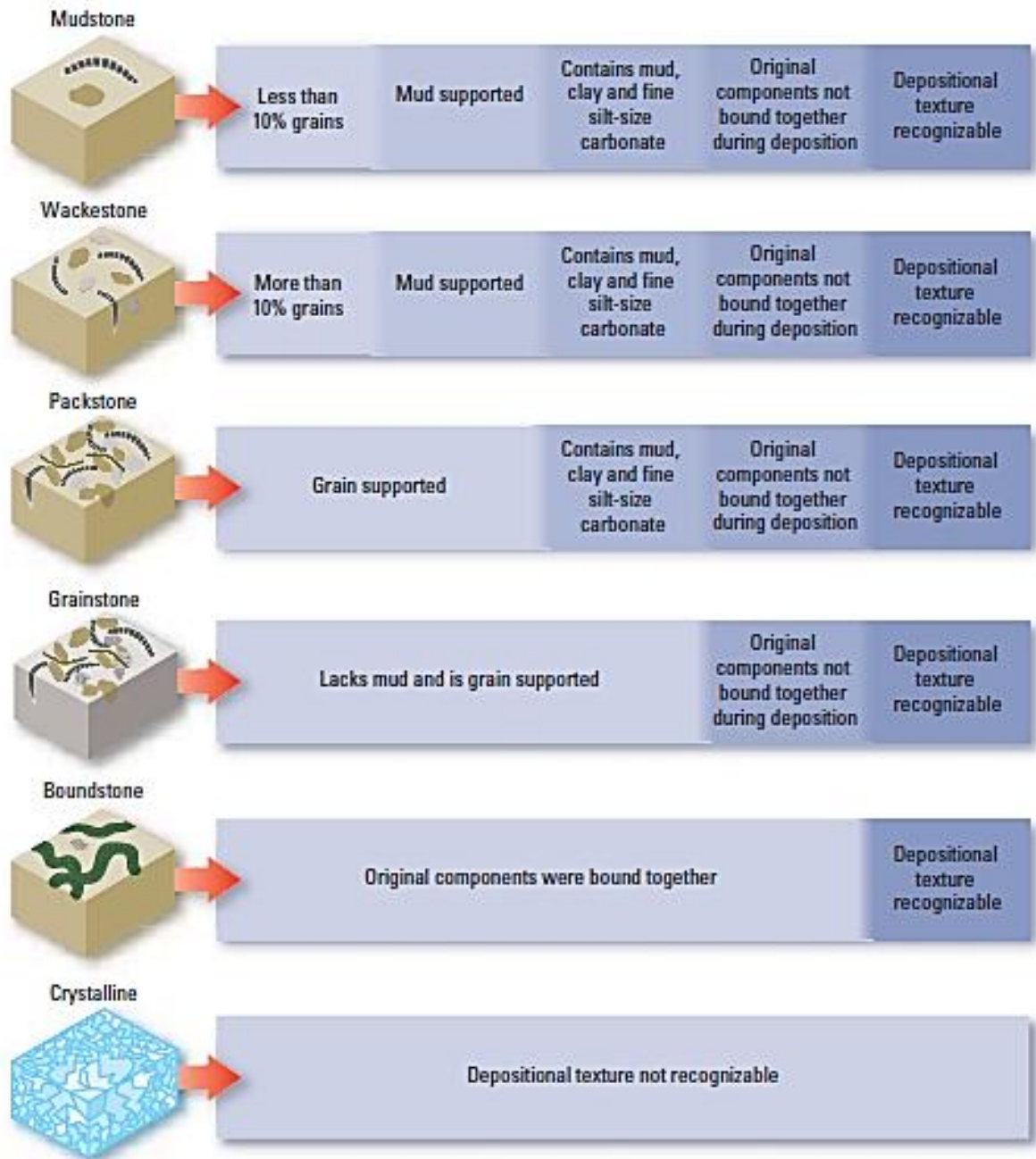


Figure 2.2.3 – Classification of limestone proposed by Dunham (1962), (Schlumberger, 2010)




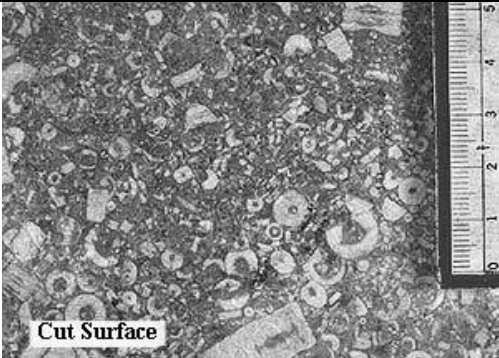

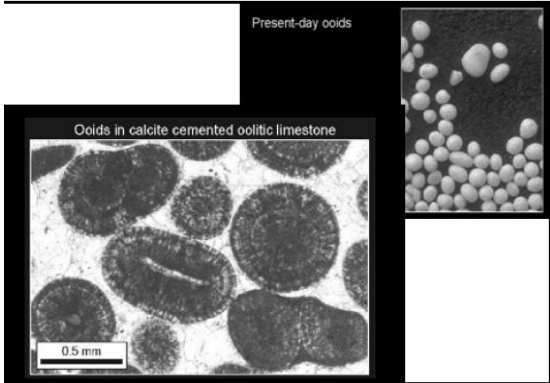


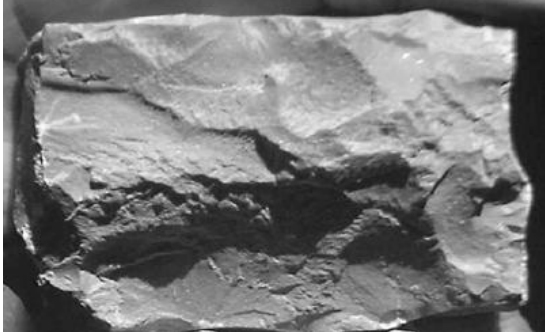
	
Coral Boundstone or Framestone	Crinoidal Packstone
	
Crinoidal Wackestone	
	
Oolitic Grainstone	Gastropod Packstone
	
Mudstone (micrite)	

Figure 2.2.4 – Carbonate rock examples (Ham, 1962)

### 2.3 Depositional environments

The facies dependence of fundamental reservoir properties such as porosity and permeability makes it essential to understand the depositional environments for the carbonate reservoir. This allows to predict what type of changes in permeability and porosity may be anticipated above or below the zone of interest (Scholle, et. al., 1983).

Biological and biochemical processes control the development of carbonate sediments. Most carbonate rocks are formed from accumulations of skeletal fragments – the remains of carbonate-secreting animals and plants by precipitation from water; either straight from the water, or induced by organisms, to make their shells or skeletons, and they form in many environments (figure 2.3.1). With a few notable exceptions, inorganic precipitation of calcium carbonate from seawater is rare (Scholle, et. al., 1983). The most important physical factors for carbonate deposition are water temperature, salinity and depth, and the volume and nature of siliciclastic sediments feeding into the depositional setting. Very low input volumes for clastic sediments allow carbonate rocks to accumulate in thick, continuous sequences (Ahr, 2008).

Many carbonate-secreting organisms, such as reef-building corals and calcareous green algae, require warm water to flourish. Today, the majority of carbonate sediments occur in the world's tropical-subtropical belt extending from 30° north to 30° south of the equator. Most of the carbonates formed during geological time have been deposited in low latitudes (Read, 1985).

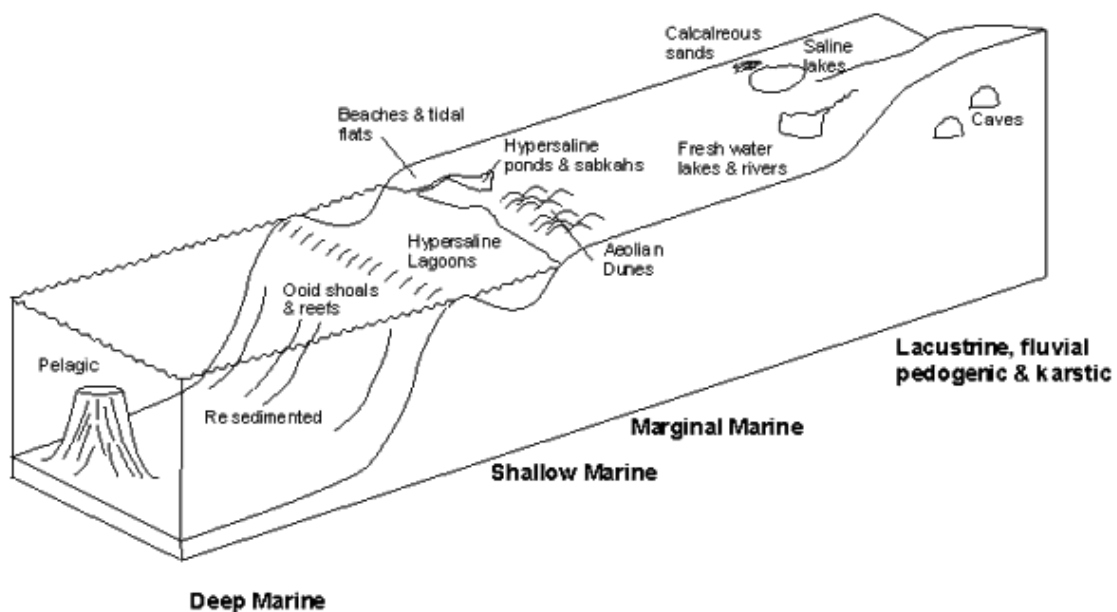


Figure 2.3.1 – Some typical environments that carbonates can form (Tucker and Wright, 1990).

According to different authors there various subdivisions of depositional environments of carbonate sediments, but the main scheme is remaining quite constant. For example, the main types of depositional carbonates environments according to Scholle, Bebout and Moore, 1991; are Subaerial exposure, Lacustrine, Eolian, Tidal Flat, Beach, Shelf, Middle Shelf, Reef, Bank Margin, fore-reef Slope, Basin Margin and Pelagic. So the carbonate rocks can be formed both in a continental and marine environment. The subaerial exposure, lacustrine and eolian environment are related to continental cases of carbonate formations. For instance, carbonate deposition can occur in non-marine lakes as a result of evaporation, in which case the carbonates are associated with other evaporate deposits, and as a result of organisms that remove CO<sub>2</sub> from the water causing it to become oversaturated with respect to calcite.

However, basically, most modern, and probably most ancient, carbonates are predominantly shallow water (depths <10-20 m) deposits. This is because the organisms that produce carbonate are either photosynthetic or require the presence of photosynthetic organisms. Since photosynthesis requires light from the Sun, and such light cannot penetrate to great depths in the oceans, the organisms thrive only at shallow depths. Furthermore, carbonate deposition in general only occurs in environments where there is a lack of siliciclastic input into the water. Siliclastic input increases the turbidity of the water and prevents light from penetrating, and silicate minerals have hardness much greater than carbonate minerals, and would tend to mechanically abrade the carbonates. Most carbonate deposition also requires relatively warm waters which also enhance the abundance of carbonate secreting organisms and decrease the solubility of calcium carbonate in seawater. Nevertheless, carbonate rocks form in the deep ocean basins and in colder environments if other conditions are right (James, 1983, Moore, 1983). The main marine carbonate depositional environments are following:

- Tidal flats are areas that flood during high tides and are exposed during low tides. Carbonate sands carried in by the tides are cemented together by carbonate secreting organisms, forming algal mats and stromatolites.
- Carbonate Platforms and Shelves. Warm shallow seas attached the continents, or in the case of epi-continental seas, partially covering the continents, are ideal places for carbonate deposition. Other shelves occur surrounding oceanic islands after volcanism has ceased and the island has been eroded (these are called atolls). Carbonate platforms are buildups of carbonate rocks in the deeper parts of the oceans on top of continental blocks left behind during continent – continent separation. Reef building organisms form the framework of most of these carbonate buildups (James, et. al., 1983).

- Deep Ocean. Carbonate deposition can only occur in the shallower parts of the deep ocean unless organic productivity is so high that the remains of organisms are quickly buried. This is because at depths between 3,000 and 5,000 m (largely dependent on latitude – deeper near the equator and shallower nearer the poles) in the deep oceans the rate of dissolution of carbonate is so high and the water so undersaturated with respect to calcium carbonate, that carbonates cannot accumulate. This depth is called the carbonate compensation depth (CCD). The main type of carbonate deposition in the deep oceans consists of the accumulation of the remains of planktonic foraminifera to form carbonate ooze. Upon burial, this ooze undergoes diagenetic recrystallization to form micritic limestones. Since most oceanic ridges are at a depth shallower than the CCD, carbonate oozes can accumulate on the flanks of the ridges and can be buried as the oceanic crust moves away from the ridge to deeper levels in the ocean. Since most oceanic crust and overlying sediment are eventually subducted, the preservation of such deep sea carbonates in the geologic record is rare, although some have been identified in areas where sediment has been scraped off the top of the subducting oceanic crust and added to the continents, such as in the Franciscan Formation of Jurassic age in California (Scholle, Moore, et. al., 1984).

Middle East carbonates occur in identifiable sequences which reflect changing marine conditions and environments (figure 2.3.2). Carbonates can be deposited in a wide range of marine environments. They typically occur in sequences which can be characterized as ramp (figure 2.3.2, a) or reef shelf (figure 2.3.2, b) settings. Low-energy environments, such as the back reef shoals, which are protected from wave and current action, are characterized by higher concentrations of lime mud while clean rocks with high original permeability are found in high-energy zones at the shoreline or around the main reef wall. If the basin area associated with either of these sections generates hydrocarbons the oil and gas should migrate up the structure (green arrow) into the porous carbonate rocks (Harris, 1984).

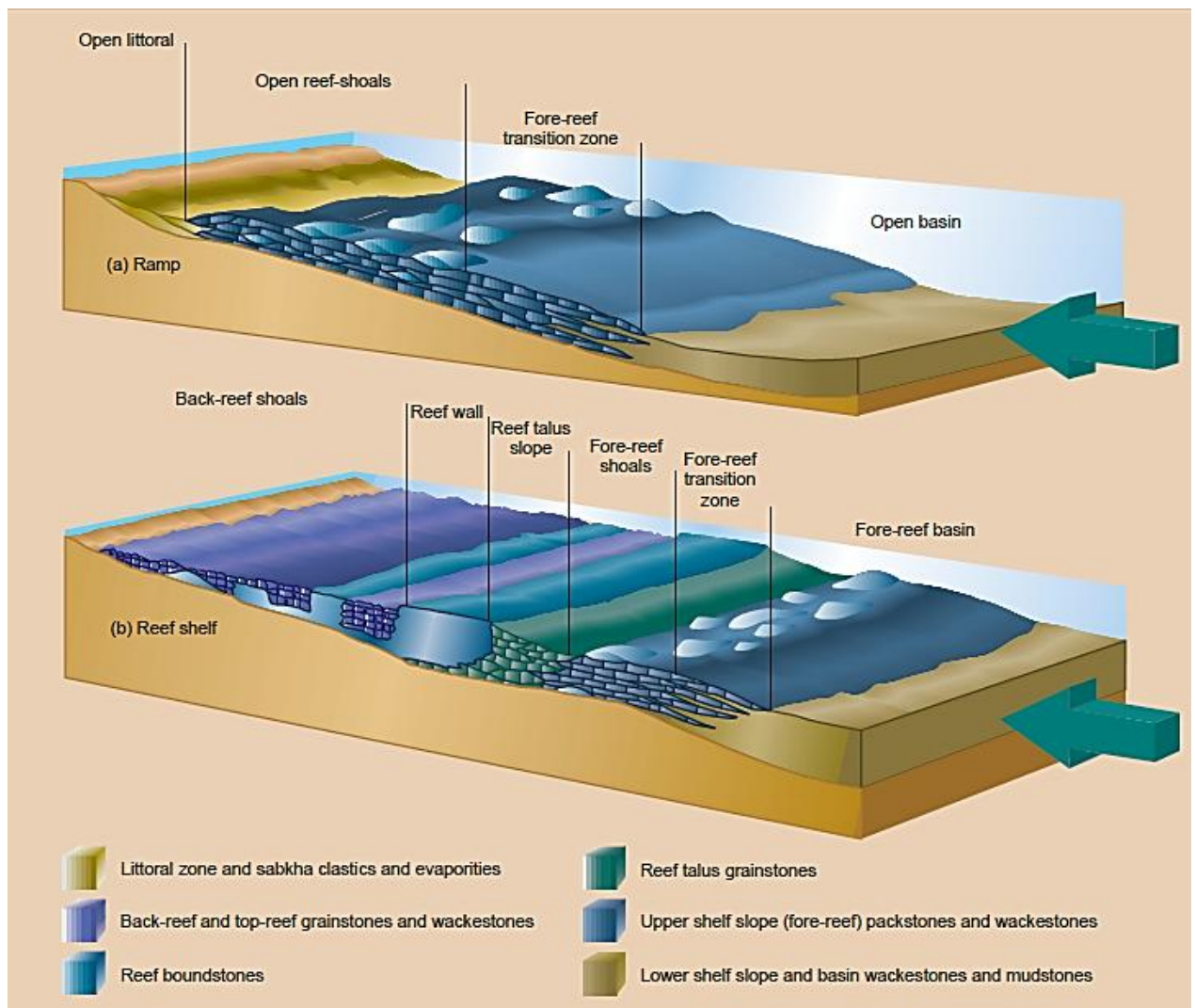


Figure 2.3.2 – Carbonates depositional environments (reefs and ramps), (Schlumberger, 2010)

In the main shelf area, carbonate skeletal sands may form barriers, beaches and shoals. Carbonate tidal deltas and sites of ooid deposition may develop along barrier coastlines at the mouths of major tidal channels that connect lagoons and the open sea. Reefs and other forms of carbonate buildup develop along the shelf margin, and may also form lagoonal barriers. Small patch reefs often form on the shelf and within the open lagoons.

In the study area there are three key depositional environments: carbonate shelves, carbonate banks or ramps and reefs.

Carbonate shelves – during transgressions gently sloping shelves and platforms become covered by shallow water carbonate sediments. Biogenic limestones build up on the shelf, and algal and oraminiferal limestones (including patch reefs) are well developed. Relatively continuous reefs

may grow along the shelf edges. The depositional units in this setting are typically interrupted and discontinuous, both laterally and vertically (figure 2.3.3).

Carbonate banks or ramps – gently sloping carbonate platforms that pass, without abrupt changes of slope, from shoreline to basin. Units in a typical shelf sequence have wide lateral continuity, making for very easy stratigraphic and/or facies correlations (figure 2.3.4). Reefs form on shelves and ramps. Linear reefs are generally developed at the edges of shelves.

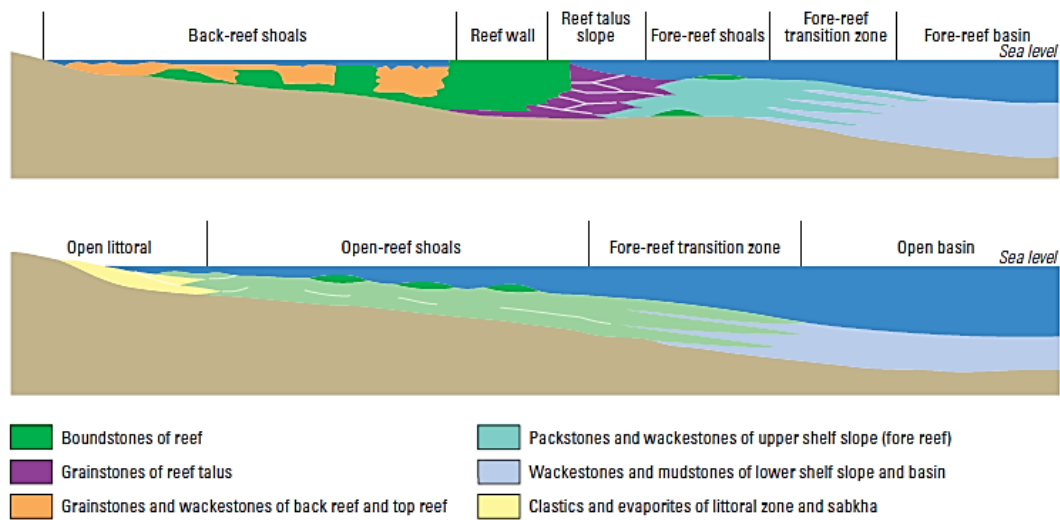


Figure 2.3.3 – Idealized shelf cross-section (Schlumberger, 2010)

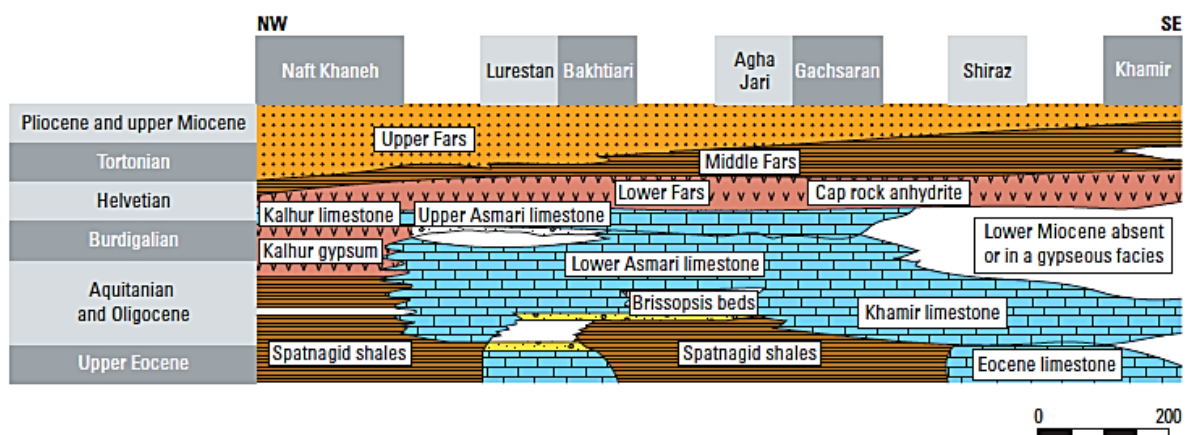


Figure 2.3.4 – Idealized ramp cross-section (Schlumberger, 2010)

Coral reefs can be classified into three main types: fringing reefs, barrier reefs and atolls (Figure 2.3.5). On ramps, the reefs develop as isolated features, making them harder to locate and exploit when they are hydrocarbon bearing.

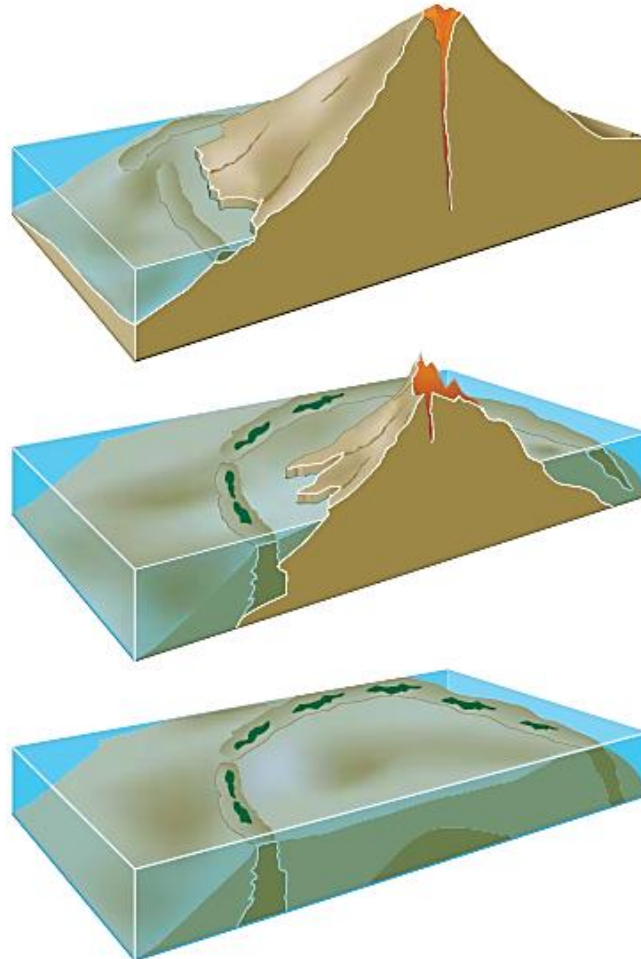


Figure 2.3.5 – Classification of reefs: fringing reefs (top), barrier reefs (middle), atolls (bottom) (Schlumberger, 2010)

Understanding of depositional environments and early diagenetic patterns are generally critical to the prediction of patterns of porosity and permeability. This is true both because depositional patterns commonly control patterns of water movement and diagenesis in carbonate rocks, and because a considerable amount of productive porosity in carbonate rocks is preserved from the depositional or early diagenetic settings. Thus, recognition of environments coupled with prediction trends can lead to important exploration advantages as well as improvements in a secondary stratigraphy (Moore, et. al., 1983).



## 2.4 Properties

Carbonates can exhibit highly varying properties (for example, porosity, permeability, flow mechanisms) within small sections of the reservoir, making them difficult to characterize. A focused approach is needed to better understand the heterogeneous nature of the rock containing the fluids and the flow properties within the porous and often fractured formations. This involves detailed understanding of the porosity, pore-size distribution, permeability, rock texture, reservoir rock type, and natural fracture systems at different scales (Ahr, 2008).

The properties such as porosity, permeability, relative permeability, and fluid saturations are linked through pore-size. Pore-size is related to the size and sorting of the particles that make up the fabric of the rock, as well as to the porosity. Fluid saturations, such as water and oil saturations, are a function of pore size, porosity, and capillary pressure. Capillary pressure is directly linked to reservoir height through the density difference of the fluids involved. Permeability is a function of porosity and pore-size. Relative permeability is a function of absolute permeability and fluid saturation, which are both linked to pore-size (Lucia, 1999).

### 2.4.1 Porosity

Porosity is an important rock property because it is a measure of the potential storage volume for hydrocarbons. Porosity in carbonate reservoirs ranges from 1 to 35%. In carbonate sediment the shape of the grains and the presence of intragrain porosity as well as sorting have a large effect on porosity. The presence of pore space within shells and peloids that make up the grains of carbonate sediments increases the porosity over what would be expected from intergrain porosity alone (Dunham 1962). The effect of sorting on porosity is opposite from that found in siliciclastics. The porosity of modern ooid grainstones averages 45% but porosity increases to 70 % as sorting decreases (Montaron, et. al., 2009). This increase is largely related to the needle shape of the mud-sized aragonite crystal. As a result, there is no simple relationship among porosity, grain size, and sorting in carbonate rocks.

Pore systems in limestones fall into two categories—primary porosity (effectively unaltered since deposition) and secondary (diagenetic-tectonic) porosity. There are three main types of primary porosity:



- framework porosity—pore space formed by rigid carbonate skeletal components such as corals;
- interparticle porosity in carbonate sands that depends on grain size, shape and distribution;
- porosity in carbonate muds provided by features such as fenestrae (bird's-eyes).

Secondary porosity includes:

- molds, vugs and caverns formed when grains or rocks are dissolved by groundwater
- intercrystalline pores produced by dolomitization
- fractured porosity formed by tectonic movements.

The porosity of carbonate sediments is generally very high at time of deposition, but is reduced or lost through cementation, compaction and pressure solution. However, this is not a one-way process (Ahr, 2008). Porosity can increase as a result of solution, dolomitization and tectonic fracturing (figure 2.4.1.1).

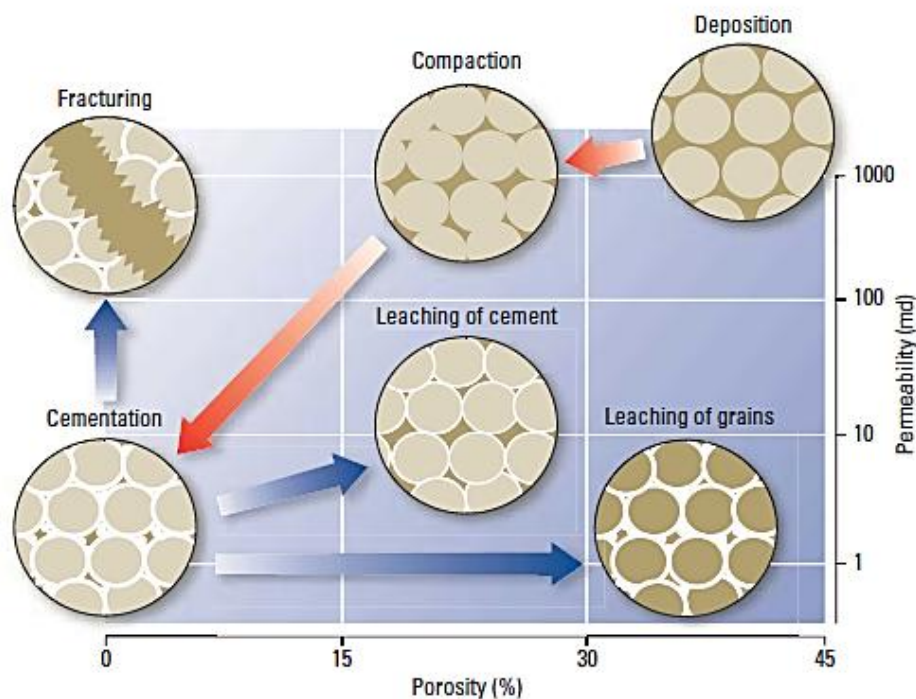


Figure 2.4.1.1 – Changings of the porosity of carbonate sediments from deposition (Schlumberger, 2010)

At deposition, carbonate sediments often have very high primary porosities (35 to 75%), but this decreases sharply as the sediment is lithified and buried to reservoir depths (figure 2.4.1.2). Primary porosity in limestones is quite different to that in sandstones. Planar grain surfaces are

rare in limestones, so pores tend to be polyconcave micropores (figure 2.4.1.3). The best primary limestone porosities are in grainstones, especially oolites and calcarenites such as back-reef lime sands.

Packstones, wackestones and mudstones that consist of pure limestone have a compact texture at time of deposition, and this compaction increases during burial. During burial, carbonate porosity is almost always reduced. Burial-related compaction can reduce the thickness of a limestone bed by up to 30% under just a few hundred meters of overburden. However, the reduction of carbonate porosity by compaction is only really significant if the carbonate remains uncemented. There is an inverse relationship between cementation and compaction in limestones (Montaron, et. al., 2009).

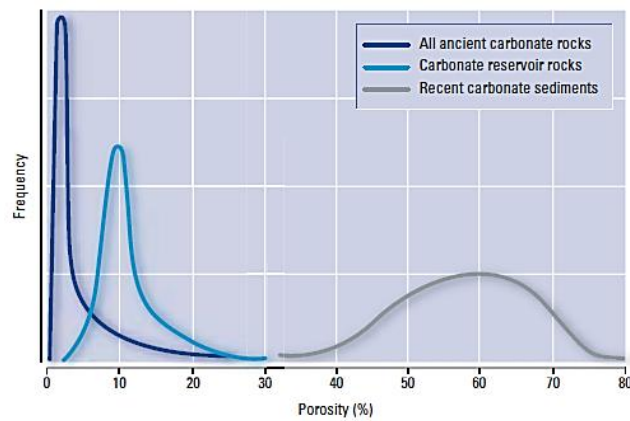


Figure 2.4.1.2 – Comparison of the primary porosity of carbonate sediments (Schlumberger, 2010)

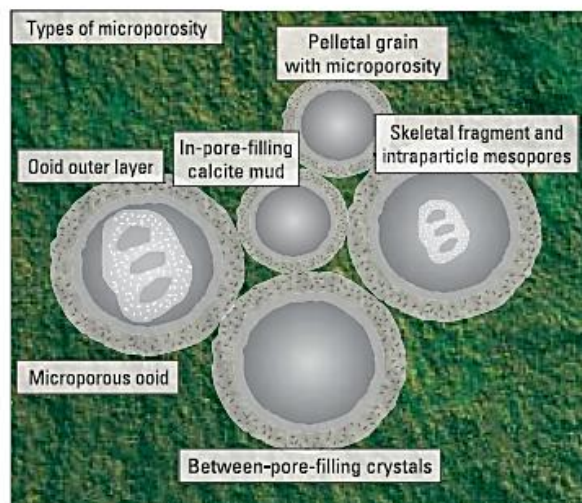


Figure 2.4.1.3 – Types of microporosity in carbonate rock (Schlumberger, 2010)

Calcium carbonate is so abundant that cementation of carbonate rocks is always likely to happen. Other minerals – such as anhydrite – do occur in the cements of carbonate rocks, but sparry calcite derived from the limestone itself is by far the most common cement. The process of pressure solution is much more important in carbonate rocks than in clastic rocks, and it is this process that allows carbonates to generate their own cements. One indication of pressure solution is the development of stylolites (or pressure seams), which are common features in many sequences. Under extreme conditions, cementation may continue until the cement becomes the single largest component in the rock (Archie, 1952).

Counteracting this cementation process is a susceptibility to solution in carbonated waters, which have taken their carbon dioxide into solution from the atmosphere, soils or other limestones. This solution process leads to the development of secondary porosity, the ultimate development of which is karst topography (Archie, 1952).

### **2.4.2 Molds and vugs in carbonate reservoirs**

Oil and gas geologists who work in carbonate reservoirs often spend a lot of time evaluating molds and vugs. Molds are pores formed by solution of an existing rock particle such as a shell fragment, crystal or grain. The resulting porosity is referred to as moldic porosity and is described according to the type of particle removed (e.g., oomoldic for an oolite from which ooids have been dissolved). If the leaching of the original particle passes the point at which it can be identified, the hole is referred to as a vug (figure 2.4.2.1). This factor, not the size of the hole, determines whether it is a mold or a vug. Extreme examples of vugs include the caverns that develop in some limestone sequences as a result of dissolution over thousands or millions of years.

A vug is a pore that (1) is somewhat equate, or not markedly elongate, (2) is large enough to be visible with unaided eye (diameter > 1/16 mm) and (3) does not specifically conform in position, shape, or boundaries to particular fabric elements of the host rock. Vuggy porosity can be subdivided into connected and disconnected types (Lucia, 1999).

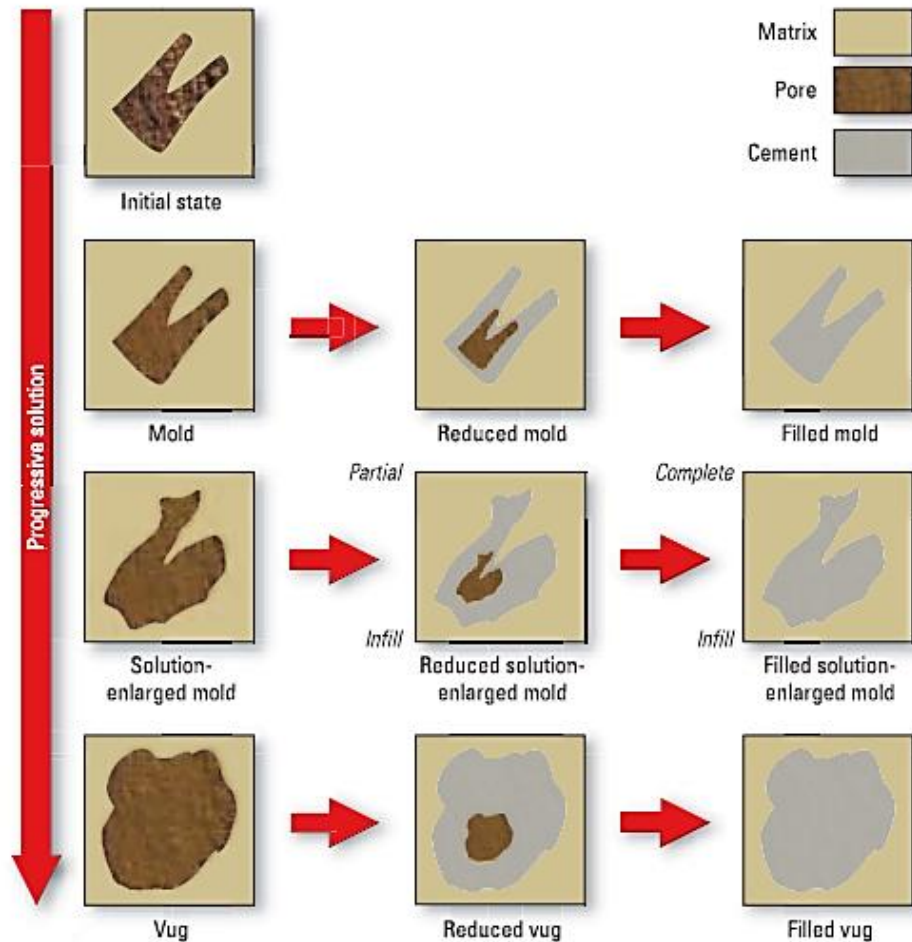


Figure 2.4.2.1 – Stages in the development of molds and vugs (Schlumberger, 2010)

### 2.4.3 Fractured porosity

Carbonate deposits are brittle substances. They do not bend easily in response to Earth movements but fracture and break. These fractures may range between tiny breaks invisible to the naked eye, to wide crevasses. Fractures create another version of secondary porosity. Most of Middle East carbonate reservoirs are present in such carbonate fractures.

Intense fracturing is present and affects the reservoir characteristics of some of the world's largest oil fields. While it is not always clear how much actual porosity is gained during the fracturing of carbonate reservoir rocks, because of the difficulty in measuring this type of porosity, there can be little doubt concerning the benefits that fractures can bring to ultimate reservoir production.

Fracturing is particularly effective and common in carbonate reservoirs because of the brittle nature of carbonates relative to the more ductile fine-grained siliciclastics with which they are often interbedded. Fracturing can take place at practically any time during the burial history of a carbonate sequence starting with shallow burial because of common early lithification. Fracturing can be associated with faulting, folding, differential compaction, solution collapse, salt dome movement, and hydraulic fracturing within overpressured zones (Lucia, 1999; Moore, et. al., 2001).

Fractures in carbonates are commonly filled with a variety of mineral species including calcite, dolomite, anhydrite, galena, sphalerite, celestite, strontianite, and fluorite (figure. 2.4.3.1). These fractures are, however, generally dominated by carbonate phases. Fracture fills are precipitated as the fracture is being used as a fluid conduit. CO<sub>2</sub> degassing during pressure release associated with faulting and fracturing in the subsurface can result in extensive, almost instantaneous calcite and dolomite precipitation in the fracture. These late carbonate fracture fills commonly have associated hydrocarbons as stains, fluid inclusions, or solid bitumen (Moore and Druckman, 1981).

Fracture porosity is exceedingly important porosity types in the subsurface. However, fractures generally enhance permeability rather than total porosity. Fracture porosity is generally only a small percentage of total reservoir porosity, but because the fractures are connected, the small fracture volume can contribute enormously to total permeability. If fracture porosity amounts only to about 1% in a thick and aerially extensive reservoir, fracture volume can be very large, justifying well spacing of hundreds to 1000 acres. A relationship between fracture porosity, fracture volume, and reservoir drainage area is shown in the figure 2.4.3.2.

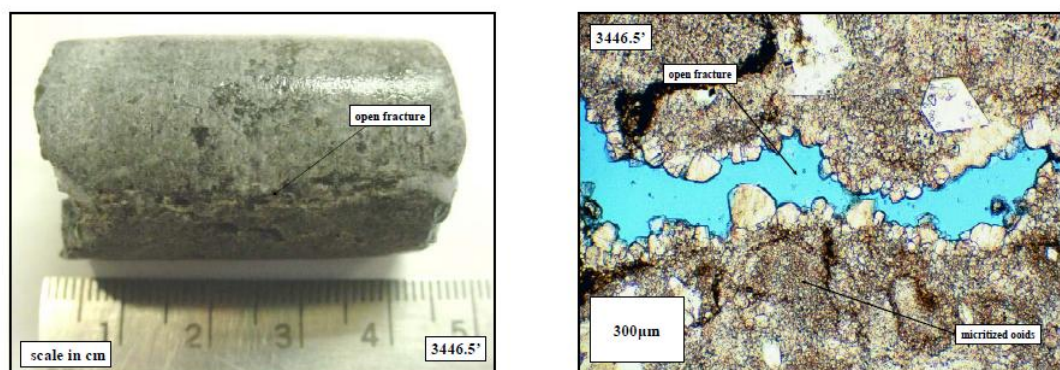


Figure 2.4.3.1 – Examples of fracture porosity in carbonate reservoirs (adopted from Lucia, 1999)

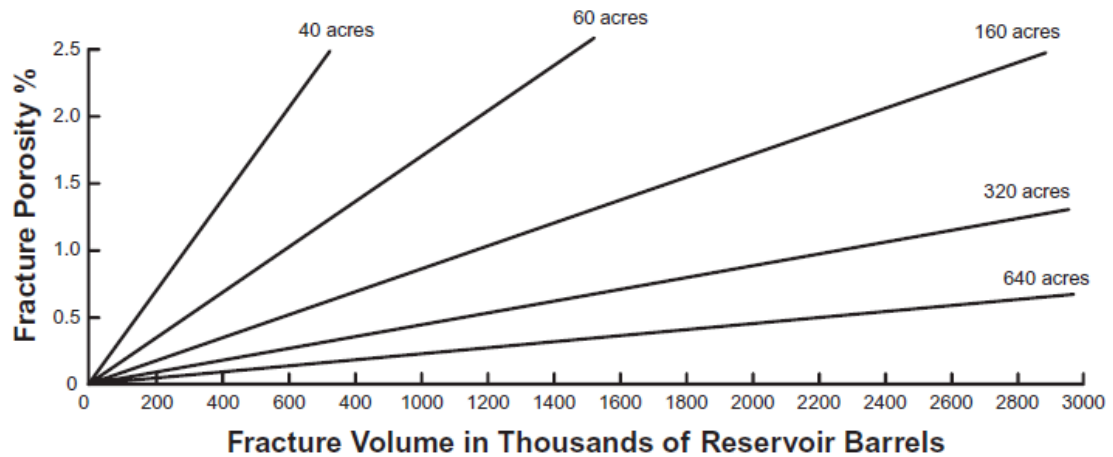


Figure 2.4.3.2 – Diagram illustrating the relationship between fracture porosity, fracture volume, and reservoir drainage area. Intuitively, smaller drainage areas have smaller fracture volume. (Ahr, 2008)

To sum up, the distribution of primary porosity, and often secondary porosity, is facies controlled. Rocks occur in characteristic assemblages or facies that are controlled by the depositional environment. Certain facies, such as reefs and fore reefs, have high primary porosities compared to other facies, such as fine-grained lagoonal deposits or outer-shelf carbonates. Therefore, to assess reservoir potential, geoscientists must conduct detailed studies of depositional environments (Archie, 1962; Ahr, 2008).

#### 2.4.4 Permeability

Carbonates are characterized by different types of porosity and have unimodal, bimodal and other complex pore size distributions, which result in wide permeability variations for the same total porosity, making difficult to predict their productivity (Lucia, 1999).

Permeability is important because it is a rock property that relates to the rate at which hydrocarbons can be recovered. Values range considerably from less than 0.01 millidarcy (md) to well over 1 darcy. A permeability of 0.1 md is generally considered minimum for oil production. Very high permeability through connected vugs and fractures is relatively common in carbonate rocks, notably in limestones rather than dolostones.



Permeability is expressed as specific permeability, effective permeability and relative permeability. Specific permeability is the permeability of a reservoir rock to a single fluid. It is measured on core samples, commonly by commercial laboratories. Effective permeability is a measure of the permeability to another fluid when the reservoir is already saturated, that is, the effective permeability to oil of a reservoir rock already saturated with water. The presence of a wetting fluid impedes the entry of a non-wetting fluid; therefore effective permeability is lower than specific or absolute permeability (Lucia, 1999).

Next to basic lithology, effective porosity and specific permeability are the most important variables used to describe reservoir rocks. Absolute permeability, or simply permeability, may vary directly with interparticle porosity in detrital reservoir rocks.

#### **2.4.5 Pore size and fluid saturation**

Pore-size is the common factor between permeability and hydrocarbon saturation. Permeability models have historically described pore space in terms of the radius of a series of capillary tubes. The number of capillary tubes has been equated to porosity so that permeability is a function of porosity and pore-radius squared (Al-Hanai, et. al., 2009)

It is common practice to estimate permeability using simple porosity permeability transforms developed from core data. However, porosity permeability cross plots for carbonate reservoirs commonly show large variability (figure 2.4.5.1), demonstrating that factors other than porosity are important in modeling permeability. In general it can be concluded that there is no relationship between porosity and permeability in carbonate rocks unless pore-size distribution is included (Lucia, 1999).

Hydrocarbon saturation in a reservoir is related to pore size as well as capillary pressure and capillary forces. For oil to accumulate in a hydrocarbon trap and form a reservoir, the surface tension between water and oil must be exceeded. This means that the pressure in the oil phase must be higher than the pressure in the water phase. If the pressure in the oil is only slightly greater than that in the water phase, the radius of curvature will be large and the oil will be able to enter only large pores. As the pressure in the oil phase increases, the radius of curvature decreases and oil can enter smaller pores (figure 2.4.5.2). It is shown that pore size is determined by grain size and sorting. (A) Only the largest pores contain oil at the base of the reservoir. (B)

Smaller pores are filled with oil as capillary pressure and reservoir height increase. (C) Smallest pores are filled with oil toward the top of the reservoir (Lucia, 1999).

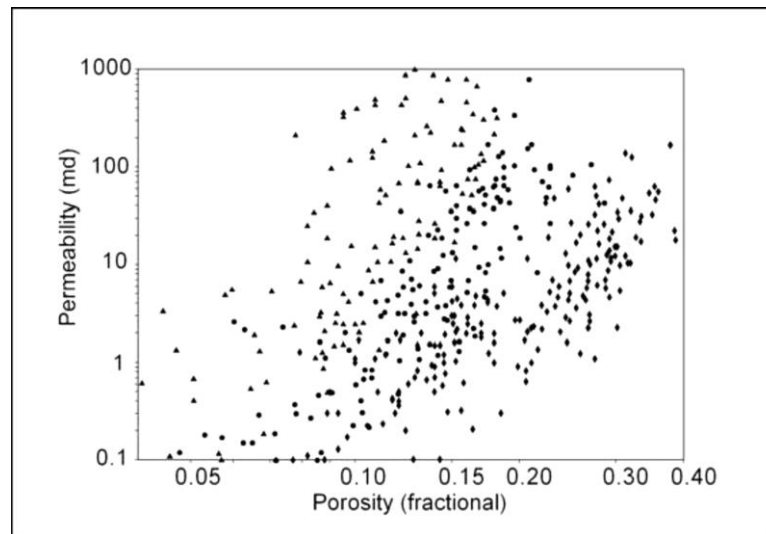


Figure 2.4.5.1 – Plot of porosity and permeability for carbonate rocks, illustrating that there is no relationship between porosity and permeability in carbonate rocks without including pore-size distribution. (Lucia, 1999)

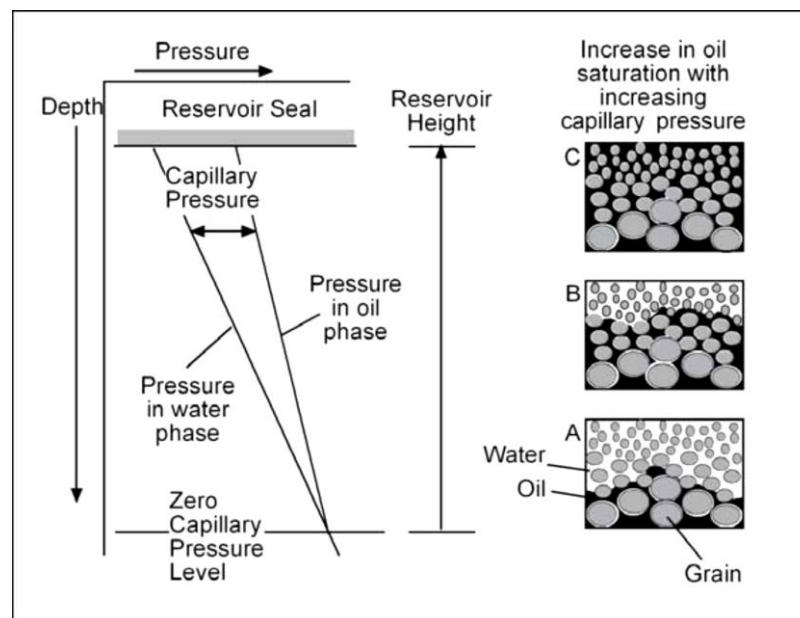


Figure 2.4.5.2 – Diagram showing smaller pores being filled with a non-wetting fluid (oil) displacing a wetting fluid (water) as capillary pressure increases linearly with reservoir height. (Lucia, 1999)



## 2.5 Diagenetic process

Once the sediments have been deposited, a range of chemical and physical processes begin to modify them – altering fundamental rock characteristics such as porosity and permeability. This is known as diagenesis.

Carbonate minerals more susceptible to dissolution, recrystallization, replacement than most siliciclastic minerals. Carbonate minerals may experience pervasive alteration of mineralogy. For instance, aragonite – calcite, dolomitization. These changes can alter or destroy original depositional textures. Porosity may be reduced or enhanced (Montaron, et. al., 2009).

After primary deposition of the original calcium carbonate bearing minerals changes during diagenetic process may result in dolostone formation, which are carbonate rocks composed almost entirely of dolomite –  $(\text{Ca,Mg})\text{CO}_3$ .

Two mechanisms of dolomitization of limestones have been proposed based on field and laboratory studies (Ahr, 2008).

- **Evaporative Reflux.** This mechanism involves the evaporation of seawater to form brine that precipitates gypsum. After precipitation of gypsum, the brine is both enriched in Mg relative to Ca and has a higher density. If the brine then enters the groundwater system and moves downward into buried limestones. This Mg-rich brine then reacts with the calcite in the limestone to produce dolomite.
- **Mixing of Seawater and Meteoric Water.** This mechanism involves the mixing of groundwater derived from the surface with saline groundwater beneath the oceans. Dolomitization is thought to occur where the two groundwater compositions mix with each in the porous and permeable limestone within a few meters of the surface.

Therefore, good porosity in carbonate reservoirs is often a result of recrystallization and, most commonly, dolomitization. In the Middle East region, approximately 20% of hydrocarbon reservoirs are dolomites. The replacement of calcium carbonate by magnesium carbonate involves a 12.3% decrease in volume (and equivalent increase in porosity) if the replacement is molecule for molecule. In many fields with partially dolomitized carbonate reservoirs; the oil is restricted to the dolomitized sections. The selective nature of dolomitization extends to its effects on the skeletal components of the carbonate sediment. Aragonite is much more easily dolomitized than calcite, so the shells of gastropods, cephalopods and corals are dolomitized earlier than those of brachiopods, ostracods or echinoderms. Calcareous algae are easily dolomitized because high-magnesium calcite is deposited on them during their lives, and the

algae themselves reduce the sulfate that would otherwise inhibit the dolomitization process. The vast mats of algae in the epicontinental seas of the great Paleozoic transgressions are undoubtedly a factor in the prevalence of Paleozoic dolomites. There is very little dolomite in the stratigraphic record since the Cretaceous (Harris, 1984; Scott, 1990; Murris, 1980).

## **2.6 Reservoir potential. Seals and traps**

The final step in describing carbonate rock as a potential reservoir for oil and gas after determination of properties is a whole consideration of formation on order to estimate the presence of potential oil trap. So trap is a part of the reservoir, where conditions of occurrence and relationship with shielding rocks provide the possibility of accumulation and long-term conservation of oil and gas. The elements of the traps are:

- porous reservoir rock to accumulate the oil and gas – in this case, limestones and dolomites.
- overlying impermeable rock to prevent the oil and gas from escaping – seal or cap.
- source for the oil and gas, typically black waxy shales.

A trap forms when the buoyancy forces driving the upward migration of hydrocarbons through a permeable rock cannot overcome the capillary forces of a sealing medium. The timing of trap formation relative to that of petroleum generation and migration is crucial to ensuring a reservoir can form.

There are three main types of traps that are based on their geological characteristics: the structural trap, the stratigraphic trap and the far less common hydrodynamic trap. The trapping mechanisms for many petroleum reservoirs have characteristics from several categories and can be known as a combination trap.

Structural traps are formed as a result of changes in the structure of the subsurface due to processes such as folding and faulting, leading to the formation of domes, anticlines, and folds. Examples of this kind of trap are an anticline trap, a fault trap (figure 2.6.1) and a salt dome trap. They are more easily delineated and more prospective than their stratigraphic counterparts, with the majority of the world's petroleum reserves being found in structural traps. Where rock layers are folded into anticlines and synclines, the oil and gas migrates to the crests of the anticlines

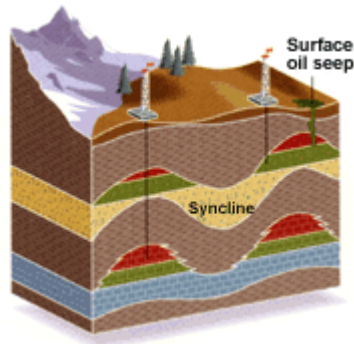
within the reservoir rock, and are trapped if overlain by an impermeable layer. If fractures occur, oil and gas may seep to the surface.



Fold (structural) trap



Fault (structural) trap



Anticlinal trap

Figure 2.6.1 – Structural traps (Discovery Drilling Funds, 2005)

Stratigraphic traps are formed as a result of lateral and vertical variations in the thickness, texture, porosity or lithology of the reservoir rock (figure 2.6.2). Examples of this type of trap are an unconformity trap, a lens trap and a reef trap.

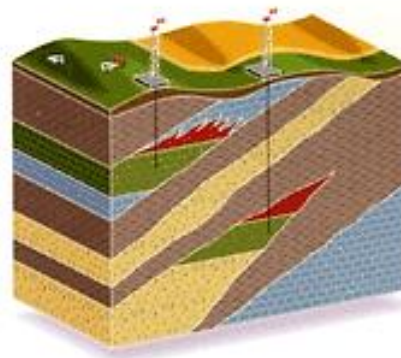


Figure 2.6.2 – Stratigraphic Pinch-Out trap: limestone reservoir loses its porosity and becomes impermeable limestone (Discovery Drilling Funds, 2005)

The unconformity trap is that where the hydrocarbons can be trapped below the unconformity by truncation, or above the unconformity when a porous bed onlaps against the unconformity

surface. Often a structural element such as tilting is required, so many of these traps can be considered combination traps (Harris, 1984).

The process most favorable to leaching is a marine regression that allows the exposure of carbonates to meteoric waters. Subsequent transgressions bury the weathered, fractured zone characterized by high solution porosity below an unconformity or at a depositional break. Nearly all of the oil in the Middle East's limestone reservoirs is pooled in this type of reservoir and trap (Skelton, et. al., 1990).

Diagenetic traps are a subtype of stratigraphic traps. These are more common in carbonate reservoirs which are more easily affected by cementation, dissolution and dolomitization (figure 2.6.3). These post-depositional processes lead to a lateral change in reservoir quality to acts as the trapping mechanism (Scott, 1990).

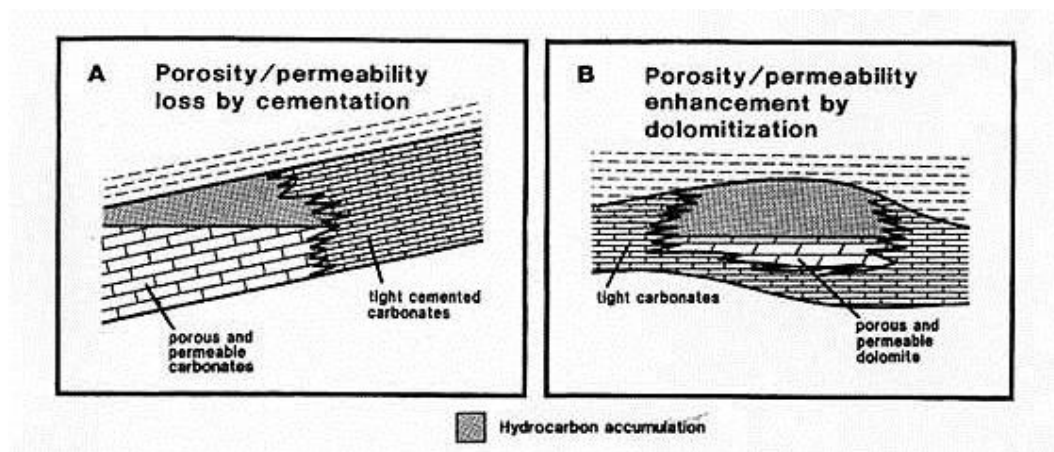


Figure 2.6.3 – Secondary diagenetic stratigraphic traps. A – Traps were created by post-depositional updip porosity occlusion. B – Traps were created by post-depositional porosity and permeability enhancement (Archie, 1952).

Sedimentological traps are also the subtype of stratigraphic traps. Several depositional systems produce isolated bodies of porous rock surrounded by impermeable rock. The most well-known examples in carbonate reservoirs are reefs within lagoonal and marine shales. Porous ancient coral reefs grew in the warm seas. They provide prolific oil and gas reservoirs. Often overlying porous rock layers are "draped," or folded over the reefs and form separate traps. Overlying impermeable rocks act as seals to the reservoirs (figure 2.6.4).

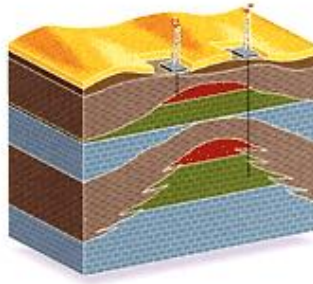


Figure 2.6.4 – Stratigraphic sedimentological trap – reef (Discovery Drilling Funds, 2005)

Hydrodynamic traps are a far less common type of trap. They are caused by the differences in water pressure that are associated with water flow, creating a tilt of the hydrocarbon-water contact.

The seal is a fundamental part of the any type of trap that prevents hydrocarbons from further upward migration. A capillary seal is formed when the capillary pressure across the pore throats is greater than or equal to the buoyancy pressure of the migrating hydrocarbons. They do not allow fluids to migrate across them until their integrity is disrupted, causing them to leak. There are two types of capillary seal whose classifications are based on the preferential mechanism of leaking: the hydraulic seal and the membrane seal (Halliburton, 2001; Gluyas, Swarbrick, 2004).

The membrane seal will leak whenever the pressure differential across the seal exceeds the threshold displacement pressure, allowing fluids to migrate through the pore spaces in the seal. It will leak just enough to bring the pressure differential below that of the displacement pressure and will reseal (Gluyas, Swarbrick, 2004).

The hydraulic seal occurs in rocks that have a significantly higher displacement pressure such that the pressure required for tension fracturing is actually lower than the pressure required for fluid displacement – for example, in evaporates or very tight shales. The rock will fracture when the pore pressure is greater than both its minimum stress and its tensile strength then reseal when the pressure reduces and the fractures close (Gluyas, Swarbrick, 2004).

Over geological time the Middle East region has passed through the equatorial belt a number of times. Optimum conditions for reef growth occurred during the Precambrian, Jurassic, Cretaceous and Middle Tertiary.

During the Miocene, between 5 M and 20 M years ago, abundant coral structures formed at shallow depths. For example, In the Red Sea, Miocene oil accumulation occurred when

evaporates were deposited on the reef, forming an excellent seal, trapping hydrocarbons in the porous reef rock. Tertiary rocks contain many of the most productive reefs found In the Middle East. The reefs of the Precambrian also contain important oil accumulations. However, some patch reefs occur in the Jurassic. These small carbonate structures were scattered across the shallowest parts of the continental shelf. The patch reefs provide good reservoirs on salt domes and anticlinal structures (Harris, 1984; Tucker, 1990).

### **3 PROSPECTING METHODS AND INTEREST VARIABLES**

The determination of hydrocarbon in place and technically recoverable reserves requires the implementation of a data acquisition scheme. The degree of understanding of reservoir continuity and properties should improve with each well drilled but will always be a subject of uncertainty.

The data collected in the pre-development, reservoir appraisal and delineation stage needs careful planning and coordination in order to extract the maximum information. The basic step in reservoir characterization is the obtaining field information. The further stages of exploration work at the reservoir or deposits directly depend on the quality of morphological, lithological and petrophysical information.

The complex investigation of carbonate hydrocarbon reservoirs via geological, geophysical and field methods has a great scientific and practical importance. The role of geophysical prospecting technics is essentially increasing when carbonates rocks are investigated because core collected not from the whole thickness of rock does not provide their authoritative description. Petrophysical measurements provide a basis for quantifying geological descriptions. Usually these measurements and descriptions are expanded in one dimension by detailed sampling of core material. However, cores are normally available from only a few wells, whereas wireline logs are available from most wells. Therefore, using correlation methods is preferably in order to associate the facies descriptions with wireline logs and core data. Such methods as drilling time logs, drill cuttings, mud logging and measurements while drilling represent the earliest information available, and can help in determining intervals for coring, thicknesses of porous, hydrocarbon bearing layers, the lithology of the section, and possibly the type of hydrocarbon (Halliburton, 2001).

Sidewall cores and core samples give information about lithology pore structure, porosity, permeability, and may help to determine depositional environments, fluid saturations and hydrocarbon type. Special core analysis techniques will indicate recovery potential (Levyant, 2010).

Bore-hole surveys: logs, wireline tests provide gross and net section thicknesses, water contacts, dips and, under favorable conditions, porosities and fluid saturations. Permeable intervals and movable hydrocarbon may be detected, and velocity data for seismic interpretation is obtained. The Repeat Formation Tester (RFT) tool can give valuable information on pressures and

zonation. Logs may be open hole or cased hole production logs (Archer, 1986; Gluyas, et. al., 2004).

Well tests and fluid sampling. generally conducted in cased hole, represent hydrocarbon type and fluid samples and give information about initial reservoir pressure, pressure gradients, permeability, thickness estimates, and well productivities.

There are a number of parameters that are needed by the exploration and development and production of a formation. These parameters are provided from a number of different sources including, seismic records, coring, mud logging, and wireline logging (Archer, 1986). Based on the abovementioned there are some main source of obtaining geological information – core sampling and analysis, geophysical well logging and seismic. The initial information for the case study of this work was also provided by these methods.

### **3.1 Core description**

The first step in quantifying a geologic model is the rock description from core material. The best sampling method is to drill 1-inch-diameter core plugs for analysis from every foot of core and to prepare a thin section from the end pieces for detailed rock description. Basic petrophysical quantification, lithology, dolomite crystal size, fabric, petrophysical class, amount and type of vugs are obtained from core description. Supplementary information includes grain types and visible interparticle porosity, is best obtained from thin sections.

Cores provide an opportunity to study the nature of the rock sequence in a well. They will provide a record of the lithology encountered and can be correlated with wireline logs. Study of the bedding character and associated fossil and microfossil record may provide an interpretation of the age and depositional environment Petro-physical measurements of porosity and permeability from samples of the recovered core allow quantitative characterization of reservoir properties in the well section. Samples from the recovered core are also used to study post depositional modification to the pore space (diagenetic studies), flow character of the continuous pore space (special core analysis studies) and character of recovered fluids and source rocks (geochemical studies) (North, 1985). The diversity of information that can be obtained from recovered core implies that a number of specialists are involved in assembling a coring program for a new well – each specialist wishing to ensure that samples are obtained



under the best possible conditions (Harris, 2010). In the figure 3.1.1 the examples of core samples is shown.

The base for determining the calculation parameters is a petrophysical relation found in the process of core description in the laboratory. Obtaining reliable petrophysical relationships for carbonate reservoirs can be achieved only with a representative core sample of sufficiently large dimensions with remaining natural structure of the pore space. This is especially important for the cavernous reservoirs in which the ratio of interstitial pores and cavities should be preserved, as in natural conditions.



Figure 3.1.1 – The examples of core sampling of carbonates (Western Siberia) (TNK, 2005)

The physical properties of reservoir rocks are largely determined by the geometry of the pore space, pore shape parameter is a quantitative expression of it. The investigation of relations between the shape pore parameter and petrophysical properties of carbonate rocks (density, porosity, permeability, electrical resistivity) makes it possible to separate the types of reservoirs in dependence on the structure of the pore space.

Changings of hydrostatic pressure, formation pressure and temperature associated with core sampling, accompanied by deformation of the carbonate rocks and alteration of their physical

properties. The scale of the alteration depends on clay content and structure of the pore space, characterized by fractured, vugs and intergrain porosity. In the rocks with a homogeneous structure of the pore space changes of petrophysical characteristics under the influence of temperature and pressure factors are small and it can be neglected by a first approximation. In reservoirs with complex geometry since the changes are more significant and may lead to a systematic error in the determination of reservoir properties from laboratory dependences obtained without taking into account reservoir pressures and temperatures (North, 1985; Harris, 2010).

Accurate estimation of parameters of carbonate reservoir depends on accuracy determination of its type. Simultaneous analysis of core and geophysical well logging give an opportunity to provide full characterization of complex carbonate reservoirs.

### **3.2 Seismic surveys**

The reliability of geophysical surveys, particularly seismic, has greatly reduced the risk associated with drilling wells in existing fields, and the ability to add geophysical constraints to statistical models has provided a mechanism for directly delivering geophysical results to the reservoir model.

Most reservoir characteristics are based on reflection seismic data, although a wide variety of other techniques are employed regularly on specific projects. Almost all seismic data collected for reservoir studies is high-fold 3-D vertical-receiver data; however, the use of converted-wave data with multiple component geophones on land and on the sea floor, and multicomponent source (on land) is increasing. The importance of fractures in carbonate reservoir development schemes has led to a number of experimental programs for multicomponent sources and receivers in an effort to identify shear-wave splitting (and other features) associated with high fracture density. Some of these techniques will find continually increasing application in the future, but at the present, most surface seismic studies designed to characterize existing reservoirs are high-quality 3-D vertical-component receiver surveys (Pennington, 2001; Sheriff, 1992).

Carbonate fractured cavernous reservoirs undoubtedly constitute complex subsurface environment. In recent years, positive experience has been accumulated in the use of the results

of seismic surveys for estimation of reserves and substantiation of development parameters in the conditions of such carbonate sections. The use of special processing techniques, different types of inversions of seismic data, seismic facies analysis, estimation and analysis of certain seismic attributes allow performing more accurate mapping of surfaces associated with top or base of the reservoir, identifying local bodies and predicting the permeability and porosity properties of fractured-cavernous type of carbonate reservoirs (Montaron, et. al., 2009).

Main geological problems, with which the seismic faced with because of specific conditions of the carbonate reservoirs, are mapping of the top and bottom of the carbonate reservoir, lithology differentiation and properties prediction (Archer, 1986).

At the interpretation stage of the morphology (top and bottom) of carbonate reservoirs the main problem is a multiple correlation (Gluyas, Swarbrick, 2004). The target reflections are almost always characterized by low amplitudes, the interference decay and seismic event discontinuities that make the interpretation process more. The main reason related to the specialty of the structure and formation derivations of carbonate reservoirs. Last research suggests that the implementation of cube acoustic impedance as an interpretation base leads to more reliable correlation and more confidence differentiation of the organic structures (Levyant, 2001)

Another problem is an existence of velocity anomalies. The basic strategy of its resolution is an integrated approach of using of all geological and geophysical information in the velocity model formation (Montaron, et. al., 1996).

The second important geological task for seismic is lithology differentiation. Seismic facies analysis may be performed as the initial stage of interpretation, as in a detailed studying. In the first case, despite the fact that great carbonate facies variability is a complicating factor of the seismic correlation process, it can also be the key of interpretation. In the case study of a local object seismic facies analysis allows to reveal the zonality within the reservoir related to various reservoir properties (Levyant, 2001). In the figure 3.2.1 the example of seismic facies analysis of the form seismic traces is shown.

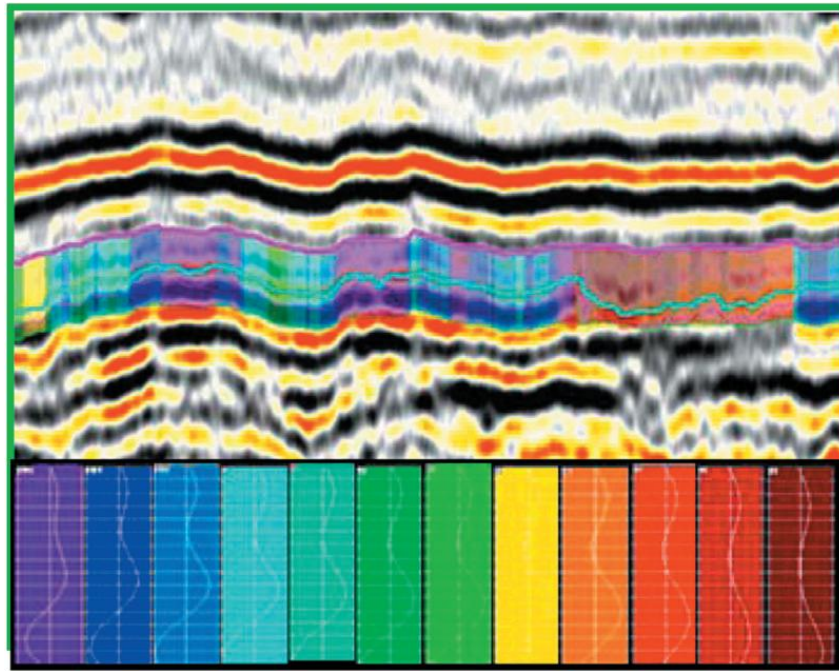


Figure 3.2.1 – The example of seismic facies analysis of the form seismic traces (Levyant, 2010)

The third geological problem is the prediction of properties, specifically porosity and permeability as key properties in the case of the carbonate reservoirs. Most existing approaches can be classified into two groups: 1 - it recounts based on both linear and multidimensional dependence and forecast properties by the technology of neural net sometimes called a direct prognosis. Such solutions can be implemented as on a dynamic phase of interpretation, and on the stage of the geological modelling as well (Archer, 1986).

For porosity prediction the inversion technology of seismic data provide optimal results. As the porosity and permeability of carbonate reservoirs are connected with the fissility of rocks the seismic methods are used to its investigation. The approach of the fissure and cavity study depends on its size. There are two areas: interpretation of fissure system that are greater than seismic wave, and interpretation of micro-fissures that are comparable with the length of the seismic waves. In the first case the geometric attributes is applied, for the second – methods of analysis of the azimuthal anisotropy of kinematic and dynamic characteristics of the wave field (Endres, Lohr, et. al., 2008).

The inferred geometric attributes traditionally include the angle of gradient, azimuth, and azimuth of gradient angles, angle of flexure and their modifications. Such geometric attributes have become standard and provides stable fissures mapping. Under favorable conditions it is possible to determine low-amplitude disturbances, lineaments and zones possibly related with

increased fracturing. The most efficient is use a combination of various attributes, and the classification methods (Sheriff, 1992; Pennington, 2001).

The great interest represents the integration of the fracturing and fissuring at the stage of geological modeling. The reference information point for modeling of fractures and fissures is a well data. Interpretation results of Formation Micro Imager (FMI) technology (figure 3.2.2) allows highlight main areas of micro-fissuring. Spatial information about the main directions of fracturing can be found of the seismic data, using the possibilities of the coherence cube technology. The obtained data about fracturing and fissuring may be used for further modelling of attributes. (Singh, 2001)

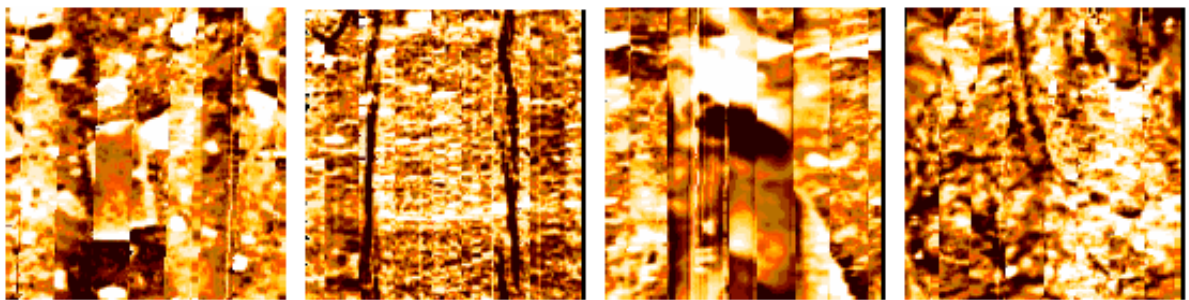


Figure 3.2.2 – Example of FMI images (Schlumberger, 2009)

Analysis of current investigation approaches and technology of complex carbonate environments suggests that there is a sufficiently rich arsenal of tools to solve the most complicated geological problems, and a plenty of practical examples convince the feasibility of their usage. All of these techniques focused on fundamental study of geological environment that provide a more detailed geological field model, which in turn allows to optimize the further development, minimize operating costs, increase a production and extend the exploitation period of a field as well.

### **3.3 Geophysical well logging**

Geophysical well logging is used to solve geological and engineering problems. In the first place geological issues include lithological determination of the facies and layers, their correlation, identification of minerals and estimation of the parameters needed for the calculation of reserves. The technical objectives include the study of geological and hydrogeological characteristics of

the reservoirs, the study of the technical condition of wells, monitoring the development of hydrocarbons.

The complexity conditions of the reservoir geometry require a comprehensive study of the physical properties. In this regard, there are a large number of geophysical well logging techniques, which combine several groups. The main ones are electrical, electromagnetic, nuclear physics, and acoustics methods. There are also thermal, magnetic, gravity, mechanical, and geochemical methods.

Effective solution of geological and technological challenges can only be based on an integrated application of geophysical methods with different petrophysical basis (electrical, nuclear, acoustic, etc.). The similarity of problems and solutions for different regions allows the model complex geophysical researches of wells drilled with the purpose of searching and exploration of similar minerals. In order to improve the effectiveness of geophysical methods a combination of such technological measures as changing wellbore fluid, increasing the diameter wells (drilling), hydrodynamic stimulation, and injection of tracer fluid is used. Analyzing the changes of geophysical parameters over time, it is possible to determine the true nature of the saturation recovery and to evaluate their initial and residual oil-and-gas content. A growing body of well logging, the complexity of the geological problems led to the development of systems of interpretation of complex data. These systems provide a preliminary assessment of the quality and selection of materials, the dismemberment of the section, the definition of bed boundaries, the allocation of mineral resources, evaluation of productivity of deposits (Sheriff, 1992).

Log measurements, when properly calibrated, can give the majority of the parameters required. Specifically, logs can provide a direct measurement or give a good indication of: porosity, both primary and secondary; permeability; water saturation and hydrocarbon movability; hydrocarbon type; lithology; formation dip and structure, sedimentary environment and also travel times of elastic waves in a formation. These parameters can provide good estimates of the reservoir size and the hydrocarbons in place.

Determining the correct lithology – be it limestone, dolomite or a combination of minerals is an important step in carbonate reservoir evaluation (Ramamoorthy, et. al., 2010). Lithology establishes the matrix density, or grain density, used for computing porosity from density tools. It is also an input for other porosity measurements, such as those from thermal and epithermal neutron measurements. An accurate porosity value is a crucial input for calculating water and hydrocarbon saturations, determining total fluid volumes and estimating reserves.

Porosity is a basic petrophysical measurement, usually obtained from well logs. It is commonly computed from bulk density data. Density porosity is sensitive to both the pore fluids and the matrix, especially the matrix. There are several methods available for computing porosity, and these often are affected by the fluids in the rock and the mineralogy. Depending on environmental conditions and operational constraints, integrating these measurements plays a role in decoupling the effects of the matrix on the porosity value.

Examples of porosity measurements include those from lithology-dependent thermal neutron, lithology-independent neutron, acoustic, thermal neutron capture spectroscopy and nuclear magnetic resonance (NMR) tools. Neutron and NMR porosity tools are blind to the presence of gas. NMR measurements are also blind to porosity filled with tar, bitumen, microporosity-bound water and hydrates.

Perhaps the most common lithology-determination method from logging data uses the photoelectric effect (PEF) measurement, which responds primarily to the minerals in the formation. This measurement is routinely acquired using formation density devices, such as the Litho-Density and LWD density tools (Ramamoorthy, et. al., 2010). Although useful in differentiating pairs of minerals among sandstone, limestone, dolomite and anhydrite, additional measurements are required when more than two minerals are present. Also, the measurement is affected by barite in drilling-mud systems, and borehole conditions such as thick mudcake and hole rugosity may render it useless.

A better method for solving complex lithologies and determining mineralogical concentrations, which may vary widely across a field depending upon the diagenetic history and fluids percolating through the reservoir, is an elemental thermal neutron capture spectroscopy measurement. For example, the ECS elemental capture spectroscopy and the LWD EcoScope tools (figure 3.3.1) offer this type of measurement. These tools measure the concentrations of specific elements that correspond to mineralogy. Various matrix properties can also be computed from the yields, including grain density. Grain density represents an effective matrix density and varies according to the elements present in the formation. It yields more accurate density porosity than when computed using a fixed-value matrix density. Texture and pore geometry are also important properties for identifying reservoir-quality rock because knowledge of correct mineralogy and porosity measurement alone is not sufficient to infer flow characteristics in carbonate reservoirs (Montaron, Stundner, Zangl, et. al., 2009).

In fact, some experts believe that characterization of pore geometry is the most important component in carbonate evaluation (Archie, 1952). Complex pore shapes and sizes often result



from reservoir deposition and the ensuing processes of dissolution, precipitation and recrystallization. Although time-consuming, core analysis can reliably identify and quantify pore geometry. The standard resistivity and porosity measurements of a triple logging suite often do not respond to changes in pore size and texture. NMR data, however, have been shown to identify changes in pore size distribution not detectable by these conventional logs (figure 3.3.2) (Montaron, et. al., 2009; Leviant, 2010).

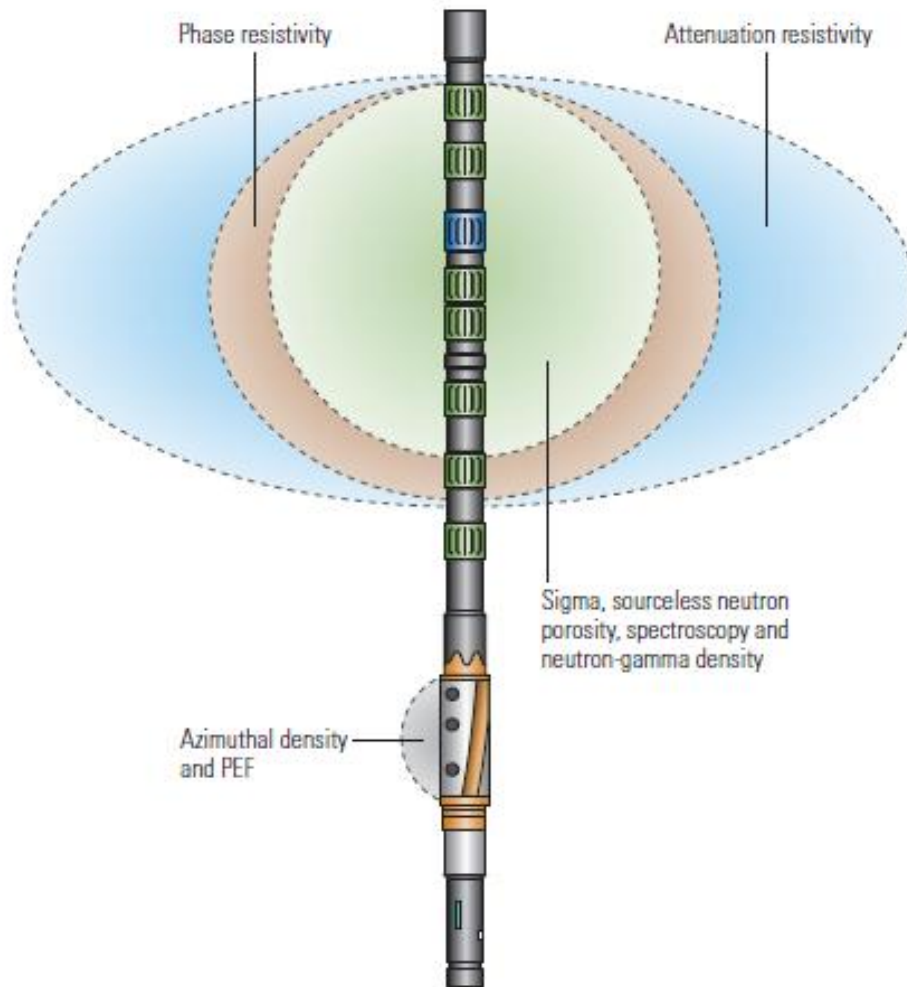


Figure 3.3.1 – EcoScope LWD tool. The EcoScope tool incorporates resistivity, neutron porosity, sigma and neutron capture spectroscopy sensors into a single compact device. Wireline and LWD tools generally use chemical sources for neutron porosity and neutron capture spectroscopy measurements. The EcoScope tool generates neutrons with a pulsed-neutron generator that operates only when mud is being pumped through the tool (Schlumberger, 2010)



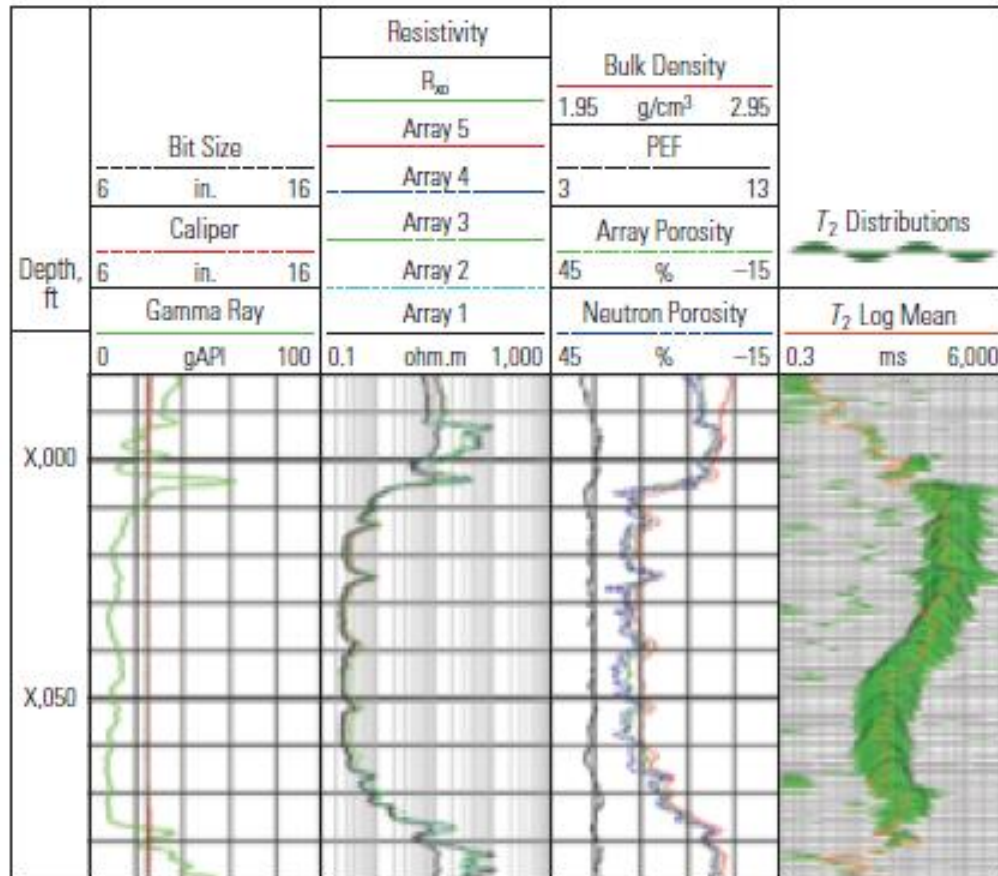


Figure 3.3.2 – Pore size and geometry. Measurements from NMR logging tools are more sensitive to pore size and geometry than are resistivity and other porosity measurements. The gamma ray log (Track 1), resistivity logs (Track 2) and porosity measurements (Track 3) are consistent throughout the interval shown. The NMR data (Track 4) indicate a large increase in pore size above X,040 ft that is not seen in the other measurements (adapted from Ramamoorthy, et. al., 2010)

Complexity of porous structure and among variety of carbonate reservoirs and phenomena associated with them create difficulties in productive layers determining in carbonate formations and in estimation of reservoirs properties. Therefore for the investigation of carbonate reservoirs it is necessary to use such geophysical prospecting methods and interpretation methodology that taking into account specific conditions of carbonate formations (Sheriff, 1992). In order to provide accurate reservoir description it is necessary to combine and take into account all geological and petrophysical information derived from different sources.

## **4 MODELLING METHODOLOGY**

A model of an oil reservoir is a spatial representation of lithologies, faces and /or petrophysical properties such as porosity, permeability for a particular application. In the petroleum industry, modelling is carried out from the evaluation of reservoir rock potential to enhanced oil recovery level.

The complexity encountered in carbonate rocks are mainly due to the heterogeneity of these systems combined with sparse sampling of data constraining reservoir geometries and properties. In carbonates, heterogeneity is caused by highly variable in situ biological growth and sedimentation processes, as well as subsequent alteration by diagenetic overprinting. The latter often occurs along fluid migration pathways, in turn determined by depositional architecture (Wayne M. Ahr., 2008).

Due to the complexity of the internal behaviour of most carbonate rocks, their heterogeneity and uniqueness conditions of filtration these fluids have a selection of collector layers, the calculation of reserves oil and gas field development management is a difficult issue. For solving these problems computer geological reservoir modelling via geostatistical approaches gives new possibilities.

### **4.1 Workflow description**

In this work the attempt of building geological model of carbonate reservoir was made by geostatistics modelling approaches. It encompasses data analysis, estimation of the top and bottom of the layers (morphological model), simulation of lithoclasses within the selected layers, simulation of permeability and porosity and a final geobody analysis defined by threshold values in permeability. These main steps are presented in the workflow of the figure 4.1.1.

The initial step of the work is data analysis. The original data is represented by set of values of porosity (Phie) and permeability (LDperm) received from geophysical logging of 19 wells and main lithological description of lithofacies composing of three layers of carbonate reservoir. In order to prepare this data for further modelling process, at the beginning of the work the univariate data analysis by calculation of the main statistics parameters was carried out along with basic data verification and grouping.

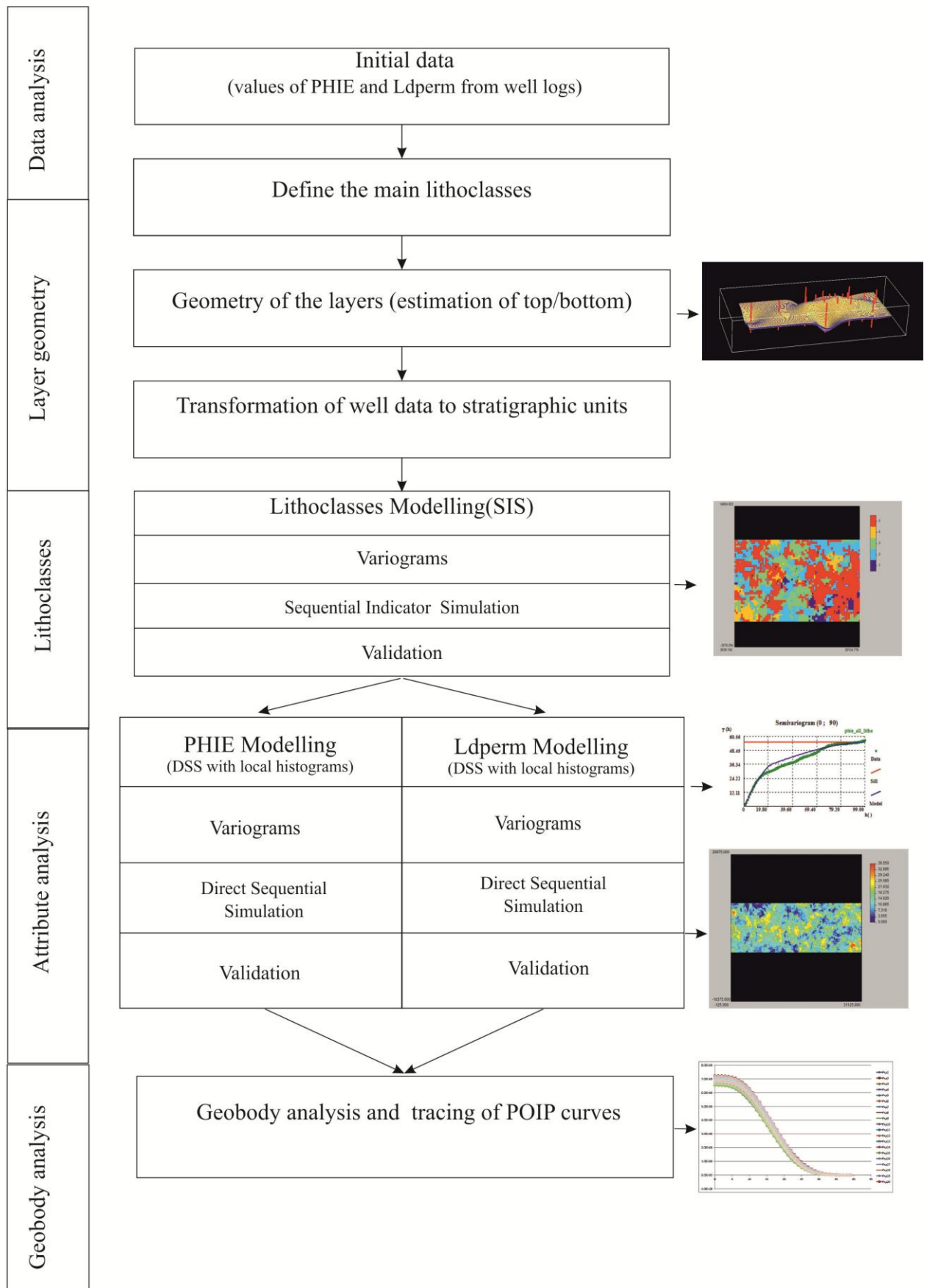


Figure 4.1.1 – Basic scheme of modelling process presented in this work: SIS – Sequential Indicator Simulation; DSS – Direct Sequential Simulation; POIP – Potential Oil in place

According to the initial values of porosity and permeability and basic lithological descriptions of presented layers from cores the main groups of lithoclasses were determined for further more clearly arranged statistical description of the reservoir.

As preparatory stage of simulation process the morphology and geometry of all layers were estimated according to initial coordinates and values of depth of the each layer. The top and bottom of each layer were estimated via ordinary kriging.

Another important preliminary step is the transformation of the data into a stratigraphical referential, instead of a simple depth referential. On this step, all lithoclasses and porosity and permeability values available from well data within the studied layer were transformed into a stratigraphical referential according the high depth of the layer (see figure 4.1.2). By this simple transformation a regular set of values for modelling was created and after modelling, a back transformation to the initial referential is required.

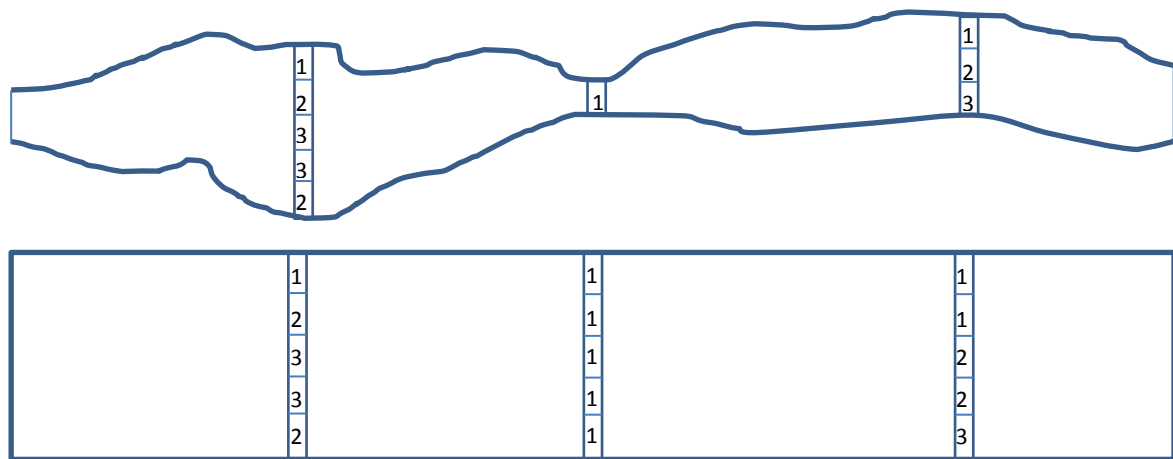


Figure 4.1.2 – Example of transformation into a stratigraphical referential

All next stages in the work are directly process of simulation of reservoirs lithology and properties. For lithoclasses the algorithm of Sequential Indicator Simulation (SIS) was used. It includes three key steps: variograms calculation and fitting of a theoretical model, simulation and validation of results.

After the simulation of the lithoclasses, simulation of the attributes porosity and permeability was carried out by Direct Sequential Simulation (DSS) with local histograms. DSS with local histograms generates the simulated images in a unique step, instead of a set of conditional images to lithoclasses and merge at the end. Simulation for both porosity (phie parameter) and permeability (Ldperm parameter) were also performed in three key steps: variograms calculation and fitting of a theoretical model, simulation and validation of results.

In order to complete the carbonate reservoir model and estimate the content of potential oil volume in the carbonate layers a geobody analysis was carried out by tracing of Oil-in-place curves according to previous simulated values of porosity and permeability of the reservoir layers.

Theoretical background for these methods is presented in the followings subchapters.

## **4.2 Background of geostatistics**

Geostatistics is a branch of statistics for geosciences focused on spatial data sets. As all geological reservoir characteristics have some level of heterogeneity, the building of 3D geologic model is a suitable solution for operating with the large amounts of data, providing its consistent analysis in three dimensions. It is also the rational approach for direct numerical input to flow simulation and pore volume calculations in reservoir management. The numerical models also give an opportunity to test or visualize multiple geologic interpretations and estimate the uncertainty of obtained geological data.

Geostatistics is related to interpolation methods, but extends far beyond simple interpolation problems, relying on the random variables theory to model the uncertainty associated with spatial estimation and simulation. Geostatistics goes beyond the interpolation problem by considering the studied phenomenon at unknown locations as a set of correlated random variables (Isaaks and Srivastava, 1989). By geostatistics techniques values of variable distributed in space or time can be analysed and/or predicted. Basically, include data analysis, spatial analysis (variograms calculation and modelling) and prediction technique (kriging estimation and simulation methods).

According to above mentioned information a base of geostatistics is a random variable  $Z(x)$ . A random variable ( $Z$ ) is a variable that can assume a set of values ( $z$ ) according a distribution law which allows us to understand and model the spatial variability. The random variable ( $Z$ ), or more specifically the distribution law, is dependent of the location, and that's why it is usual to present  $Z(u)$  associated to a location  $u$ . The random variable is also dependent of the known information, which means, the distribution law changes when the information of the not sampled location  $z(x)$  increases.

A random variable can be of two types: continuous – variables that can assume an infinite number of real values (for example, temperature or chemical grades, porosity, permeability and

density, thickness and depth) and categorical – when can be assume a discrete set of numeric values or disjunctive categories (lithology, colours, weathered level).

The cumulative distribution function (*cdf*) of a continuous random variable  $Z(u)$ , can be expressed by:

$$F(u; z) = Prob\{Z(u) \leq z\}$$

When the *cdf* is presented for a location  $u$ , taking into account a set of  $n$  neighbour samples of location  $u$ ,  $Z(u_\alpha) = z(u_\alpha)$ ,  $\alpha = 1, \dots, n$  it is used the designation “conditional to”:

$$F(u; z|(n)) = Prob\{Z(u) \leq z|(n)\}$$

In geostatistics, most of the information related with an unsampled location  $z(u)$  is given by the neighbour samples  $u'$  of the same attribute  $z$  or another  $y$  if correlated. Thus, it is important to model the correlation or dependence between the random variables  $Z(u_\alpha) = z(u_\alpha)$ ,  $\alpha = 1, \dots, n$  and  $Z(u_\alpha) = z(u_\alpha)$ ,  $\alpha = 1, \dots, n$ ,  $Y(u_{\beta'}) = y(u_{\beta'})$ ,  $\beta' = 1, \dots, n'$ .

A random function is a set of random variables defined for the same area in study  $\{Z(u), u \in \text{study area}\}$ .

As a random variable is characterized by their *cdf*, a random function is characterized by the set of  $K$ - *cdf* given for  $K$  locations,  $k = 1, \dots, K$ .

$$F(u_1, \dots, u_k; z_1, \dots, z_k) = Prob\{Z(u_1) \leq z_1; \dots; Z(u_k) \leq z_k\}$$

As a univariate *cdf* of the random variable  $Z(u)$  is used to characterize the uncertainty of  $z(u)$ , the multivariate *cdf* is used to characterize the joint uncertainty of the  $K$  values  $z(u_1), \dots, z(u_k)$ .

The geostatistical methods suggest that the random variables simultaneously present a random pattern, which means, for small distances random variations exists; a structured pattern and, therefore, predictable (geology, grades, etc.).

The random component may be more or less predominant, in dependence on the variability of the phenomenon and their sampling, for instance, existence of different procedures for the quantification of the same attribute, or errors due to data collection.

The basic geostatistics assumption is that the statistical distribution of the difference of values of a variable between pairs of points (samples) is similar in all study area and depends only on the

distance and orientation of pairs of points. So, the geostatistics uses the location of each sample towards the neighbour samples.

Given the impossibility of fully evaluate, in space or time, the distribution of the property in study, the characterization is usually based on a limited set of data obtained by several samples. The data collection presents specific characteristics associated with a certain degree of uncertainty and unique achievements making it impossible to repeat the observation in a determined space and time.

There are two main approaches in geostatistics: estimation and simulation (Deutsch and Journel, 1992; Goovaerts, 1997; Soares, 2006). The estimation technique is a geostatistical interpolation based on the formalism of kriging and provides generation of an average picture of the variable. There are some variations of kriging (ordinary, simple) or kriging with indirect information (cokriging, collocated cokriging, kriging with an external drift), or one that are applied to categorical variables (indicator kriging) or continuous.

In estimation process the probable prediction of attribute distribution at the location without sampling is being got via kriging, by minimalizing the error variance. However, the map obtained by kriging may not have the same variogram and variance as the original data.

The simulation process allows to obtain a set of images as a whole that equiprobable quantifies of a local and global uncertainty. It provides an infinite number of realizations of the map each of which has approximately the same variogram and variance as the original data. Thus the simulation technique presents for further investigation a set of attribute distribution maps. Each map is equally represents the feasible uncertainty in the distribution of the geological properties.

### **4.3 Variograms and spatial continuity**

To successfully implement the geostatistics techniques it is necessary to use some specific methods of data evaluation as spatial continuity that the univariate statistics could not provide.

In geostatistics the dependence between observations can be evaluated with the variogram tool. Variogram is a quantitative measure of spatial variability or continuity is needed to characterize the detailed distribution of attributes within the reservoir.

The experimental variogram  $\gamma(\vec{h})$  is calculated by the half-sum of the squares of differences between pairs of measurements in the direction of the vector  $\vec{h}$  and separated by  $|\vec{h}|$ , where  $N(\vec{h})$  is the number of pairs of points separated by a vector  $\vec{h}$ .

$$\gamma(\vec{h}) = \frac{1}{2N(\vec{h})} \sum_{\alpha=1}^{N(\vec{h})} [z(u_{\alpha}) - z(u_{\alpha} + \vec{h})]^2$$

For a specific direction, or set of directions, the values of  $\gamma(\vec{h})$  are usually represented graphically with the distance (module of vector  $\vec{h}$ ). The increment of  $\gamma(\vec{h})$ , with the distance, depends of the gradient of a sample value changes related with the distance. When  $\gamma(\vec{h})$  stabilizes the maximum correlation distance is reached.

There are two another ways of spatial continuity measurement:

Covariance

$$C(h) = \frac{1}{N(h)} \sum_{i=1}^{N(h)} v_i \cdot v_{i+h} - m(h) \cdot m(-h)$$

The spatial covariance  $C(\vec{h})$  is related with the variogram  $\gamma(\vec{h})$  by  $\gamma(\vec{h}) = C(0) - C(\vec{h})$  where  $C(0) = C(|\vec{h}| = 0)$  is the statistical variance of the data.

And correlation

$$R(h) = \frac{C(h)}{\sigma(h) \cdot \sigma(-h)}$$

The main parameters of variogram are: (scheme is shown in the figure 4.3.1)

$h$  – (lag) – separation distance;

$C$  – (sill) – plateau reached by the variogram. Roughly equivalent to overall variance of data values;

$a$  – (range) – Distance at which the variogram reaches its plateau  $\diamond$  “correlation distance”

$C_0$  (nugget effect) – Short scale variability and sampling error.



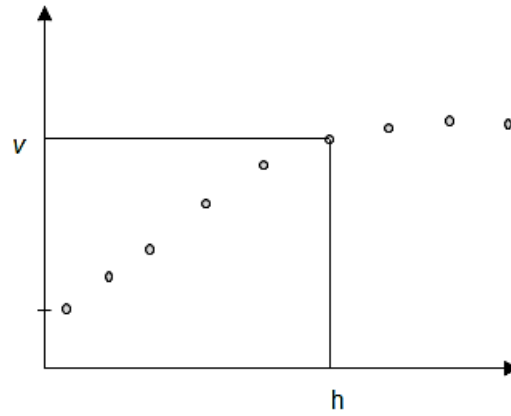


Figure 4.3.1 – Representation of the main variogram parameters

After computing the experimental variogram, the next step is to define a model variogram. This variogram is a simple mathematical function that models the trend in the experimental variogram. In turn, this mathematical model of the variogram is used in kriging computations. The kriging and conditional simulation processes require a model of spatial dependency, because kriging requires knowledge of the correlation function for all-possible distances and azimuths. Also the model makes a smooth in the experimental statistics and introduces geological information. And kriging cannot fit experimental directional covariance models independently, but depends upon a model from a limited class of acceptable functions.

The theoretical model can be defined by a unique function, or a sum of theoretical functions as the sum of two positive-defined. The final model can be isotropic or not, as it is constant or not, according to the various directions. There are three most common theoretical functions (their diagrams are shown in the figure 4.3.2):

Spherical

$$\gamma(h) = \begin{cases} C \left[ \frac{3}{2} \left( \frac{h}{a} \right) - \frac{1}{2} \left( \frac{h}{a} \right)^3 \right] & \text{if } h \leq a \\ C & \text{if } h > a \end{cases}$$

Exponential

$$\gamma^*(h) = C \cdot \text{Exp} \left( \frac{h}{a} \right) = C \left[ 1 - \text{Exp} \left( -\frac{h}{a} \right) \right]$$

Gaussian

$$\gamma(h) = C \left[ 1 - \text{Exp} \left( -3 \left( \frac{h}{a} \right)^2 \right) \right]$$

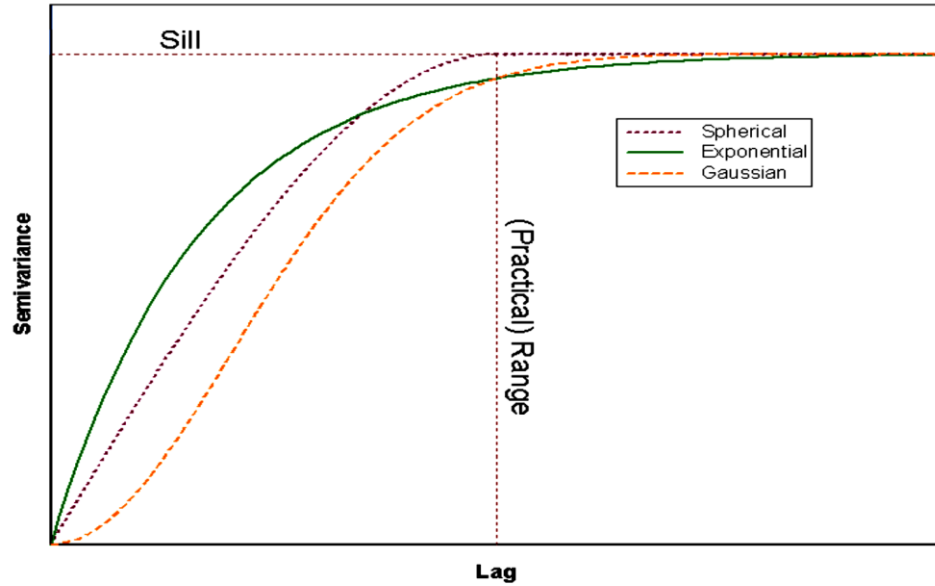


Figure 4.3.2 – Representation of theoretical models with the same range (adapted from Matheron, 1989)

The spherical and exponential models exhibit linear behaviour in the origin, appropriate for representing properties with a higher level of short-range variability.

In some cases if the individual variograms are very smooth because of the skew distribution of data and great amount of data, it is difficult to estimate all individual variograms accurately. For such cases, the concept of multiphase spatial variograms is used (Soares, 1998). The multiphase variogram is estimated by:

$$\gamma(h) = \frac{1}{2} E \left\{ \sum_{k=1}^K [I_k(x) - I_k(x+h)]^2 \right\}$$

After the calculation of experimental multi-phase variograms, the modelling process proceeds as in case of usual variograms: first find anisotropies between the different directions; then fit the experimental points with a theoretical function (for instance, exponential or spherical types).

#### 4.4 Estimation

Contouring maps by hand or by computer requires the use of some type of interpolation procedure. Kriging is a geostatistical technique for estimating attribute values at a point, over an area, or within a volume. It is often used to interpolate grid node values in mapping and contouring applications. In theory, no other interpolation process can produce better estimates (being unbiased, with minimum error); though the effectiveness of the technique actually depends on accurately modeling the variogram. The accuracy of kriging estimates is driven by the use of variogram models to express autocorrelation relationships between control points in the data set. Kriging also produces a variance estimate for its interpolation values. The theory behind interpolation and extrapolation by kriging was developed by the Georges Matheron. Kriging provides optimal interpolation; generates best linear unbiased estimate at each location; employs variogram model. (Isaaks and Srivastava, 1989).

Kriging interpolates the value  $Z(x_0)$  of a random field  $Z(x)$  at an unobserved location  $x_0$  from observations  $z_i = Z(x_i), i = 1, \dots, n$  of the random field at nearby locations  $x_1, \dots, x_n$ . Kriging computes the best linear unbiased estimator  $Z^*(x_0)$  of  $Z(x_0)$  based on a stochastic model of the spatial dependence quantified either by the variogram  $\gamma(h)$  or by expectation  $\mu(x) = E[Z(x)]$  and the covariance function  $C(h)$  of the random field. The kriging estimator is given by a linear combination

$$Z^*(x_0) = \sum_{i=1}^n w_i(x_0) \cdot Z(x_i)$$

of the observed values  $z_i = Z(x_i)$  with weights  $w_i(x_0), i = 1, \dots, n$  chosen such that the variance (also called kriging variance or kriging error):

$$\begin{aligned} \sigma_k^2(x_0) &= \text{Var}(Z^*(x_0) - Z(x_0)) \\ &= \sum_{i=1}^n \sum_{j=1}^n w_i(x_0) \cdot w_j(x_0) \cdot C(x_i, x_j) + \text{Var}(Z(x_0)) - 2 \sum_{i=1}^n w_i(x_0) \cdot C(x_i, x_0) \end{aligned}$$

is minimized subject to the unbiasedness condition:

$$E(Z^*(x_0) - Z(x_0)) = \sum_{i=1}^n w_i(x_0) \cdot \mu(x_i) - \mu(x_0) = 0$$

The kriging variance must not be confused with the variance:

$$\text{Var}(Z^*(x_0)) = \text{Var}\left(\sum_{i=1}^n w_i \cdot Z(x_i)\right) = \sum_{i=1}^n \sum_{j=1}^n w_i w_j \cdot c(x_i, x_j)$$

of the kriging predictor  $Z^*(x_0)$  itself.

Depending on the stochastic properties of the random field different types of kriging apply. The type of kriging determines the linear constraint on the weights  $w_i$  implied by the unbiasedness condition; i.e. the linear constraint, and hence the method for calculating the weights, depends upon the type of kriging. There are the typical methods of kriging: simple kriging assumes a known constant trend:  $\mu(x) = 0$ ; ordinary kriging assumes an unknown constant trend:  $\mu(x) = \mu$ , also universal kriging, indicator kriging uses indicator functions instead of the process itself, in order to estimate transition probabilities; lognormal kriging interpolates positive data by means of logarithms.

Consequently, estimation of attributes by kriging techniques give an opportunity of taking into account the spatial process (variogram) and also the redundant data and possible anisotropies in the most optimal manner.

#### 4.5 Indicator background

The indicator approach operates on discrete parameters like geologic facies or rock types. Indicator geostatistics generates multiple distributions of material zones. An indicator approach is widely used in geostatistics in order to estimate lithological parameters because this geological data is categorical. An advantage of the indicator geostatistics approach is that it allows to provide geological interpretation of the results. In addition, indicator simulations can be conditioned to existing site data. Indicator variable is a variable that has binary characteristics:

$$I(x) = \begin{cases} 1 \\ 0 \end{cases}$$

These variables can be used to differentiate lithology type or rock-types, for example,

$$I(x) = \begin{cases} 1 & \text{if sand} \\ 0 & \text{if shale} \end{cases}$$

Indicator variables can also be used for intervals of continuous variables

$$I(x) = \begin{cases} 1 & \text{if } \phi(x) \leq 0.05 \\ 0 & \text{if } \phi(x) > 0.05 \end{cases}$$

$I(x)$  – In each spatial location  $x$  of an area  $A$ , and in a binary system, an indicator variable has two possible outcomes  $X$  and its complementary  $X^c$ : (figure 4.5.1)  $A = X \cup X^c$ .

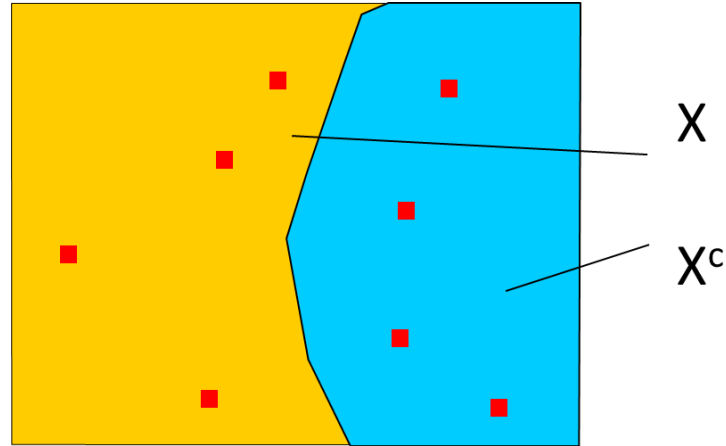


Figure 4.5.1 – Representation of a binary map and a binary variable

$$I(x) = \begin{cases} 1 & \text{if } x \in X \\ 0 & \text{if } x \in X^c \end{cases}$$

The set of  $N$  available samples in  $A$  is coded in one of the two possible states “1” or “0”, according the probability of belonging to  $X$  or  $X^c$  -  $I(x_i), i = 1, \dots, N$ , and can be interpreted as a realisation of a random function  $I(x)$ . From the realization  $I(x_i) = 1, \dots, N$ , it is possible to compute the mean (measure of the proportion of rock-type  $X$  within  $A$ ):

$$m_I = \frac{1}{N} \sum_{i=1}^N I(x_i)$$

And the variance:

$$\sigma_I^2 = \frac{1}{N} \sum_{i=1}^N (I(x_i) - m_I)^2 = m_I(1 - m_I)$$

The spatial continuity of  $X$  and  $X^C$  within  $A$  can be measured by the bi-point statistics covariance,  $C_I(h)$ , or the indicator variogram,  $\gamma_I(h)$ :

$$\gamma_I(h) = \frac{1}{2N(h)} \sum_{i=1}^{N(h)} [I(x_i) - I(x_{i+h})]^2$$

$$C_I(h) = C_I(0) - \gamma_I(h)$$

Both indicator covariance and variogram are an average measure of the spatial contiguity of the two rock-types  $X$  and  $X^C$  within  $A$ :

1. In each non-sampled location  $x$  in  $A$ , estimation of the probability of belonging to rock-type  $X$  -  $[prob\ x \in X]$ . The result is a probability map not a binary map.
2. Transformation of the probability map into a binary map reproducing the shape of the two rock-types  $X$  and  $X^C$ .

The best estimator of the proportion / mean of rock-types  $X$  in  $A$  is the global kriging estimation of the indicator variable in  $A$ , which is equivalent to the average of the punctual estimated values by kriging:

$$[X]^* = \frac{1}{M} \sum_{i=1}^M [I(x_i)]^*$$

$$[X^C]^* = 1 - [X]^*$$

The binary map of  $X$  will be constituted by the points  $x_u$  with highest estimated probabilities of belonging to  $X$  -  $[I(x_u)]^*$  - until the number of points reached the estimated proportion of  $X$  in  $A$ ,  $[X]^*$ .

If the estimated indicator values  $[I(x_u)]^*$ , estimated in a grid of  $M$  points in  $A$ , are sorted by decreasing order, the rock-type  $X$  will be constituted by the first  $N$  values where  $\frac{N}{M} = [X]^*$ .

This algorithm combines the two criteria concerning the shape: the maximization of the local probabilities and the reproduction of the global probability of  $X$  in  $A$ .

Indicator kriging estimates the probability of an attribute at each grid node (e.g., lithology, productivity). Summarizing, the technique requires the following parameters: coding of the attribute in binary form, as 0 or 1; prior probabilities of both classes; spatial covariance model of the indicator variable. So an indicator maps is very informative, providing a detailed spatial description of the lithology or rock-types.

#### **4.6 Simulation**

Stochastic modelling, also known as conditional simulation is an important geostatistical technique for modelling of reservoir attributes. The main advantage of the approach to mapping is the ability to model the spatial covariance before interpolation. The covariance models make the final estimates sensitive to the directional anisotropies present in the data. If the mapping objective is reserve estimation, then the smoothing properties of kriging in the presence of a large nugget may be the best approach. However, if the objective is to map directional reservoir heterogeneity (continuity) and assess model uncertainty, then a method other than interpolation is required (Hohn, 1988).

Conditional simulation models are becoming more accepted into our day-to-day reservoir characterization-modeling efforts because the results contain higher frequency content, and lend a more realistic appearance to our maps when compared to kriging (Srivastava, et. al., 1994).

In an industry that has become too familiar with layer-cake stratigraphy, with lithological units either connected from well-to-well or that conveniently pinch out halfway, and contour maps that show gracefully curving undulations, it is often difficult to get people to understand that there is much more inter-well heterogeneity than depicted by traditional reservoir models. Because stochastic modeling produces many, equi-probable reservoir images, the thought of needing to analyse more than one result, let alone flow simulate all of them, changes the paradigm of the traditional reservoir characterization approach. Some of the realizations may even challenge the prevailing geological wisdom, and will almost certainly provide a range of predictions from optimistic to pessimistic (Yarus, et. al., 1994).

In geostatistics stochastic simulation is the process of drawing equally probable, joint realizations of the component Random Variables from a Random Function model. These are usually gridded realizations, and represent a subset of all possible outcomes of the spatial distribution of the attribute values. Each realization is as called a stochastic image (Deutsch and Journel, 1992)

The aim of sequential simulation is to reproduce desirable multivariate properties through the sequential use of conditional distributions. Suppose the continuous variable  $Z(x)$  has a global cumulative distribution function and stationary variogram. It is necessary reproduce the histogram of original variable in the regions to be reconstructed.

The sequential simulation algorithm of a variable follows the classical procedure.

- 1) Define a random path visiting all nodes to be simulated. Each node will be computed only once and the number of its conditional data will be limited to a specified range. The conditional data include the original data and simulated data.
- 2) At each node  $x_u$ , determine the local cumulative distribution function at each node to be simulated.
- 3) Draw a value from the cumulative distribution function and add it to the simulated data set.
- 4) Return to step 1 and compute the next node until all the unknown nodes in the random path are simulated.

There are several simulation algorithms to generate images, which based on this main approach but with specific details and characteristics according to initial information. In the work the sequential indicator simulation and direct sequential simulation were used therefore there is brief description below.

#### 4.6.1 Sequential Indicator Simulation

Sequential Gaussian simulation (SGS) and Sequential Indicator simulation (SIS) have emerged as powerful tools for stochastic imaging of Earth Science phenomena and are currently widely accepted fast simulation algorithms.

These sequential simulation procedures make use of the same basic algorithm for different data types. The general process is

1. Select at random grid node ( $x_0$ ), a point not yet simulated in the grid.
2. Use kriging to estimate the mean ( $m_i$ ) of each category  $i$  at location of grid note ( $x_0$ )
3. Build a pseudo cumulative distribution law with the estimated means;
4. From the pseudo cumulative distribution law, draw a random category (Monte Carlo);



5. Include the newly simulated value  $I_s(x_0)$  in the set of conditioning data. This ensures that closely spaced values have the correct short scale correlation.
6. Repeat the process until all grid nodes have a simulated value.

In order to provide this process it is necessary to make an election of the simulated grid node. The order in which grid nodes are randomly simulated influences the cumulative feedback effect on the outcome. The selection process is random, but repeatable:

- For each simulation, shuffle the grid nodes into an order defined by a random seed value.
- Each random seed corresponds to a unique grid order.
- Different random seed values produce a different path through the grid.
- Although the total possible number of orderings is very large, each random path is uniquely identified and repeatable.

Sequential Indicator Simulation (SIS) is a method used to simulate discrete or categorical variables. By filling a grid with categorical values, it uses the same methodology as SGS, which represent “lithofacies” (pay/non-pay, or sand/shale). SIS requires the following input parameters such as a priori probabilities (proportions) of two data classes (Indicators -denoted as I) coded as 0 or 1, for example:

$$I(x) = \begin{cases} 1 & \text{if } z(x) = \text{sand} \\ 0 & \text{if } z(z) = \text{shale} \end{cases}$$

indicator histogram and the indicator spatial correlation mode.

#### 4.6.2 Direct Sequential Simulation

In this work also the techniques of Direct Sequential Simulation (DSS) was used. Recent development in geostatistical theory (Journel, et. al., 1994) denoted that in order to obtain variogram reproduction in the resulting simulations, any type of local conditional distribution can be used to simulate values, as long as its mean and variance identifies the kriging mean and kriging variance. This statement is a clear extension of the Gaussian simulation paradigm where

the kriging mean and variance are imposed on the standard normal distribution. DSS allows variogram reproduction under non-Gaussian assumptions, however, it does not ensure reproduction of the global histogram of the data, and neither does DSS allow, through its construction, the reproduction of indicator variograms.

Therefore, a direct sequential simulation approach is presented in this paper, which need not use any prior or posterior transformation, but can reproduce the histogram of reference data as well. The main strategy of the DSS is the same as in the sequential simulation procedure.

For continuous variables, the Direct Sequential Simulation (DSS), unlike SGS, uses the original variable without any previous transformation of the data. For instance, as SGS uses a prior transformation of the data to a Gaussian distribution, and a back-transformation at the end, it is sometimes difficult to reproduce the variograms of the original variable mainly for extremely skew distributions. This effect increases if secondary variables are used within a co-simulation procedure.

The DSS uses the local mean and variance to resample the global cumulative distribution law  $F_Z(z)$ , and build a new local cumulative distribution function  $F'_Z(z)$  with intervals centred on the local estimated average and with a range proportional to the local conditional variance. Those two local parameters, mean and variance, are estimated by simple kriging:

$$[z(x_o)]^* - m = \sum_{\alpha} \lambda_{\alpha} (z(x_{\alpha}) - m)$$

One way to define the intervals and get the simulated value  $z^s(x_0)$  from  $F'_Z(z)$  is to select a subset of  $n$  contiguous values  $z(x_i)$  of the global experimental histogram whose mean and variance of the selected values is equal to the local estimated mean  $[z(x_o)]^*$  and estimation variance  $\sigma_{ks}^2(x_0)$ :

$$\frac{1}{n} \sum_{i=1}^n [z(x_i) - [z(x_o)]^*]^2 = \sigma_{ks}^2(x_0) \quad \text{and} \quad \frac{1}{n} \sum_{i=1}^n z(x_i) = [z(x_o)]^*$$

Another way to define the function is to use a Gaussian distribution law only as a helper function to re-sample intervals  $F_Z(z)$  and not to transform the original data to Gaussian distribution.

In conclusion, reservoir modelers recognize two fundamentally different aspects of stochastic reservoir models. The reservoir architecture is usually the first priority, consisting of the overall structural elements (for example, faults, top and base of reservoir), then defining the lithoclasses based on the depositional environment (shallow zone or, deep-water fan.). Once the spatial arrangement of the different flow units is modeled, we must then decide how to populate them with rock and fluid properties. The important difference between modeling facies versus modeling rock properties is that the former is a categorical variable, whereas the latter are continuous variables.

#### 4.7 Geobody analysis

Geobody analysis in the work is meant the estimation of potential oil reserves that is in carbonate reservoir rock. In order to provide this the method of tracing of Potential oil-in-place curves was used.

Potential oil-in-place (POIP) is the amount of crude first estimated to be in a reservoir. Oil initially in place differs from oil reserves, as POIP refers to the total amount of oil that is potentially in a reservoir and not the amount of oil that can be recovered. Calculating POIP requires determining how porous the rock surrounding the oil is, how high water saturation might be and the net rock volume of the reservoir.

Accurate calculation of the value of POIP requires knowledge of:

- volume of rock containing oil
- percentage porosity of the rock in the reservoir
- percentage water content of that porosity
- amount of shrinkage that the oil undergoes when brought to the Earth's surface

It is calculated by using the formula

$$N = \frac{7758V_b\phi(1 - S_w)}{B_{oi}} [stb]$$

Or

$$N = \frac{V_b\phi(1 - S_w)}{B_{oi}} [m^3]$$

where

- $N$  = POIIP (barrels)
- $V_b$  = Bulk (rock) volume (acre-feet or cubic metres)
- $\phi$  = Fluid-filled porosity of the rock (fraction)
- $S_w$  = Water saturation – water-filled portion of this porosity (fraction)
- $B_{oi}$  = Formation volume factor (dimensionless factor for the change in volume between reservoir and standard conditions at surface).

Gas saturation  $S_g$  is traditionally omitted from this equation. The constant value 7758 converts acre-feet to stock tank barrels. An acre of reservoir 1 foot thick would contain 7758 barrels of oil in the limiting case of 100% porosity, zero water saturation and no oil shrinkage. If the metric system is being used, a conversion factor of 6.289808 can be used to convert cubic meters to stock tank barrels. A 1 cubic meter container would hold 6.289808 barrels of oil.

In an industry this calculation not only relies on computations attribute values from log data but also on the size and shape of a reservoir, and correlations of logs from many wells in the field. Also a lot of additional information (Dipmeter data and seismic data) is used for providing comprehensive calculation. Then in order to calculate oil reserves is a portion of oil volume that is the technically and economically recoverable from the reservoir, the current recovery factor for oil field is being taken into account. However in our case even without these additional information there is an opportunity to evaluate the approximately the oil volume according to the initial data of porosity and permeability after prediction of their distribution made by simulation. In conclusion, this method provides brief estimation that can be easily carried out with a simple technique based on different types and quantity of available information. According to the obtained results it is possible to compare and correlate with other field information and conclude about further process of exploration or developing of reservoir giving predictions and also to estimate economical parameters of the work. In proportion to accumulation of more detailed information it is easily changed recalculated model. The minimization of uncertainty in reservoir simulation is time dependent and occurs as more reservoir simulation performance prediction is confirmed by historical field measurement.

## 5 CASE STUDY

The underwritten steps of the work was carried out according to initial information, theoretical background and workflow description

### 5.1 Data presentation and basic statistics

The studied reservoir is located in the Middle East. The main geological structure of the field consists of a single lengthened anticline with a NE-SW orientation, measuring approximately 27 km along the major axis and 8 km at the perpendicular, corresponding to a surface area of about 160 km<sup>2</sup> (North, 1985). The geological structure of this reservoir is a carbonate rich sequence of *Maashtrichiana* age (Upper Cretaceous) deposited during an actively growing paleohigh in shallow marine subtidal to intertidal and supratidal conditions. The Cretaceous rocks are dominated by limestones with shales and sandstone interbeds. This formation consists of limestones, mainly packstones, which were deposited in a shallow water environment, representing a regressive phase. There are two principal sealing formations – anhydrite and shales (Scott R.W., 1990).

The initial data represents three carbonate interlayers. Well data came from 19 vertical wells (geographical representation is shown in Figure 5.1.1) that cross all identified units and allow to provide geological identification into the 5 main lithoclasses. Table 5.1.1 contains all identified lithoclasses and displays the corresponding rock type and indicative mean and variance of porosity and permeability values.

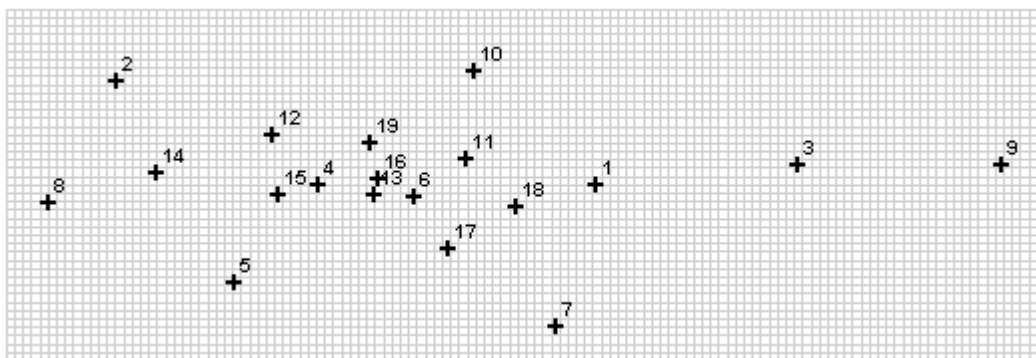


Figure 5.1.1 – Aerial view of the entire field with superposition of the stochastic simulation grid and well locations.

The stochastic models presented in this work characterize the reservoir properties in a discrete grid of points, covering the volume, which bounds the entire reservoir. The unitary block in the grid selected for the stochastic model is 250 by 250 meters for both X and Y directions and 1

foot in the vertical direction. Taking into account the dimensions of the reservoir, the total number of blocks is laterally 124 in the X direction and 42 in the Y direction. The number of blocks in the Z direction depends from the maximum thickness of each layer.

Cumulative curves for porosity and permeability are presented in the figure 5.1.2 and figure 5.1.3, respectively.

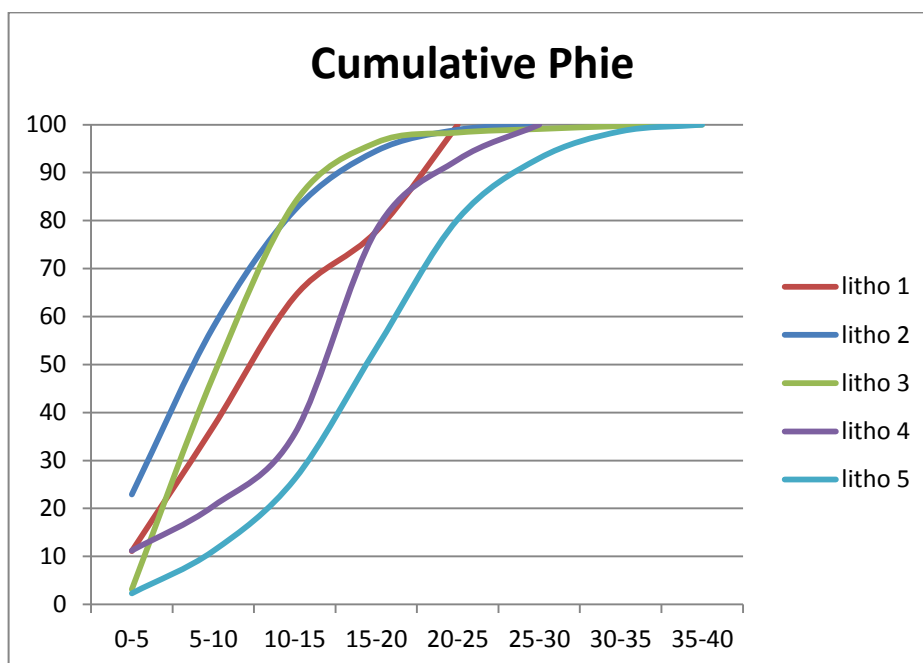


Figure 5.1.2 – Cumulative curves of PHIE for each lithoclass

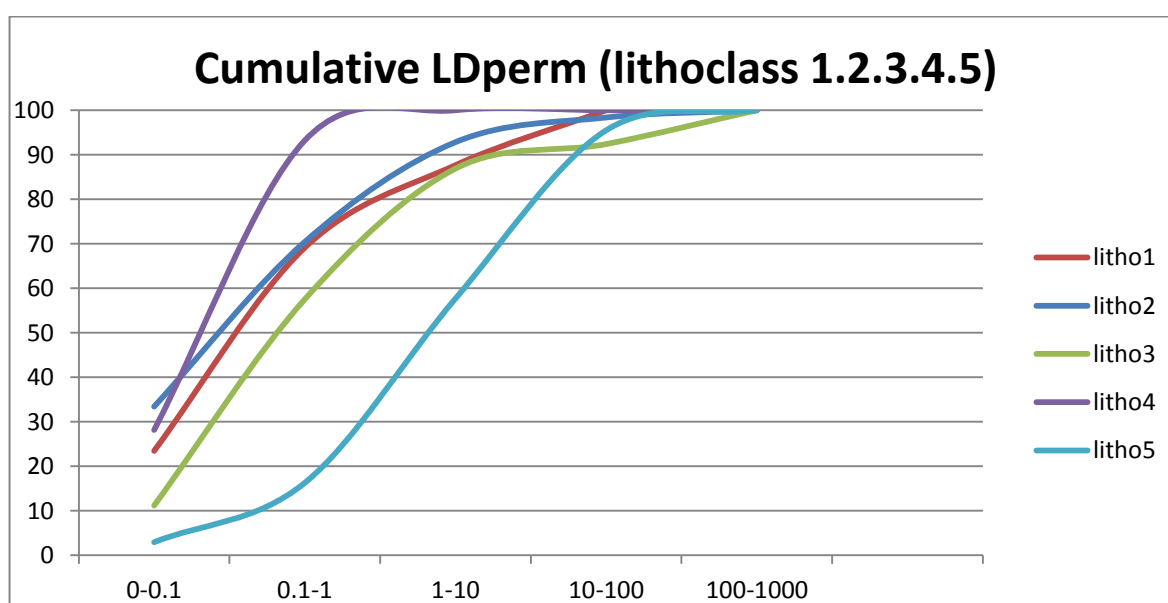


Figure 5.1.3 – Cumulative curves of permeability

Table 5.1.1 – Lithoclasses identified in the present oil field: typical rock types and porosity and permeability mean and variance

lithoclass	Rock type	PHIE		LDperm	
		mean	variance	mean	variance
1	Shale	13.36	45.54	2.58	26.54
2	Mudstone	9.65	32.66	6.63	1395.71
3	Mudstone to wackestones	11.11	23.06	28.71	10084.61
4	Wackestones	15.68	48.25	3.72	20.79
5	Moldic dolomites/ grain to packstone	19.26	49.02	23.25	2694.94

The figure 5.1.4 represents the percentage of each lithoclasses. According to the diagram the least lithoclass is the lithoclass 1. Such small quantity of the samples might have the negative influence on the modelling process. This fact will be proven in the appropriate subsection.

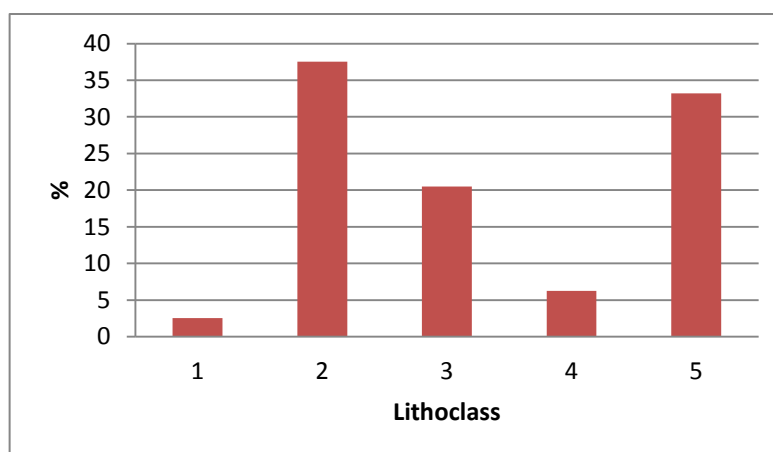


Figure 5.1.4 – Proportion of each lithoclasses

## 5.2 Layer top and bottom morphology

In order to obtain the model of reservoir the common necessary first step is the modelling of morphology. Thereby in this paper, ab initio morphology of top and bottom was modelled. It was completed according to coordinates of the wells. Parameters of the grid for computing top and bottom layers are showed in the table 5.2.1. This reservoir grid was used for all further modelling steps (lithoclasses and properties).

Table 5.2.1 – Parameters of grid used for computing variograms and kriging process

	Lower left point	Upper right point	Number of blocks	Spacing	Discretization
<b>X</b>	125	30875	124	250	1
<b>Y</b>	125	10375	42	250	1
<b>Z</b>	0	0	1	1	1

The process of morphology modelling consisted in two main stages – calculating variograms and estimation via ordinary kriging. All variograms in this work were calculated in geoMS software. Basic analysis showed that for the kriging process the omnidirectional variograms would use so that the others presented quite smooth results. The derived omnidirectional variograms are shown in the figure 5.2.1. The kriging was performed for each surface. The example of surface map for the top is shown on the figure 5.2.2. Top and bottom was imported into GOCAD software and the result is shown in the figure 5.2.3. According to obtained map the modelling structure presents the anticlinal one.

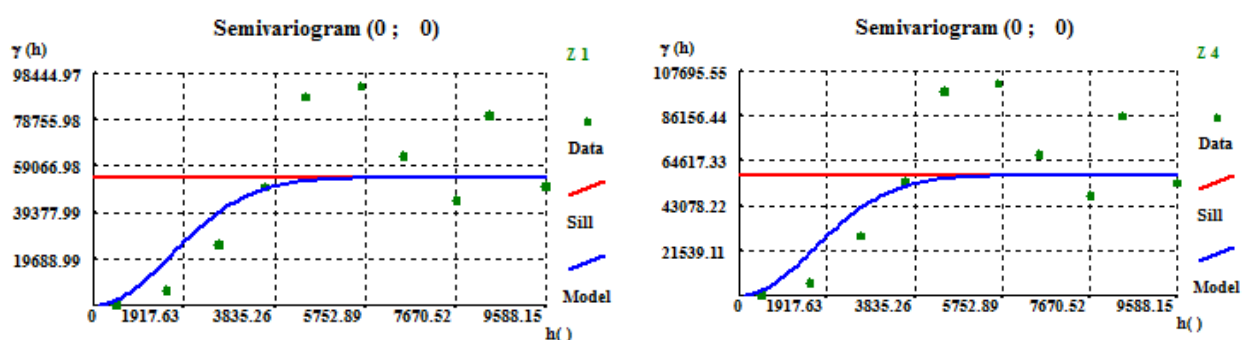


Figure 5.2.1 – Omnidirectional variograms for every surface

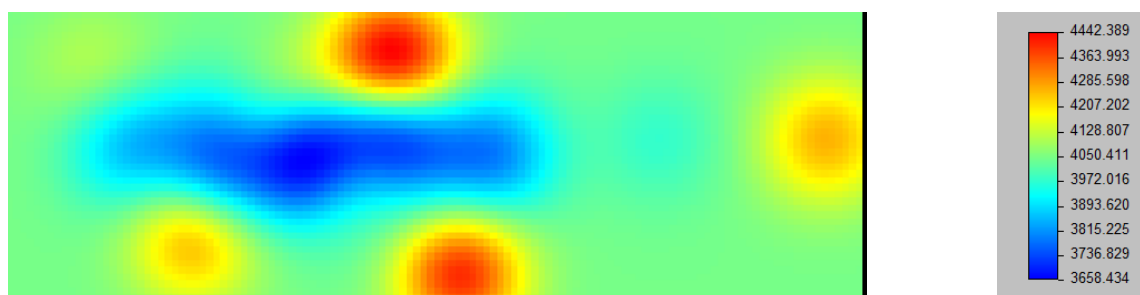


Figure 5.2.2 – Map of the top of the first layer



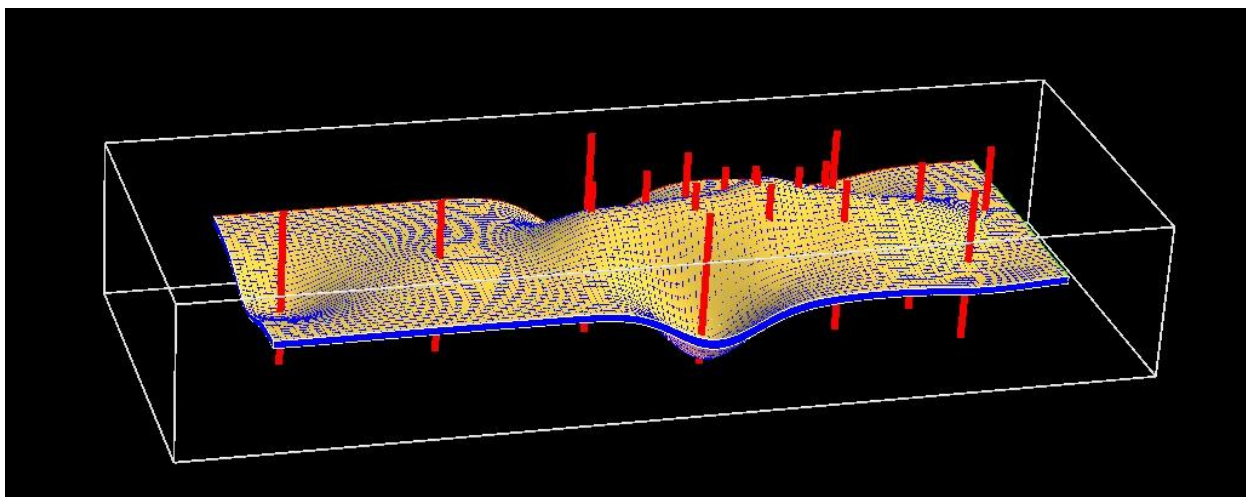


Figure 5.2.3 – Obtained morphology of the studied layer and location of wells

### 5.3 Transformation into stratigraphic units

The next important step for all further work is the referential transformation of the initial data. This transformation is necessary to compute horizontal variograms according to stratigraphical referential and provide the correct modelling of lithoclasses and properties of the reservoir by means of simulation techniques. This step allows to transform a volume delimited by two regular surfaces into regular parallelepiped shape. On this step all the values of lithoclasses or porosity and permeability from the wells are proportionally stretched to the maximum thickness of the layer. The example of results of PHIE parameter transformation performed by geoMS software is shown in the figure 5.3.1.

According to the output files with transformed data the statistic tables were composed and cumulative curves for porosity and permeability according to each lithoclasses were obtained (figures 5.3.2, 5.3.3 respectively). Comparison of these cumulative curves and ones before transformation shows small differences between values but at the end back transformation will restore the original proportions for lithoclasses and conditional histograms for properties.

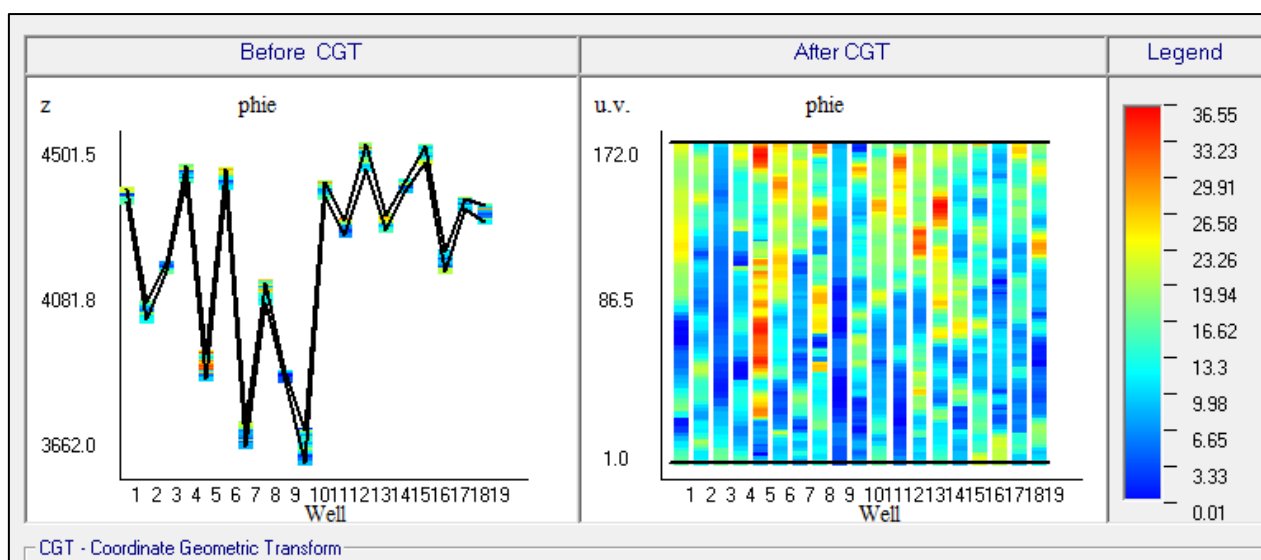


Figure 5.3.1 – The example of coordinate geometric transformation for PHIE parameter

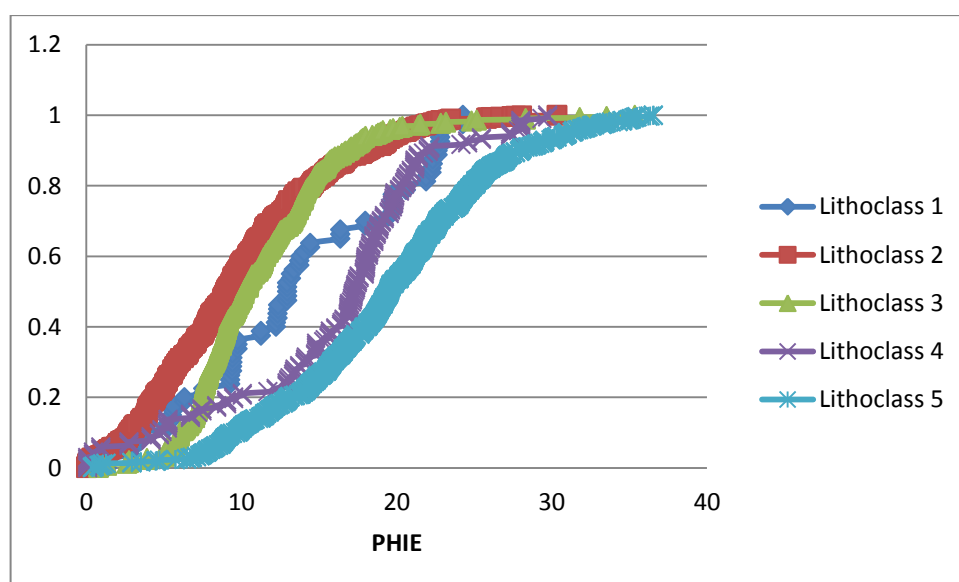


Figure 5.3.2 – Cumulative curves of PHIE parameter for each lithoclass

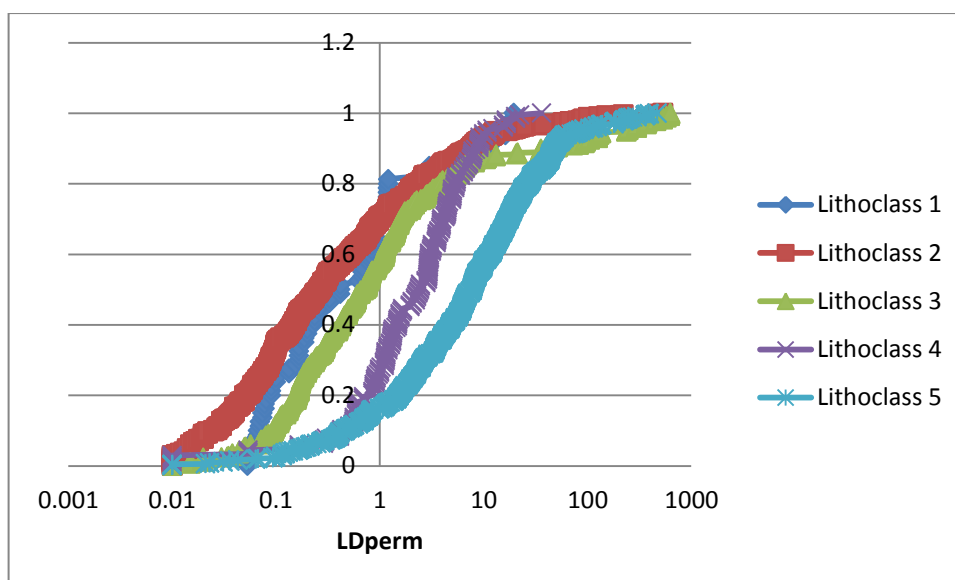


Figure 5.3.3 – Cumulative curves of LDperm parameter for each lithoclass

#### 5.4 3D geological model of lithoclasses

Modelling of the lithoclasses is the next step. Common previous procedure for this stage is the computing indicator variograms. In the case of this work the variograms were made for each lithoclass in two directions: horizontal and vertical (s.u. – stratigraphical unit). The obtained variograms had different level of representation because of the low proportion for lithoclass 1 and 4, comparing with the higher proportions of lithoclasses 2 and 5 shown in the figure 5.4.1. In concordance with these results and as lithoclasses 2 and 5 exhibit similar ranges for the further modelling process the multi-phase variograms were computed. Theoretical models were fitted for multi-phase variograms for two directions (figure 5.4.2). Only one exponential structure was used. The main model parameters are shown in the table 5.4.1.

Table 5.4.1 – Theoretical model parameters for the multi-phase variograms of lithoclasses

Direction	Model	Range	Sill
Horizontal	exponential	2500 m	0.702
Vertical	exponential	50 s.u.	0.702

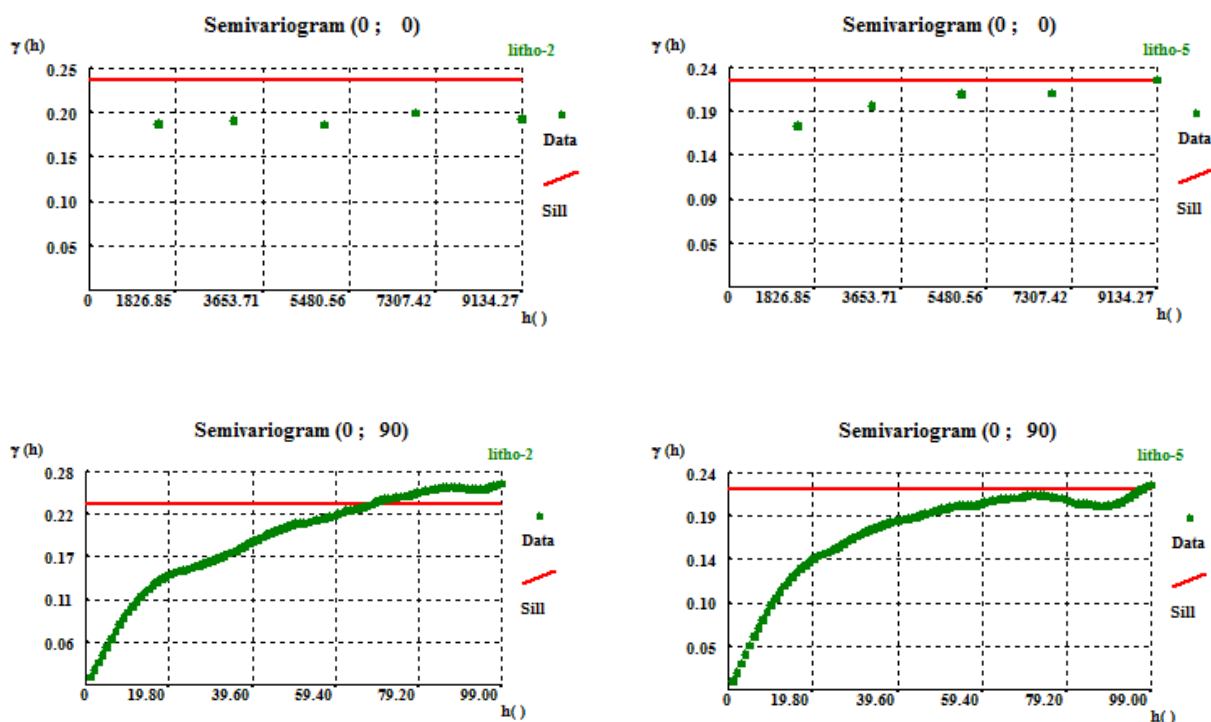


Figure 5.4.1 – Variograms for lithoclasses 2 and 5 for both directions (horizontal and vertical)

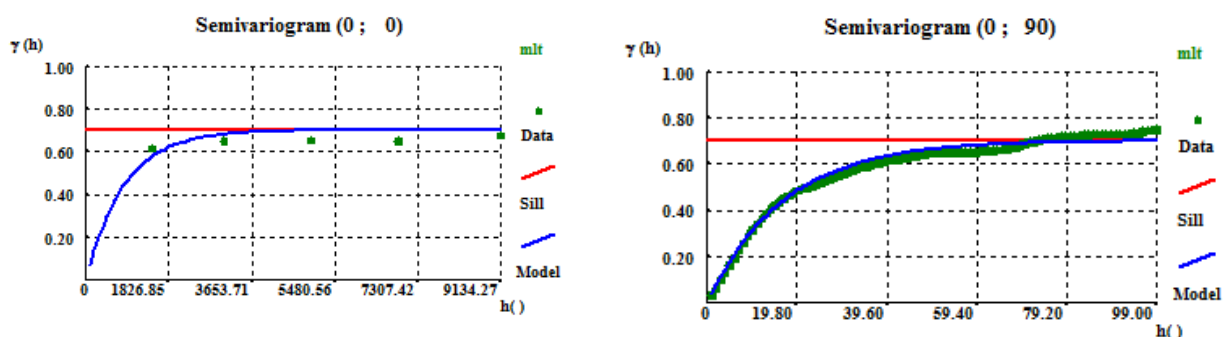
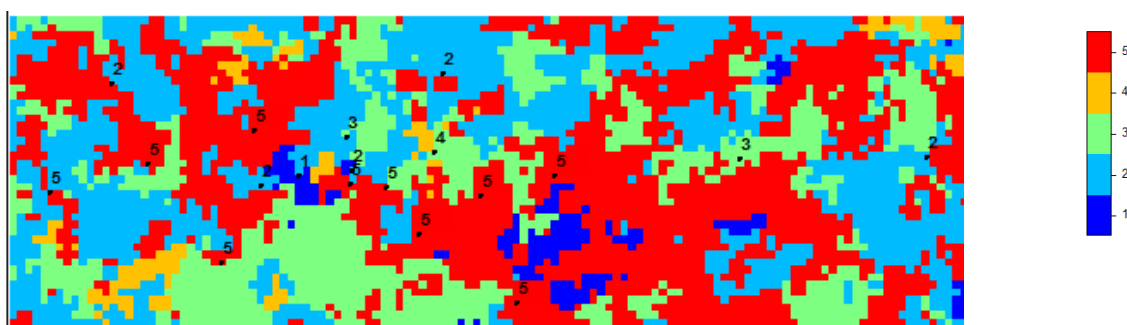
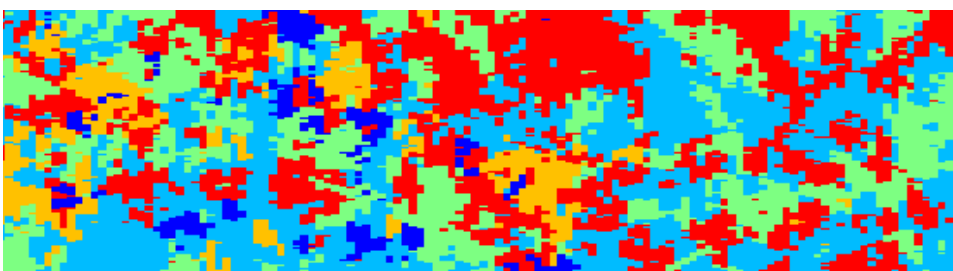


Figure 5.4.2 – Multi-phase variograms for lithoclasses with fitted theoretical model

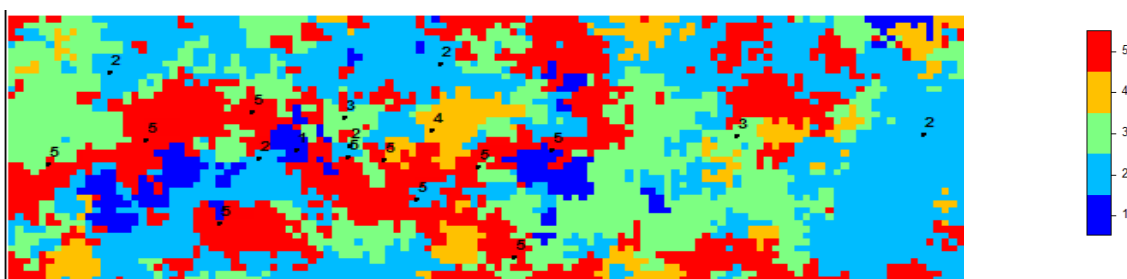
The next stage of the modelling is the lithoclasses simulation. In order to implement it the method of Sequential Indicator Simulation was used with spiral search as a grid search method with 20 nodes maximum. In this work 30 images of lithoclasses were simulated. The two simulations of the lithoclasses are shown in the figure 5.4.3., both in one level and one cross-section.



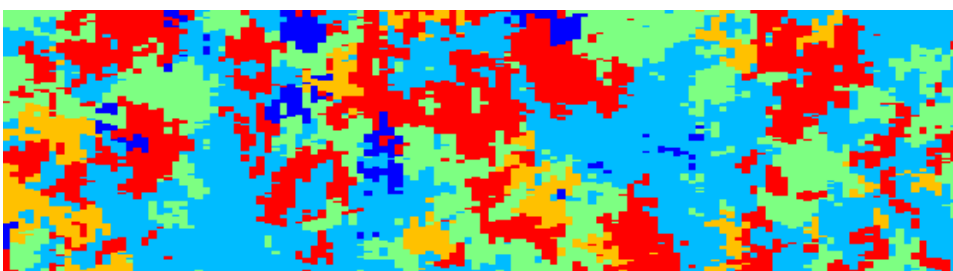
Horizontal map



Cross-section



Horizontal map



Cross-section

Figure 5.4.3 – Two realization of simulation of the lithoclasses: left – horizontal; right – cross-section, where colours represent each lithoclass

The final step of the modelling process is the validation stage. First the comparison of the well and simulated data were carried out (figure 5.4.4). As can be seen from it the well data register the simulated data. Also the proportions of lithoclasses were compared for grid and well data (table 5.4.2). As it can be seen the differences between the well and grid data are quite small.

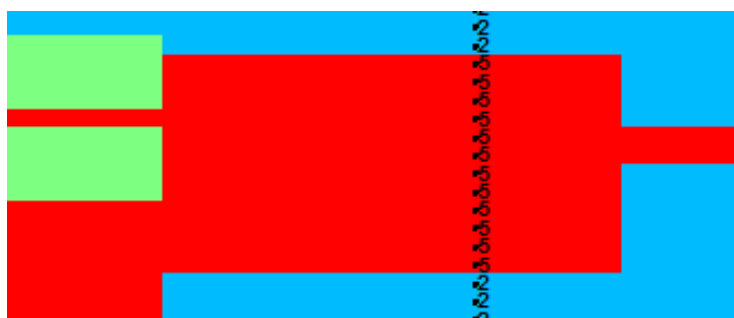


Figure 5.4.4 – Comparison of the well and simulated data

Table 5.4.2 – Main univariate statistic parameters for well and simulated data

Lithoclass	Well data	Grid data (Simulation 1)	Grid data (Simulation 2)
1	0.0248	0.0254	0.0262
2	0.3752	0.3724	0.3715
3	0.2050	0.2063	0.2048
4	0.0627	0.0644	0.0679
5	0.3323	0.3315	0.3295

Also the multi-phase variograms were compared for the one simulated image and the theoretical model fitted before (figure 5.4.5). The comparison of these models represented the appropriate results.

Thereby the simulation of the lithoclasses was successfully provided. The results could be used for further modelling steps.

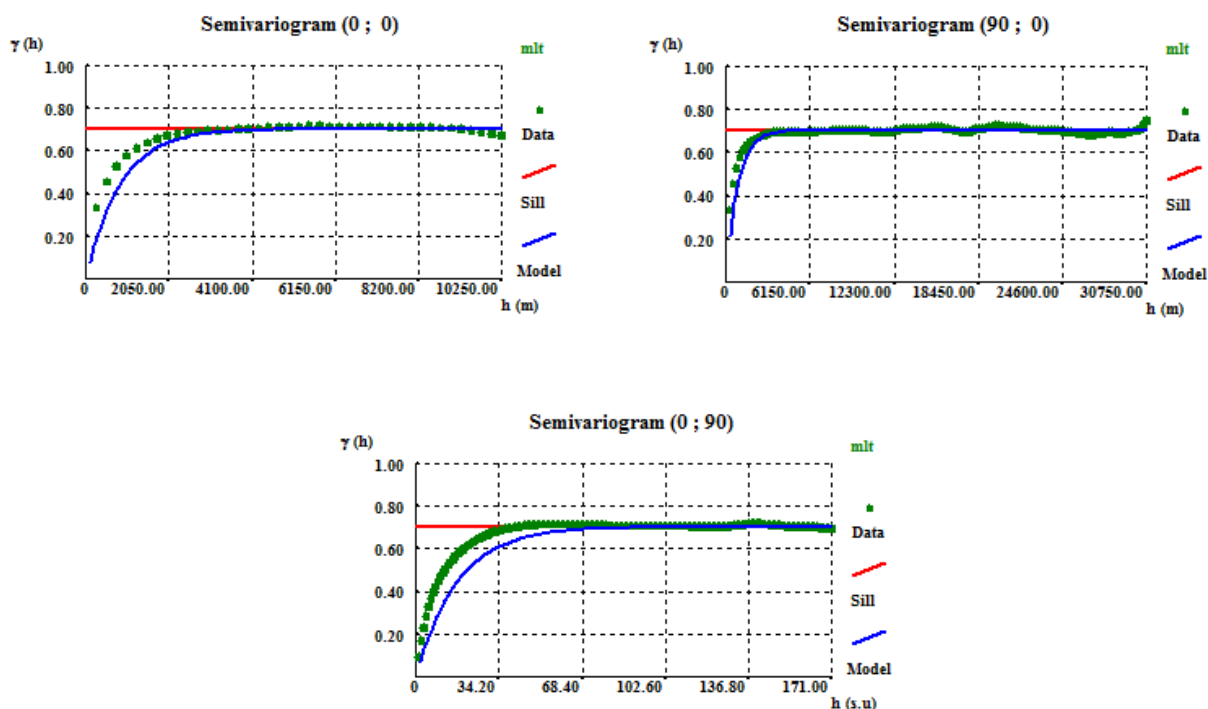


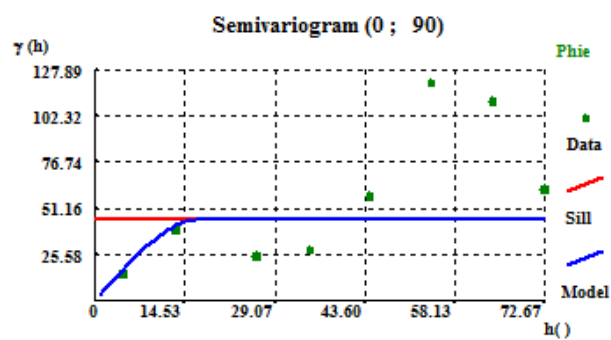
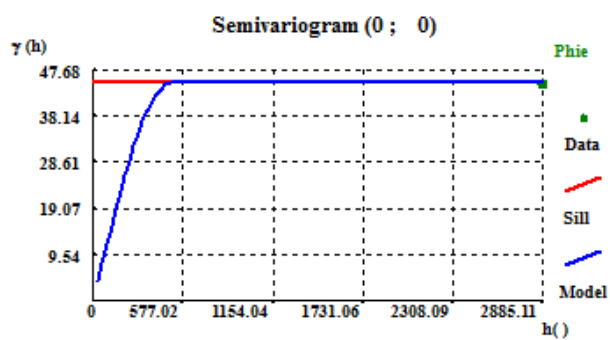
Figure 5.4.5 – Multi-phase variogram of one simulated image (horizontal and vertical) and the theoretical model fitted to the well data

### 5.5 3D model of porosity

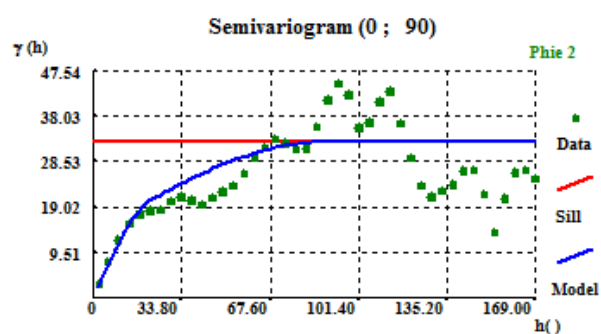
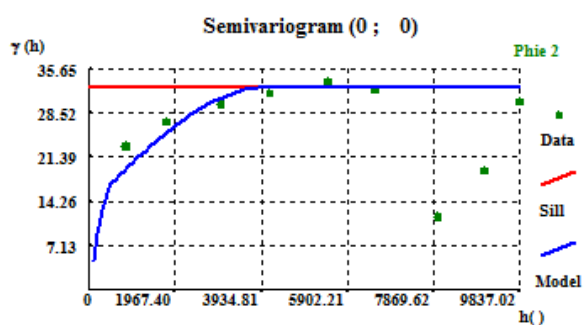
The next stage is the attributes modelling. The modelling of porosity (PHIE parameter) was conditioned to the 3D model of lithoclasses.

The first step also as for the modelling of lithoclasses is computing variograms in two directions. The obtained variograms of PHIE for each lithoclass are shown in the figure 5.5.1 with fitted theoretical models as well. The main parameters of the fitted theoretical models for each lithoclass are shown in the table 5.5.1. Also the variograms of PHIE independently of lithoclasses were computed.

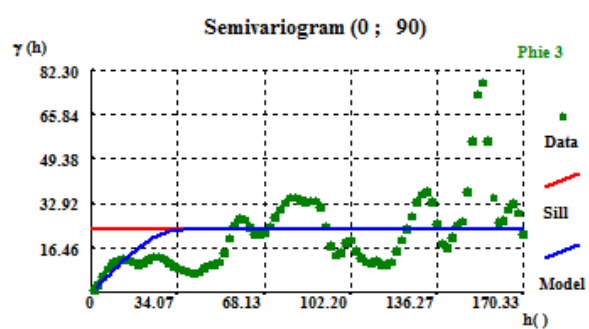
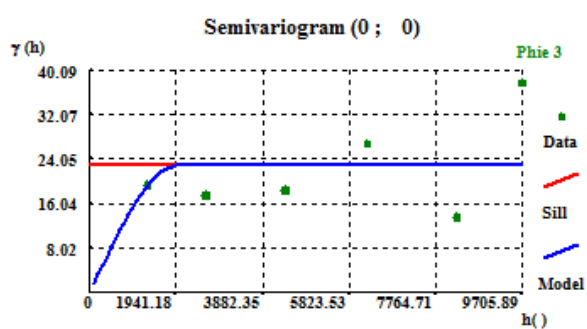
## Lithoclass 1



## Lithoclass 2

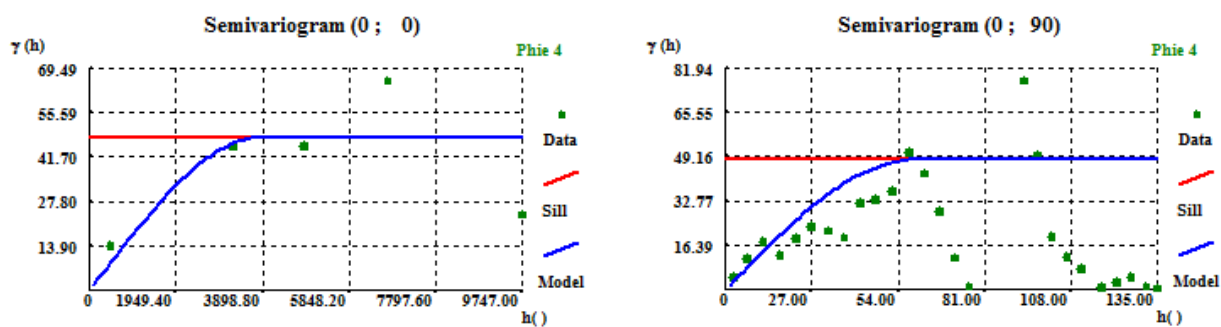


## Lithoclass 3

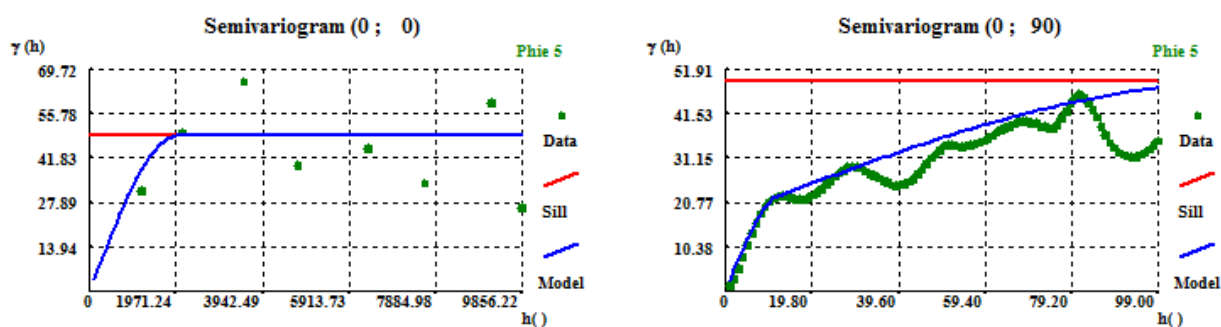


## Lithoclass 4





## Lithoclass 5



## Independently of lithoclasses

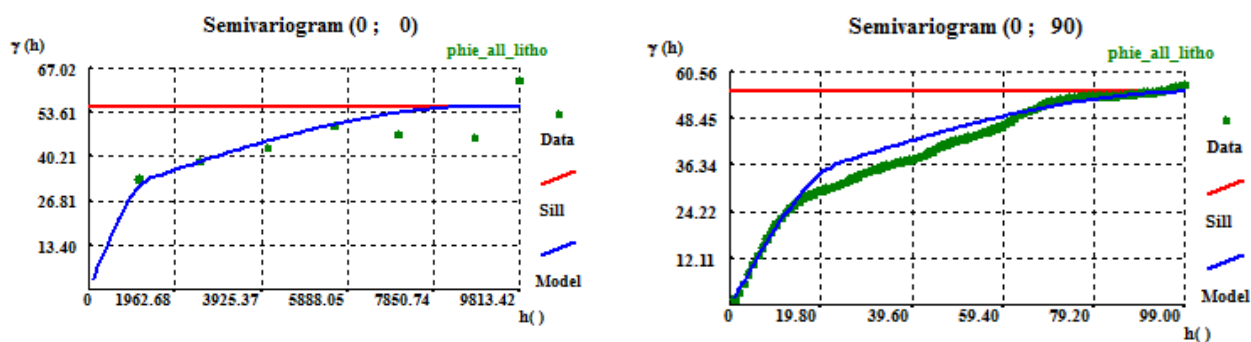


Figure 5.5.1 – Variograms of PHIE for each lithoclass and fitted theoretical models

For the first lithoclass the horizontal variogram is absent because there are only 2 wells with shale and they are located at the distance about 3000 meters from each other. In this case the model was fitted presumptively with spherical structure with similar sill and range (500 m) that is approximately equal to the distance between wells in the structure.

According to the obtained variograms for the lithoclass 2, 5 and independently of lithoclasses variogram two spherical structures were used to fit the model. Actually the sum of two structures with the same sill was used, for instance for lithoclass 5:

$$\gamma(h)_H = \text{SPH}(C=17.62; a=2000) + \text{SPH}(C=31.3; a=2000)$$

$$\gamma(h)_V = \text{SPH}(C=17.62; a=12) + \text{SPH}(C=31.3; a=120)$$

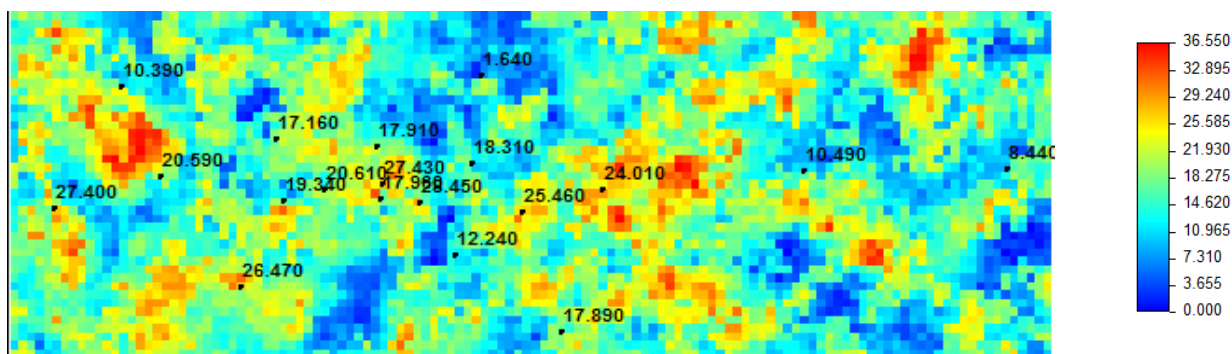
The comparison of all results lead to the using the theoretical model fitted for PHIE independently of lithoclasses for the further realization of the simulation algorithm. It should be noted that there is the advantage of DSS approach that give an opportunity of using global histogram in case if the local histograms showed very different and unclear results.

Table 5.5.1 – Parameters of the theoretical models of variograms for PHIE

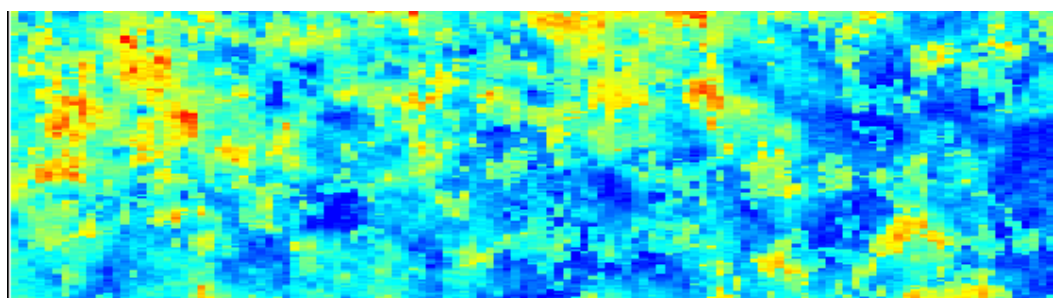
Lithoclass	Direction	Model 1, 2	Range 1	Sill 1	Range 2	Sill 2
1	Horizontal	Spherical	500 m	50		
	Vertical	Spherical	17 s.u.	50		
2	Horizontal	Spherical	500 m	13.597	4000 m	19
	Vertical	Spherical	22 s.u.	13.597	88 s.u.	19
3	Horizontal	Spherical	2000 m	23		
	Vertical	Spherical	35 s.u.	23		
4	Horizontal	Spherical	3900 m	48		
	Vertical	Spherical	59 s.u.	48		
5	Horizontal	Spherical	2000 m	17.62	2000 m	31.3
	Vertical	Spherical	12 s.u.	17.62	120 s.u.	31.3
independently of lithoclasses	Horizontal	Spherical	1400 m	27.249	9000 m	28.135
	Vertical	Spherical	24 s.u.	27.249	102 s.u.	28.135

Using the Direct Sequential Simulation algorithm conditional simulation of porosity according to lithoclasses with local histograms at local average was provided, as the result the 90 simulated

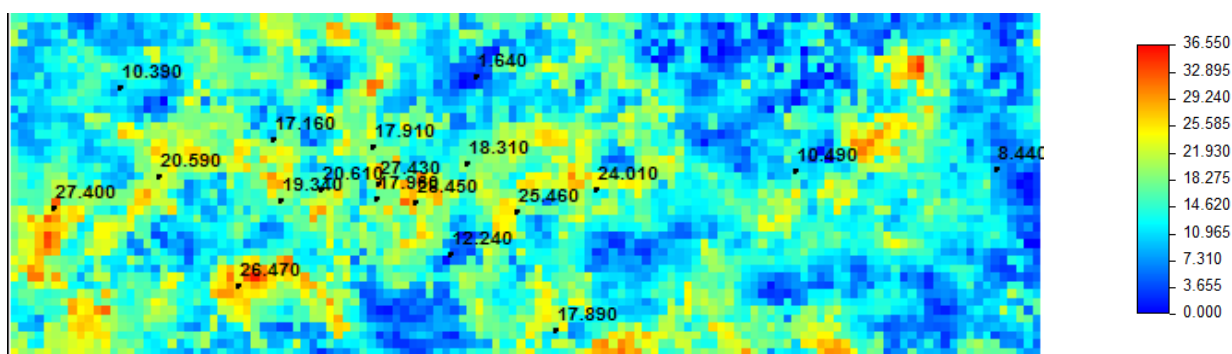
maps of PHIE constraining to all lithoclasses were obtained (for each of 30 images of lithoclasses three simulation of PHIE were made). The examples of one map of PHIE for the first and second images of lithoclasses are shown in the figure 5.5.2. The obtained PHIE maps represented quite accurate correspondence to maps of lithoclasses. Also the average map of PHIE constraining to the lithoclasses was computed (figure 5.5.2). As can be seen from the comparison of the PHIE and lithoclasses maps, the boundaries of each lithoclass represent quite exactly on the average map of PHIE.



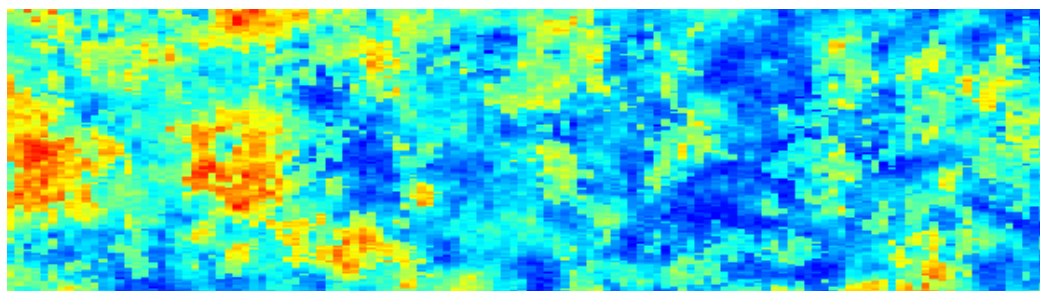
Realization 1 for the first image of lithoclasses (horizontal)



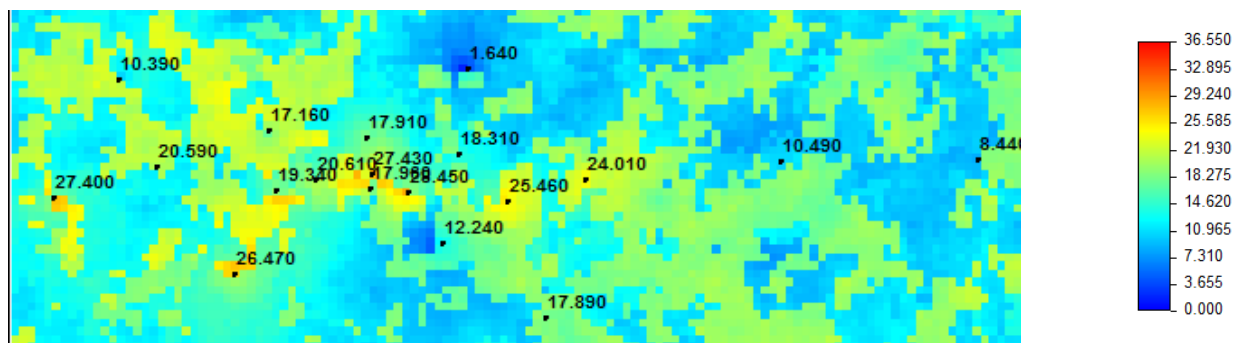
Cross-section



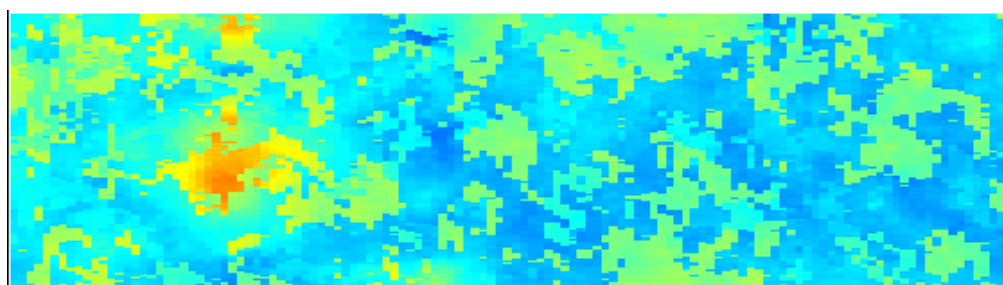
Realization 1 for the second image of lithoclasses (horizontal)



Cross-section



Average map (horizontal)



Cross-section

Figure 5.5.2 – The obtained maps of PHIE for first and second images of lithoclasses (horizontal and cross-section) and an average map of phie (30)

In the process of modelling porosity as in case of lithoclasses modelling, validation is the essential step. Three main compared parameters were also used in order to prove accuracy of obtained simulation maps. With reference to comparison of the well and simulated data (figure 5.5.3) simulated map exactly registers well data. Also the main statistic parameters were compared. The main parameters of grid and well data univariate statistic are shown in the figures 5.5.4 and 5.5.5, respectively, provide appropriate agreement. The third step of validation is

comparison of variograms computed for obtained map (figure 5.5.6) with fitted theoretical model. The comparison of these models represented the appropriate results.

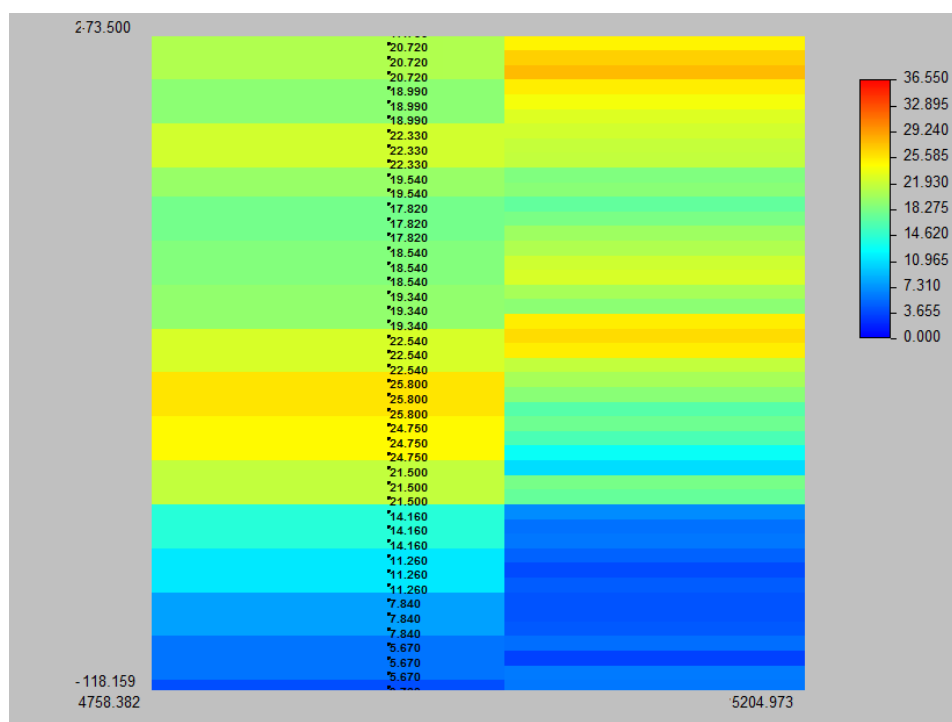


Figure 5.5.3 – Simulated map of Phie with overlaid well data

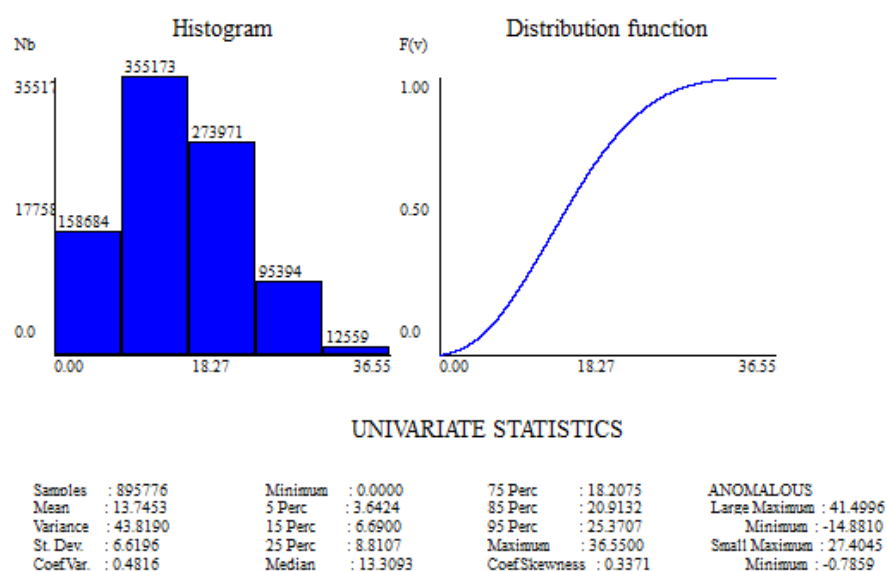


Figure 5.5.4 – Univariate statistics of grid

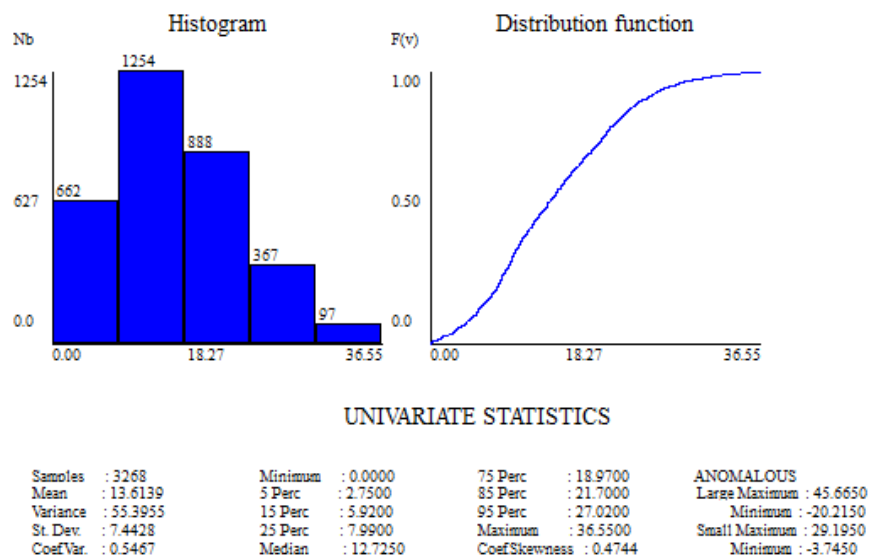


Figure 5.5.5 – Univariate statistics of well data

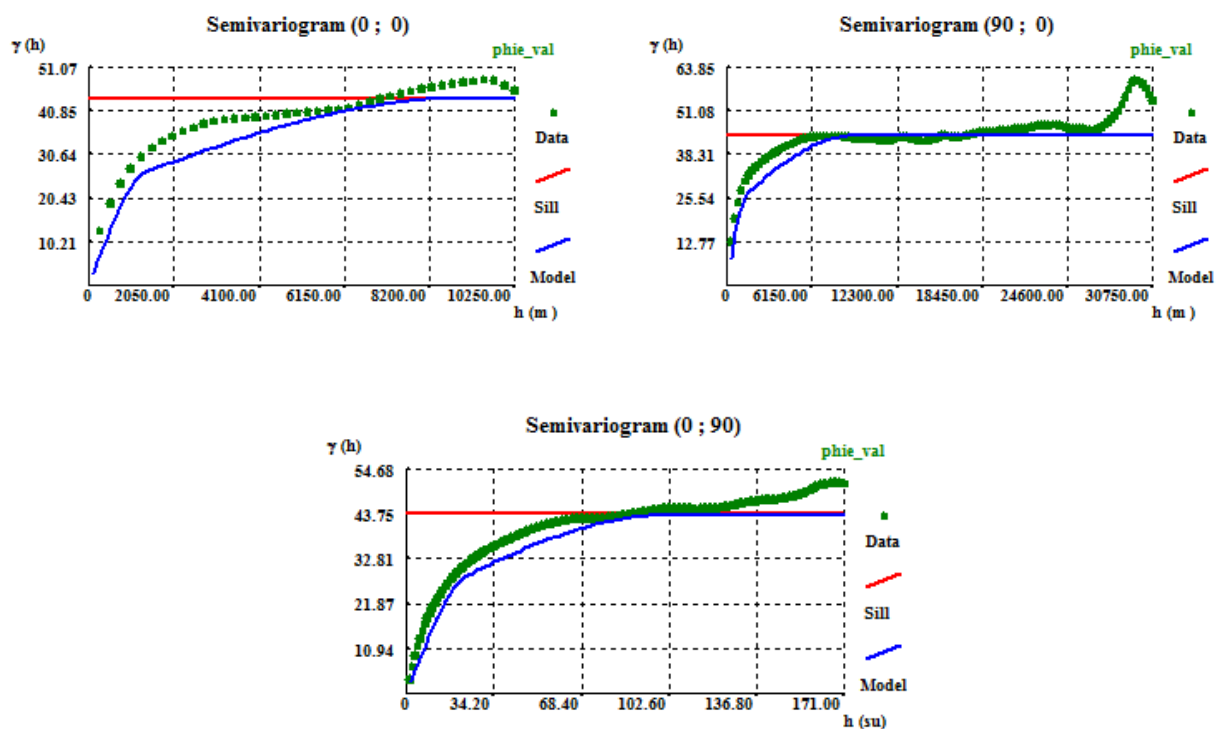


Figure 5.5.6 – Variograms for one simulated images of PHIE conditioning to the lithoclasses

### 5.6 3D model of permeability

As in previous simulation case there are two main stages – computing variograms and simulation.

Variograms were built for each lithoclass separately and for all lithoclasses together. The theoretical models were fitted. As in case of porosity more accurate results were obtained from the variograms for all lithoclasses. Modelling of permeability variograms is more complicated process because the permeability distribution law is high skew. In order to achieve a better experimental variogram representation a threshold value of 40 md for permeability was admitted. Variograms that were used for simulating process is shown in a figure 5.6.1. Parameters of fitted theoretical model that were used for modelling process are presented in the table 5.6.1. Thus for further modeling process the global variogram was used. As in case of porosity simulation was made by Direct Sequential Simulation method. Simulation of permeability was also pursued constraining to each 30 maps of lithoclasses. As a result 90 maps of permeability were obtained. In the figure 5.6.2 the realizations for the first and second images of lithoclasses are presented as the average map of LDperm (horizontal view and cross-section). It can be seen that these simulated maps accurately reflects the lithoclass image.

Table 5.6.1 – Parameters of the theoretical model fitted for LDperm for all lithoclasses

Lithoclass	Direction	Model	Range	Sill
for all lithoclasses	Horizontal	Exponential	3000 m	51.9
	Vertical	Exponential	50 s.u	51.9

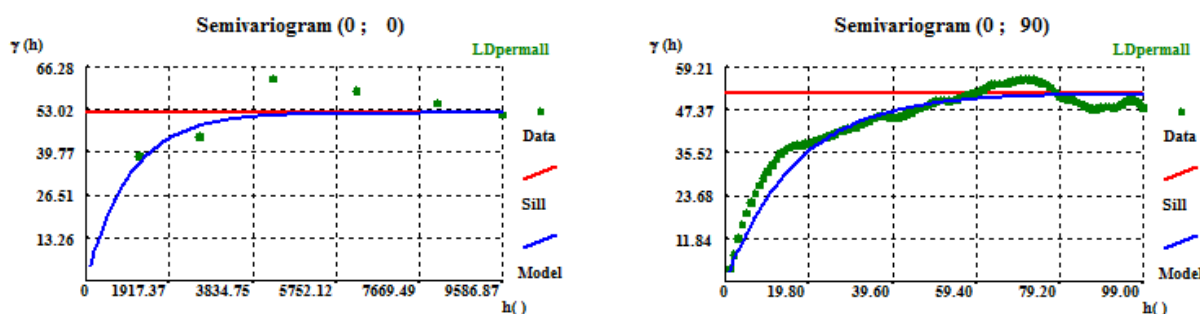
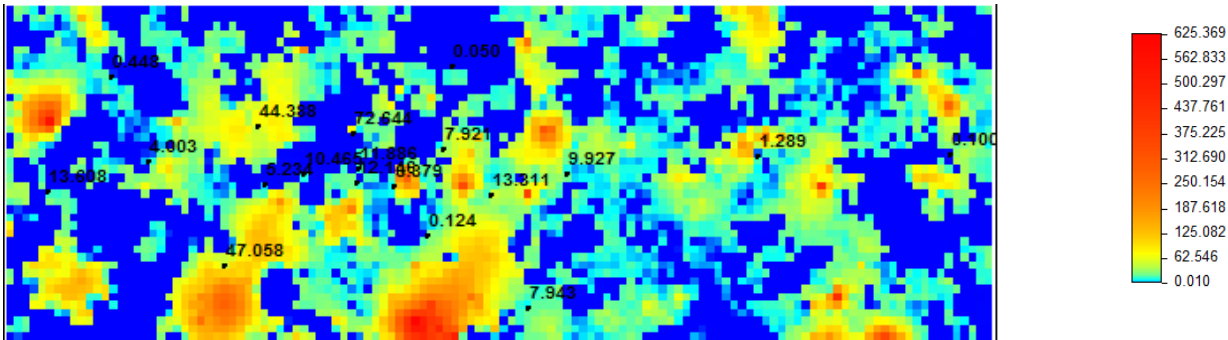
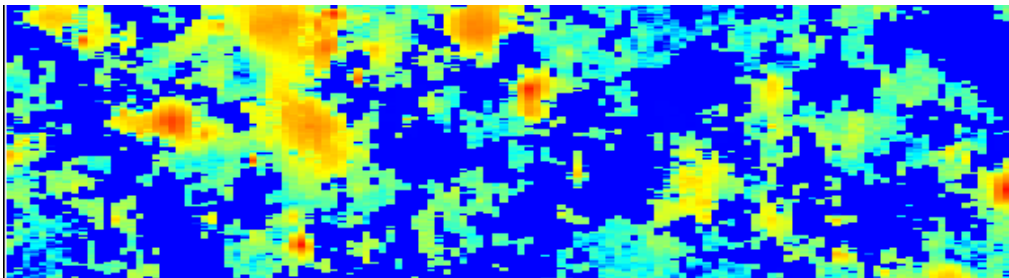


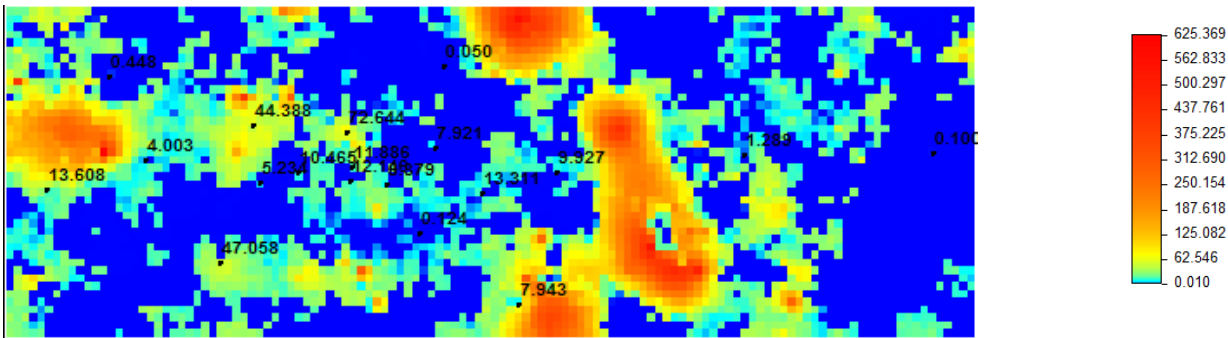
Figure 5.6.1 – Variograms of LDperm for all lithoclasses with fitted theoretical model



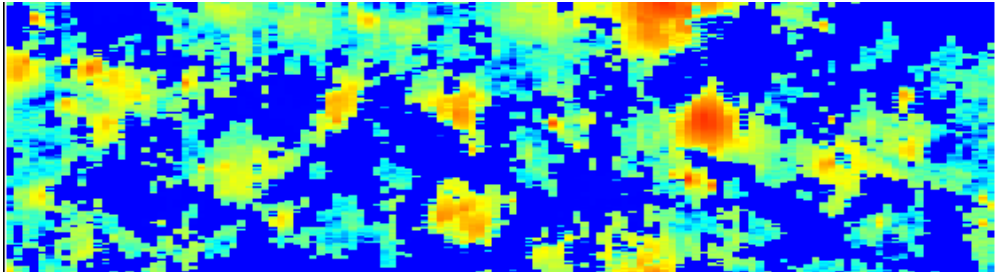
Realization 1 for the first image of lithoclasses (horizontal)



Cross-section

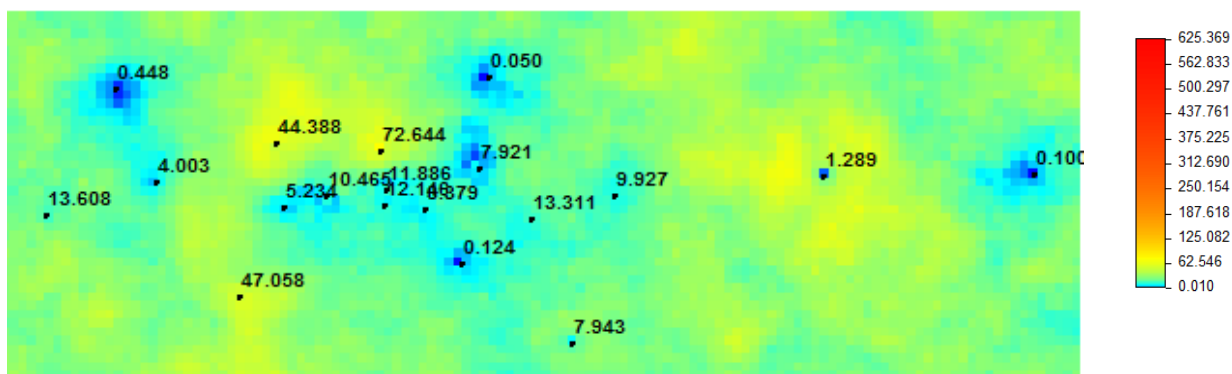


Realization 1 for the second image of lithoclasses (horizontal)

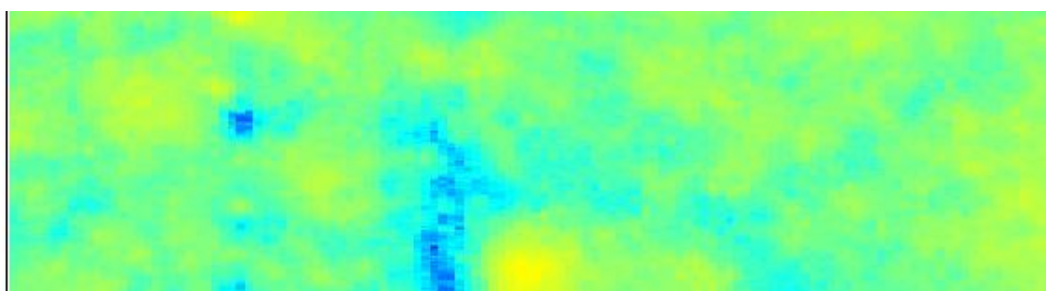


Cross-section





Average map (horizontal)



Cross-section

Figure 5.6.2 – Two realizations of LDperm for the first and second images of lithoclasses (horizontal and cross-section) and the average map of LDperm (logarithmic scale)

In what concerns validation, firstly the comparison of well data and simulated images was made by overlaying those data (figure 5.6.3). It can be seen that simulated map matches real values at well locations. The next step is statistic comparison, and basic statistics are shown in diagrams for well and grid data (the figure 5.6.4 and 5.6.5, respectively).

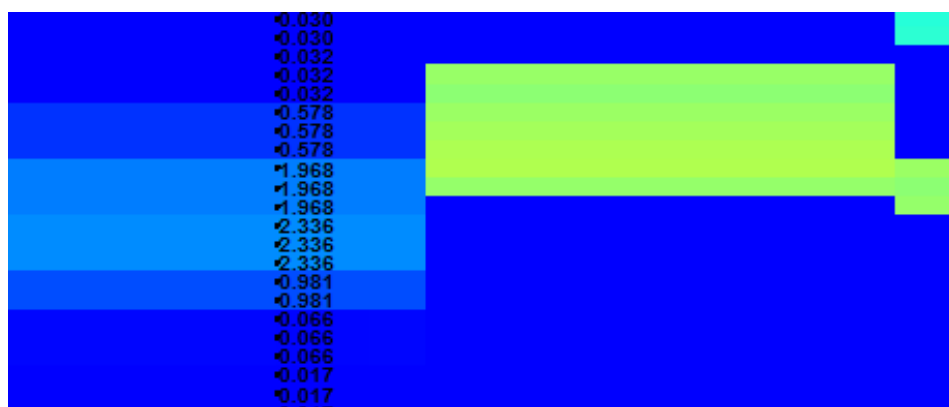


Figure 5.6.3– Simulated map of LDperm with overlaying well data

The differences between statistic parameters of the real data and simulated values can be explained by specific character of permeability values distribution (high skew) condition to lithoclasses. As the simulation was made constraining to lithoclasses with local histogram in case of permeability disconformity tends to be higher than in case of porosity simulation.

The third step of validation is variogram comparing. The variograms of permeability for simulated map are shown in the figure 5.6.6. In order to fit the theoretical model the same range was used, but it should be noted, that because of determination of threshold of permeability (40 md) in the stage of computing variograms the different sill was used.

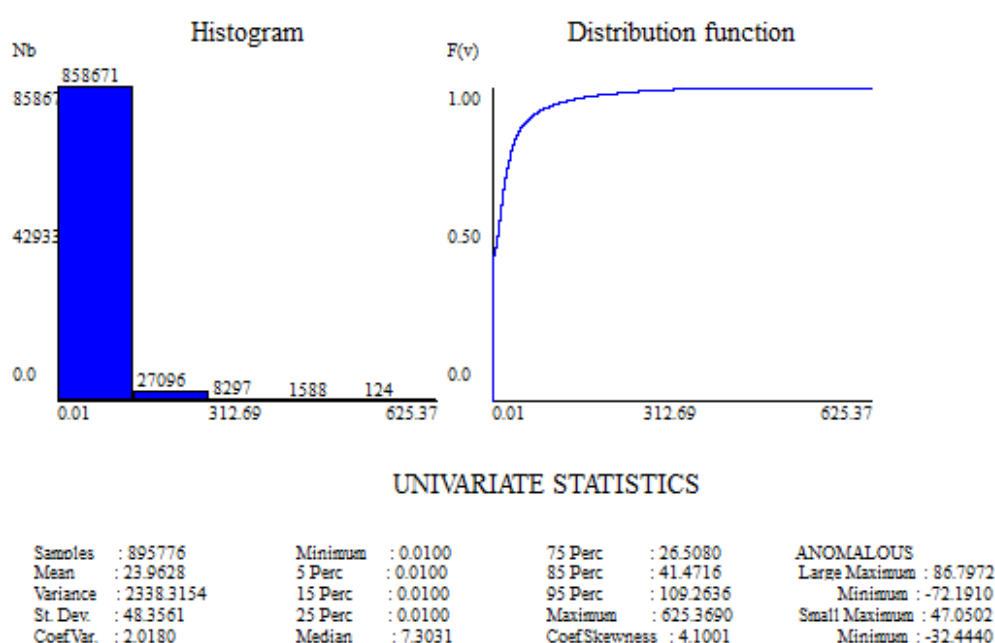


Figure 5.6.4 – Univariate statistic for one simulated image of LDperm

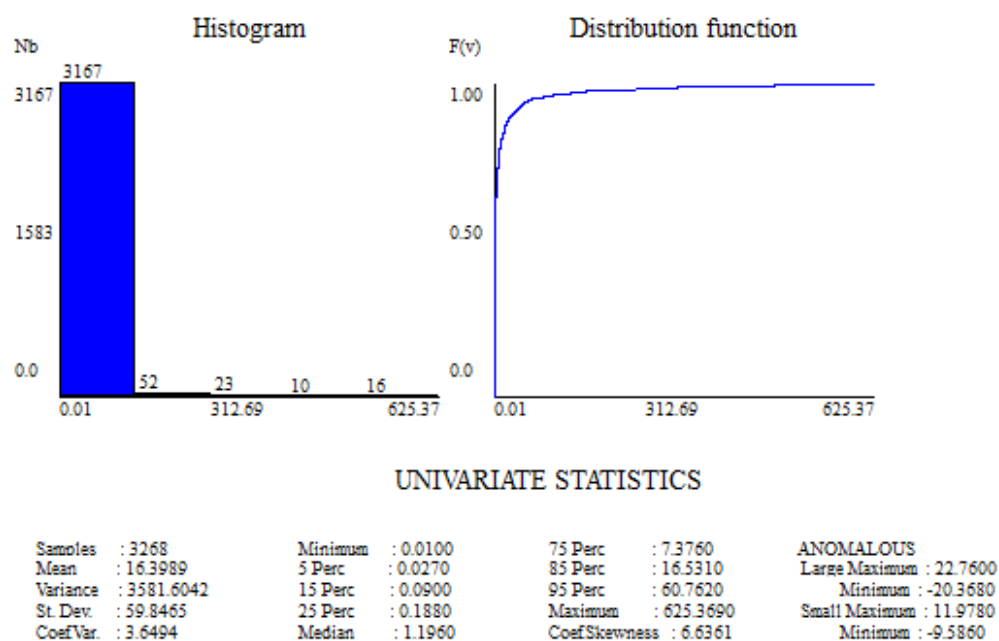


Figure 5.6.5 – Univariate statistic for well data

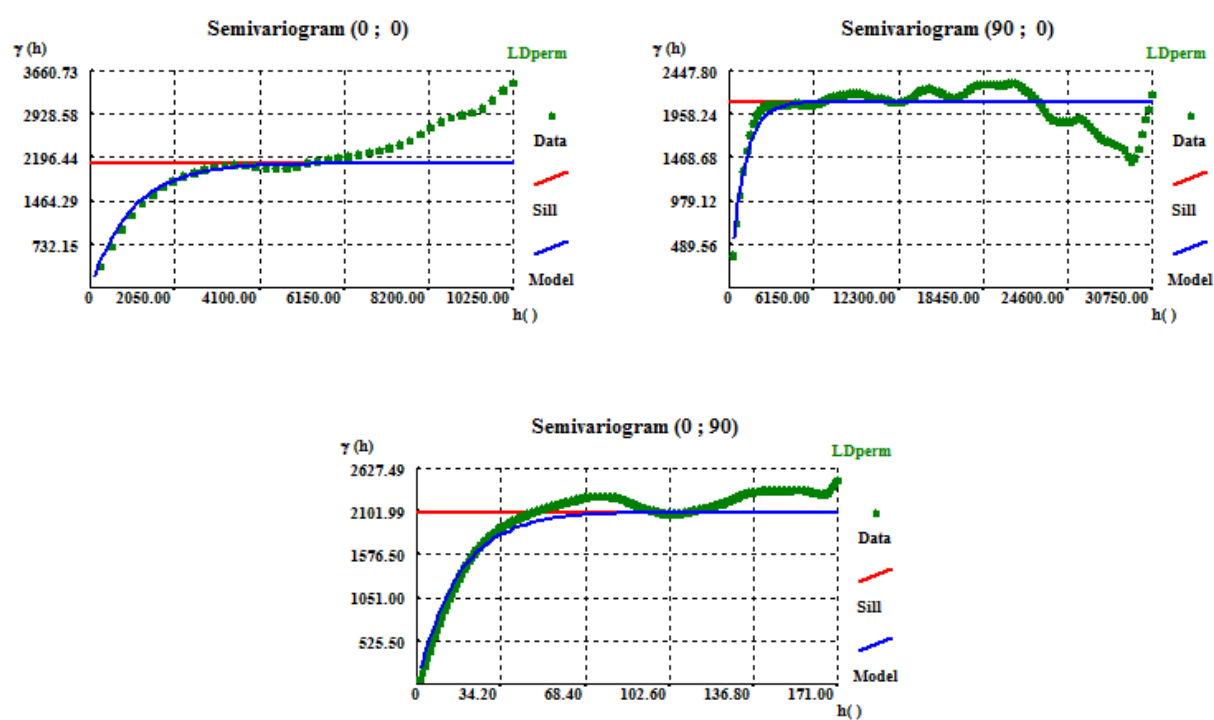


Figure 5.6.6 – Variograms for simulated maps of LDperm

According to validation stage the simulation of permeability was carried out accurately. It is proved that method of direct sequential simulation is shown appropriate results for modelling of properties distribution even in case of high heterogeneity and skew distributions.

### **5.7 Analysis of geobodies**

Accurately estimating the reserves of hydrocarbons in the reservoir is extremely important. Therefore the final in reservoir modelling is geobody analysis that including Potential Oil In Place (POIP) curves calculation. This analysis can give the complete information for reservoir characterization and provide the quantitative calculation of reserves. Curves of OIP refer to the total amount of oil that is potentially in a reservoir. Consideration of main properties of reservoir such as porosity and permeability for this calculation provides the reliable results and completed the process of reservoir modelling.

Prior to the calculation of POIP the back transformation of all grid models to the original referential was performed. POIP was computed using two approaches:

- a) Potential volume of oil based only on porosity (figure 5.7.1);
- b) Potential volume of oil based on porosity within high permeability geobodies (figure 5.7.2)

For case b) geobodies of permeability high than 50 md were calculated for each permeability images and overlaid with the homologous porosity images.

As these types of curves represent the oil volume in a reservoir the most productive volume of reservoir can be determined from the curves. It also can be used for the reserves estimation and evaluation of the most productive part of the reservoir.

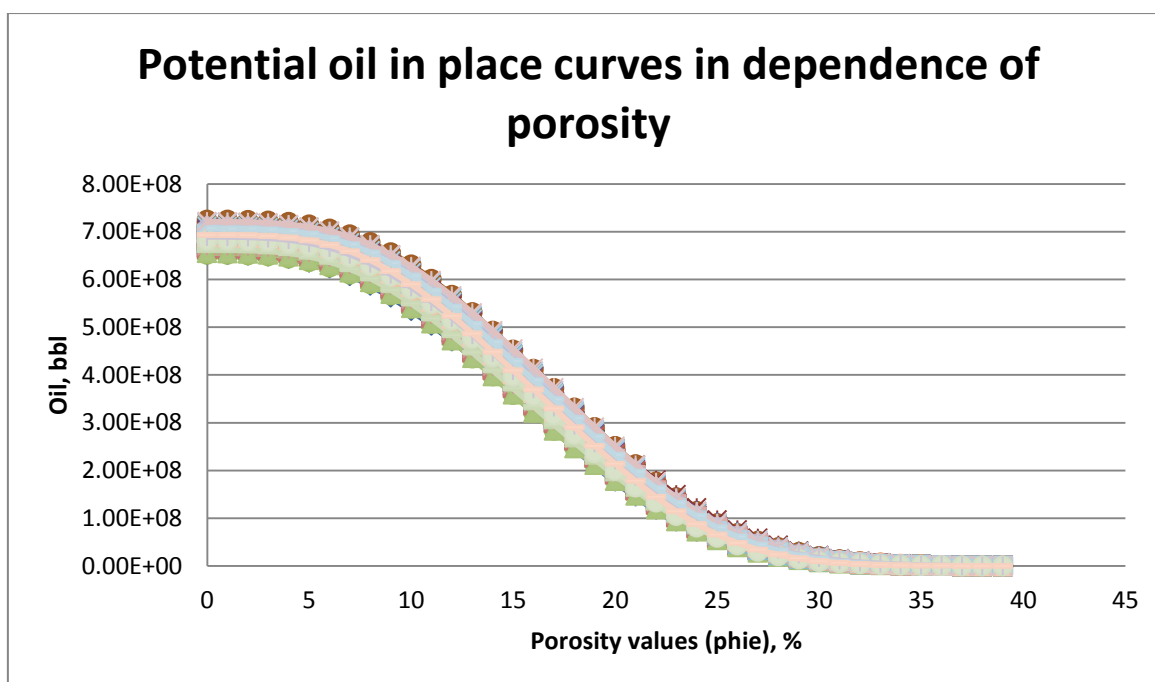


Figure 5.7.1 – Potential oil in place curves for case a)

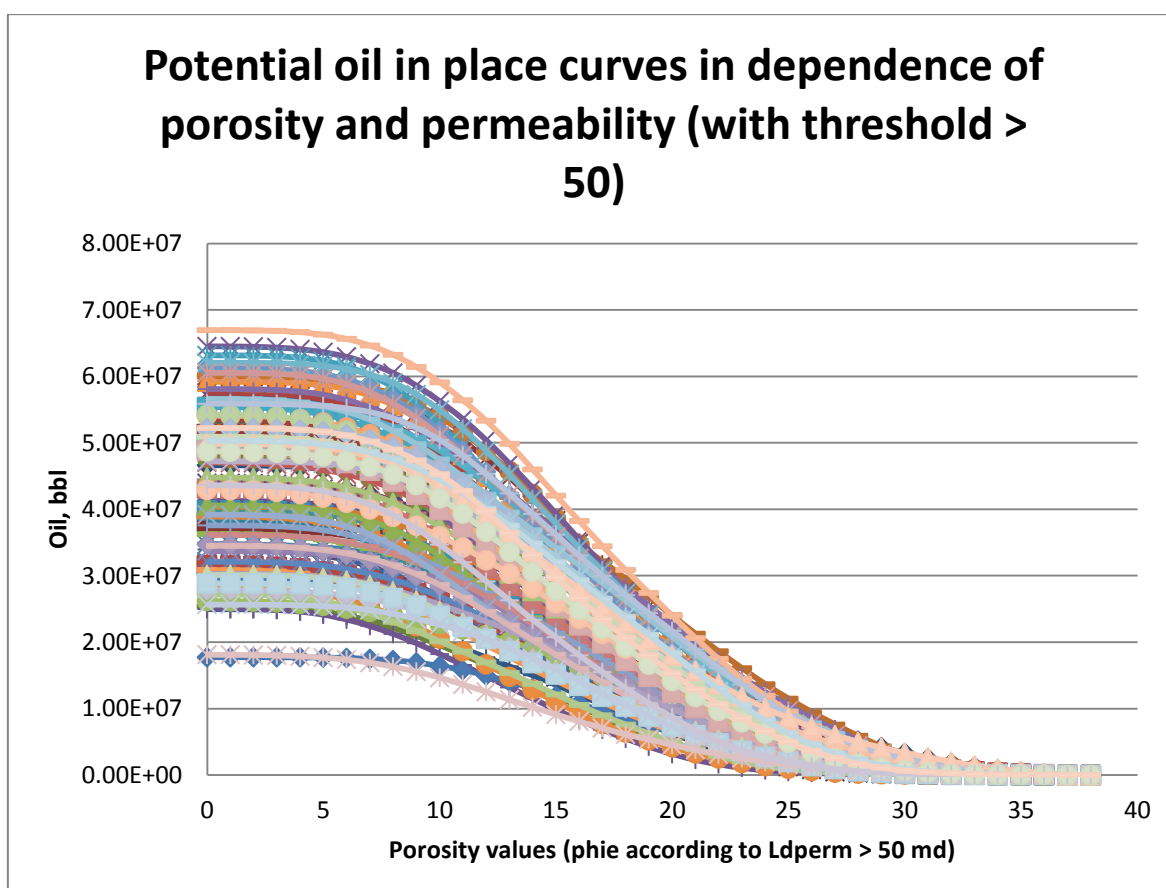


Figure 5.7.2 – Potential oil in place curves for case b)

## 6 FINAL REMARKS

Nowadays according to a current situation in a petroleum world when the largest and easy-recovery fields is in a depletion stage and prospecting is associated with a great challenge due to complexity of the reservoirs structure and deep depth of deposits occurrence, the geostatistics methods is becoming more and more actual. The drilling with a complete core recovery in a deep-seated massive reservoir rock is quite expensive and in combination with high exploration and exploitation costs make the hydrocarbon extraction almost unprofitable and lead to a growing of energy prices. In this critical situation the stochastic modelling provides advantages. Even having rather limited quantity of core material or information obtained from geophysical logging curves the complete model of the reservoir can be computed with low level of uncertainty by last estimation and simulation techniques.

Whereas the carbonate reservoirs present the significant part of the reservoir rocks in the world and a large portion of the oil and gas in the Middle East is contained in carbonate reservoirs, including several giant fields. Also reservoirs in other regions are depleted the Middle East carbonates have a potential to become a dominative producer of oil and gas. Processing of numerical model of carbonate reservoir based on logging initial data was made in this paper.

Carbonate reservoirs can be rather challenging. Their complex lithology and porosity variations make them difficult to characterize and develop efficiency. The way of solving problems is modern techniques that provide reliable information of essential reservoir parameters such as morphology, lithology and porosity and permeability variations and describe their spatial distribution.

Reservoir modelers recognize two fundamentally different aspects of stochastic reservoir models. The reservoir architecture is usually the first priority, consisting of the overall structural elements (for example, top and bottom of reservoir), and lithology of layers, then to generate probable distributions of reservoir attributes based on the conditioning data of sample data of a properties such as porosity or permeability observed at wells or derived from logs or cores.

The data obtained from cores has great level of heterogeneity, because in the most cases it is unprofitable to carry out full core sampling. The log data provide indirect measurement of attributes of borehole environment. The distribution of reservoir characteristics within non-sampling and non-logging reservoir volume is a main challenge and simultaneously the most important aspect for further reservoir development.

Geostatistics methods are means for obtaining the probable distribution of reservoir attributes via estimation and simulation techniques. The estimation method that was used in this work in order to model morphology of reservoirs based on variograms and ordinary kriging. Then for lithology and attributes modelling in the work the two most commonly forms of reservoir simulation were used: Sequential Indicator Simulation for categorical variables, such as lithoclasses and Direct Sequential Simulation with local histograms for continuous variables, such as porosity and permeability. It is important to note that the attributes were simulated according to obtained lithoclass images. The simulation process was based on global variograms as the distribution of the initial data represents smooth transition between properties and lithoclasses and also is very skew. The DSS with local histogram proposed in this work for attribute modelling showed the appropriate results and its proceeding were more facilitated took less time. The performed validation test showed that the simulated images provide accurate representation of the real data, also, for instance, the comparison of the average maps of porosity and lithoclasses maps showed that the boundaries of each lithoclass represent quite exactly on the average map of porosity, so the work is applicable. As new fields information becomes available it is possible to enhanced the model using the techniques, such as seismic data.

The 3D geological model of carbonate reservoir rocks presented in this work gives an opportunity to estimate the distribution of reservoir characteristics and thereby to obtain the reservoir model and evaluate ways of further development of reservoir in the most efficient way by considering different realizations. In addition based on simulation techniques the curves of potential oil in place were calculated in dependence on cut-off values of porosity and permeability that in turn let to estimate the potential volume of oil within the most productive part of reservoirs. So this work is an example of base geological model of carbonate reservoir which could be created by geostatistics techniques based on only well logs data.

In conclusion, by implementation of modern geostatistical approach the model of reservoir was obtained. However there is uncertainty in the reservoir model, but it is often difficult to assess the amount of uncertainty. One of the biggest benefits of geostatistical stochastic modeling is the assessment of risk or uncertainty in our model. To paraphrase Professor Andre Journel "... it is better to have a model of uncertainty, than an illusion of reality."

**REFERENCES**

- Ahr, W.M., 2008. Geology of carbonate reservoirs, the identify cation, description, and characterization of hydrocarbon reservoirs in carbonate rocks. John Wiley and Sons, USA.
- Al-Hanai, W., Russell, S.D., Vissapragada, B., 2009. Complexity of carbonate reservoirs. Schlumberger.
- Almeida, J.A., 1999. Use of geostatistical models to improve reservoir description and flow simulation in heterogeneous oil fields. PhD thesis IST-161.
- Amilcar, S., 2001. Direct Sequential Simulation and Co-simulation. Mathematical Geology, Vol.33, No.8, 9 11-926.
- Archer, I.S., 1986. Petroleum engineering: principles and practice. Graham and Trotman Inc., USA.
- Archie, G.E., 1952. Classification of carbonate reservoir rocks and petrophysical considerations. AAPG Bulletin 36: 278-298.
- Basic Petroleum Geology and Log Analysis , 2001, Halliburton.
- Burkhard, J., 2010. Oil and gas trends and challenges. Microsoft Global Energy Forum, Houston, Texas, USA.
- Caers, J., 2001. Direct sequential indicator simulation. Stanford University, Department of Petroleum Engineering, Stanford, USA.
- Deutsch, C., Journel, A. G., 1992, GSLIB: Geostatistical software library and User's Guide. Oxford University Press, New York.
- Endres, H., Lohr, T., Trappe, H., 2008. Quantitative fracture prediction from seismic data. Petroleum Geoscience, 14: 369—377.
- Gluyas, J., Swarbrick, R., 2004. Petroleum Geoscience. Blackwell Science Ltd, Blackwell Publishing Company.
- Goovaerts, P., 1998. Geostatistics for natural resources evaluation. Oxford University Press.
- Ham, W.E., 1962. Classification of carbonate rocks. A symposium, The American Association of Petroleum Geologists, Tulsa, USA.
- Harris, P.M., Frost, S.H., Seiglie, G.A., Schneidermann, N., 1984. Regional unconformities and depositional cycles, Cretaceous of the Arabian Peninsula, in J. S. Schlee., Interregional unconformities and hydrocarbon accumulation. AAPG Memoir 36: 67-80.
- Harris, P.M., 2010. Delineating and quantifying depositional facies patterns in carbonate reservoirs: Insight from modern analogs. AAPG Bulletin, 94 (1): 61-86.
- Isaaks, E.H., Srivastava, R.M., 1989. An introduction to applied geostatistics. Oxford University Press.



- James, N.P., Scholle, P.A., Bebout, D.G., Moore, C.H., 1983. Carbonate depositional environments. AAPG Memoir 33: 346-462.
- Jef, C., 2000. Adding local accuracy to Direct Sequential Simuiation. Mathematical Geology, Vol. 32, No.7, 81 5- 850.
- Jordan, C.F., Connally, T.C., Vest, H. A., 1985. Middle Cretaceous Carbonates of the Mishrif Formation, Fateh Field, Offshore Dubai, U.A.E., in P. O. Roehl and P. W. Choquette, eds., Carbonate Petroleum Reservoirs. Springer-Verlag, New York: 426-442.
- Levyant, V.B., 2010. Guidelines on the using transformations of seismic data to calculate hydrocarbons in carbonate reservoirs. Moscow, CGE - 250.
- Loucks, R.G., Sarg, J.F., 1993. Carbonate sequence stratigraphy. Recent developments and applications. AAPG MEMOIR 57.
- Lucia, F.J., 1999. Carbonate reservoir characterization. An Integrated Approach. Second Edition, Springer-Verlag, Berlin, Heidelberg.
- Matheron, G., 1989. Estimating and choosing, Springer-Verlag, Berlin.
- Montaron, B., Stundner, M., Zangl, G., 2009. Middle East and Asia Reservoir review: enhancing carbonate reservoir characterization. Middle East & Asia Reservoir Review Volume, No. 9.
- Moore, C.H., 2001. Carbonate reservoirs. Porosity evolution and diagenesis in a sequence stratigraphic framework. Elsevier Science B.V., Amsterdam. The Netherlands.
- Murris, R. J., 1980. Middle East stratigraphic evolution and oil habitat. AAPG Bulletin, v. 64: 597-618.
- North, F.K., 1985. Petroleum Geology. Unwin Hyman Inc., Winchester, USA: 191-206.
- Nur, A.M., Wang, Z., 1989. Seismic and acoustic velocities in reservoir rocks, 1: Experimental studies: Soc. Expl. Geophys.
- Pennington, W.D., 2001. Reservoir geophysics. Geophysics, vol. 66, no. 1: 25–30.
- Ramamoorthy, R., Boyd, B., Neville, T.J., Seleznev, N., Sun, H., Flaum, C., 2010. For more on difficulties with carbonate reservoir evaluation. A New Workflow for Petrophysical and Textural Evaluation of Carbonate Reservoirs, Petrophysics 51, no. 1: 17-31.
- Read, J.F., 1985. Carbonate platform fades models. AAPG Bulletin, v. 69: 1-21.
- Scholle, P.A., Bebout, D.G., Moore, C.H., 1983. Carbonate Depositional Environments. AAPG Memoir 33.
- Scott, R.W., 1990. Chronostratigraphy of a Cretaceous carbonate shelf, southeastern Arabia, in A. H. F. Robertson, M. P. Searle, and A. C. Ries, eds. The geology and tectonics of the Oman region. Geological Sodety Special Publication 49: 89-108.
- Sheriff, R.E., Ed., 1992. Reservoir geophysics. Soc. Expl. Geophys.

- Singh, U., Van Der Baan, D., 2001. FMS/FMI borehole imaging of carbonate gas reservoirs, Central Luconia Province, offshore Sarawak, Malaysia. AAPG Bulletin: 1162-1163.
- Skelton, P.W., Nolan, S.C., Scott, R.W., 1990. The Maastrichtian transgression onto the northwestern flank of the proto-Oman mountains sequences of rudist-bearing beach to open shelf facies, in A. H. F. Robertson, M. P. Searle and A. C. Ries, eds. The geology and tectonics of the Oman region. Geological Society Special Publication 49: 521-547.
- Soares, A., 1998. Sequential indicator simulation with correction for local probabilities. Mathematical Geology, 30: 761–765.
- Soares, A., 2001. Direct Sequential Simulation and Co-simulation. Mathematical Geology, 33(8): 911-926.
- Sokolov, A.N., 2011. Reserves, production and consumption of fossil fuels in the world and in Russia. Institute of Oil and Gas Problems of Siberian Branch of the Russian Academy of Sciences, Yakutsk, Russia.
- Solow, A.R., 1986. Mapping by simple indicator kriging: Mathematical Geology, v. 18: 335-352.
- Stone, D.G., 1994. Designing seismic surveys in two and three dimensions. Soc. Expl. Geophys.
- Tucker, M.E., Wright, V.P., 1990. Carbonate Sedimentology. Blackwell Publishing.
- Yarus, J.M., Chambers, R.L., 1995. Stochastic modeling and geostatistics—principles, methods, and case studies. AAPG.